

AN ABSTRACT OF THE THESIS OF

Liang Xian for the degree of Doctor of Philosophy in

Electrical and Computer Engineering presented on August 2, 2006.

Title: Space Time Coding in MIMO Systems

Abstract approved: _____

Huaping Liu

Multiple-input multiple-output (MIMO) antenna technology is promising for high-speed wireless communications without increasing the transmission bandwidth. Space time coding (STC) is a scheme that employs multiple antennas to increase transmission rate or to improve transmission quality. STC is used widely in mobile cellular networks, wireless local area networks (WLAN) and wireless metropolitan area networks (WMAN). However, there are still many unsolved or partially solved issues in STC. In this thesis, I propose a new STC design from cyclic design. I then propose a systematic method to design quasi-orthogonal space time block codes (QOSTBC) for an arbitrary number of transmit antennas, and derive the optimal constellation rotation angles to achieve full diversity. I also propose an analytical method to derive the exact error probabilities of orthogonal space time block codes (OSTBC). In order to improve the error performance, I introduce an adaptive power allocation scheme for OSTBC. Combining STC with continuous phase modulation (CPM) is an attractive solution for mobile communications for which power is limited. Thus, I apply OSTBC to binary CPM with modulation index $h = 0.5$, and develop a simplified receiver for such scheme. Fi-

nally, I present a decoding method to reduce the complexity of QOSTBC without degrading its error performance.

©Copyright by Liang Xian

August 2, 2006

All Rights Reserved

Space Time Coding in MIMO Systems

by

Liang Xian

A THESIS

submitted to

Oregon State University

in partial fulfillment of
the requirements for the
degree of

Doctor of Philosophy

Presented August 2, 2006
Commencement June 2007

Doctor of Philosophy thesis of Liang Xian presented on August 2, 2006

APPROVED:

Major Professor, representing Electrical and Computer Engineering

Director of the School of Electrical Engineering and Computer Science

Dean of the Graduate School

I understand that my thesis will become part of the permanent collection of Oregon State University libraries. My signature below authorizes release of my thesis to any reader upon request.

Liang Xian, Author

ACKNOWLEDGMENTS

First of all I would like to express my sincere gratitude to my advisor Dr. Huaping Liu for his continuous encouragement, support and guidance throughout my graduate studies. I am very thankful for his patience and always believing in me during the ups and downs of my Ph.D. research. His broad knowledge and logical way of thinking have been of great value for me. His technical advice and constructive comments have provided a good basis for this thesis. I would also like to thank Intel Corp. for providing me the opportunity to work with the great people that I met along the way.

I am deeply indebted to Dr. Gabor C. Temes, Dr. Michael H. Scott, Dr. Un-Ku Moon and Dr. Zhongfeng Wang for their efforts and time to serve on my Ph.D. committee.

My thanks to all the members in my lab for their help and friendship. Special thanks to Jie Gao, Orhan C. Ozdural, Shiwei Zhao, Weiting Chen and Yu Zhang for always being available for technical discussions.

Finally, I would like to express my deepest gratitude for the constant support, understanding and unconditional love that I received from my parents, my parents-in-law and my wife Jinna. This thesis is also a gift for my dear boy Daniel.

TABLE OF CONTENTS

	<u>Page</u>
1 INTRODUCTION	1
1.1 Background and Motivation	1
1.2 Objective and Contributions	3
1.3 Notation Summary	5
2 SPACE-TIME BLOCK CODES FROM CYCLIC DESIGN	8
2.1 System Model	8
2.2 New Codes From Cyclic Design	10
2.2.1 The rank criterion	10
2.2.2 The determinant criterion	11
2.2.3 New full-rate full-diversity codes from cyclic design	12
2.3 Numerical Results and Discussion	14
2.4 Conclusion	17
3 OPTIMAL ROTATION ANGLES FOR QUASI-ORTHOGONAL SPACE-TIME CODES WITH PSK MODULATION	18
3.1 Optimal constellation rotation for PSK	18
3.1.1 The optimal rotation angles	23
3.1.2 Relative coding gain between $Q=2n$ and $Q=2n-1$	24
3.2 Conclusion	25
4 RATE-ONE SPACE-TIME BLOCK CODES WITH FULL DIVERSITY	26
4.1 System Model	27
4.2 Generalized Quasi-Orthogonal Codes	29
4.2.1 Code construction	29
4.2.2 Generalized fast decoding	33

TABLE OF CONTENTS (Continued)

	<u>Page</u>
4.2.3 Optimal constellation rotation for quasi-orthogonal codes . . .	34
4.3 Simulation Results	38
4.4 Conclusion	40
5 EXACT ERROR PROBABILITY FOR SPACE-TIME BLOCK-CODED MIMO SYSTEMS OVER RAYLEIGH FADING CHANNELS	41
5.1 Performance Analysis	41
5.1.1 Rate 1 codes	42
5.1.2 Rate 3/4 complex codes	45
5.1.3 Rate 1/2 complex codes	47
5.1.4 Differential space-time block codes	50
5.2 Conclusion	51
6 AN ADAPTIVE POWER ALLOCATION SCHEME FOR SPACE-TIME BLOCK CODED MIMO SYSTEMS	53
6.1 System model	54
6.2 SNR Analysis	55
6.3 Adaptive power allocation	57
6.3.1 Minimum Feedback Allocation Scheme (Antenna Selection) .	57
6.3.2 A New Adaptive Power Allocation Scheme	58
6.3.3 The New Scheme with Imperfect Feedback	62
6.4 Numerical Examples and Discussion	64
6.5 Conclusion	67
7 SIMPLIFIED RECEIVER DESIGN FOR STBC BINARY CPM WITH MODULATION INDEX $H = 1/2$	68

TABLE OF CONTENTS (Continued)

	<u>Page</u>
7.1 System Model	69
7.2 Code Design Based on Laurent Decomposition.....	71
7.3 Low-Complexity Decoding.....	75
7.3.1 The receiver without FIR	75
7.3.2 The receiver with FIR	78
7.3.3 The receiver with decision feedback.....	82
7.4 Performance Analysis.....	85
7.5 Simulation Results	87
7.6 Conclusion	89
8 LOW-COMPLEXITY MAXIMUM LIKELIHOOD DECODING FOR QUASI-ORTHOGONAL SPACE-TIME CODES	93
8.1 Low-Complexity ML Decoding and Simulation Results.....	93
8.2 Conclusion	98
9 SUMMARY	99
BIBLIOGRAPHY	100

LIST OF FIGURES

Figure	Page
2.1 Error performance of cyclic code ($N = 3, M = 1$, QPSK)	15
2.2 Error performance of cyclic code ($N = 4, M = 1, 2$, QPSK)	16
3.1 An example of an even-sized constellation \mathcal{A} : 16PSK.	20
3.2 An example of an odd-sized constellation \mathcal{A} : 7PSK.	20
3.3 Constellation \mathcal{X} formed by $(x_1 - \tilde{x}_1)^2$, where $x_1, \tilde{x}_1 \in \mathcal{A}$ as shown in Fig. 3.1	21
3.4 Constellation \mathcal{X} formed by $(x_1 - \tilde{x}_1)^2$, where $x_1, \tilde{x}_1 \in \mathcal{A}$ as shown in Fig. 3.2	21
4.1 Constellation \mathcal{X} and $\mathcal{Y} = e^{j\pi/6}\mathcal{X}$	36
4.2 Performance comparison between \mathbf{G}_5 and theoretical lower bound ($N = 5, M = 1, 2$ bits/s/Hz).	38
4.3 Performance comparison between \mathbf{G}_5 and theoretical lower bound ($N = 5, M = 1, 4$ bits/s/Hz).	39
5.1 Rate 1 codes with BPSK modulation.	45
5.2 Rate 3/4 codes with QPSK modulation.	48
5.3 Rate 1/2 codes with QPSK modulation.	50
5.4 Differential codes with BPSK modulation, full rate.	52
6.1 BER versus parameter u ($M = 2, N = 1, 2$)	64
6.2 BER versus E_b/\mathcal{N}_0 curves for different schemes ($M = 2, N = 1$, BPSK)	65
6.3 BER versus E_s/\mathcal{N}_0 curves for different schemes ($M = 2, N = 2$, QPSK)	66
7.1 The modified Alamouti scheme ($M = 2$) for MSK with precoding based on Laurent decomposition.	75
7.2 Receiver structure of space-time block coded BCPM0.5 with 2 transmit antennas.	80
7.3 GMSK with $BT = 0.3, L = 3$	81
7.4 Equivalent system model for space-time block coded GMSK with 4 antennas.	82

LIST OF FIGURES (Continued)

<u>Figure</u>	<u>Page</u>
7.5 Performance of space-time block coded GSMK ($BT = \infty$, $L = 1$, $M = 2$).	88
7.6 Performance of space-time block coded GSMK ($BT = 0.5$, $L = 2$, $M = 2$).	89
7.7 Performance of space-time block coded GSMK ($BT = 0.3$, $L = 3$, $M = 2$).	90
7.8 Performance of space-time block coded GSMK with 3 transmit antennas	91
7.9 Performance of space-time block coded GSMK with 4 transmit antennas	92
8.1 The virtual constellation and actual constellation for 64QAM.	94
8.2 CDF of condition numbers of channel matrices for QOC and SM. . . .	96
8.3 Performance comparison of maximum likelihood and the proposed decoding schemes for PSK signals.	97
8.4 Performance comparison of maximum likelihood and the proposed decoding schemes for QAM signals.	98

Space Time Coding in MIMO Systems

1. INTRODUCTION

1.1. Background and Motivation

MIMO systems use multiple transmit and receive antennas to create multiple spatial channels between the transmitter and the receiver. MIMO systems have been shown to provide high spectral efficiencies [1–34], which form the basis to increase the data rates without increasing the bandwidth. If perfect channel state information (CSI) is available at the receiver, the average capacity grows linearly with the smaller of the numbers of transmit and receive antennas under certain channel conditions. The major potential advantage of MIMO is that either the quality in terms of bit error rate (BER) or the data rate of the system can be improved. The performance improvement of MIMO systems can be assessed by using diversity gain and spatial multiplexing gain. It is not possible to achieve maximum diversity and multiplexing simultaneously because there is a tradeoff between them [35]. Diversity gain is achieved by transmitting the same signal over multiple independent fading environments, e.g., in the time, frequency, and spatial domains. Space-time coding transmits signal across the spatial and time domains simultaneously in order to achieve diversity gain without increasing bandwidth.

In [36], Alamouti proposed an OSTBC for systems with two transmit antennas. Later, orthogonal design was extended to the systems with arbitrary number of transmit antennas in [37–39]. The most important aspect of orthogonal design is its full diversity and low-complexity maximum likelihood (ML)

decoding. These properties make OSTBC be an attractive transmission scheme in practical systems. Space time trellis coding (STTC) [40] is another space time coding scheme which combines trellis code with space time coding in order to achieve both diversity gain and coding gain [40]; however, encoding and decoding complexities of STTC are higher than those of OSTBC.

Spatial multiplexing gain could be evaluated by using the linear increase in capacity without additional bandwidth resources. This gain is realized by transmitting independent data streams from individual antennas to maximize data rates. Vertical Bell Labs layered Space-Time (V-BLAST) proposed in [41, 42] is an effective approach to achieve spatial multiplexing gain. V-BLAST is also directly called spatial multiplexing (SM). By using channel coding, interleaving, and mapping, information bits can also be transmitted across time and space domains. Therefore, V-BLAST can be considered a type of space time coding. The interference among the signals transmitted simultaneously from different transmit antennas considerably increases the detection complexity. The optimal detection scheme is the ML scheme where the receiver compares all possible combinations of the transmitted symbols with the observed ones. It suffers from significant increase in complexity, which grows exponentially with the number of transmit antennas and the size of signal constellation. It could become prohibitive with a large number of antennas and high-order modulations. Thus, several suboptimal detection schemes have been developed, e.g. zero-forcing (ZF), minimum-mean-square error (MMSE) and V-BLAST, at this time, V-BLAST stands for a nulling and cancelling detection scheme instead of a transmission scheme. Both ZF and MMSE can decouple different spatial streams by matrix inversion. ZF results in poor performance without considering the noise enhancement. MMSE has a better performance than ZF by considering the tradeoff between noise enhancement

and interference suppression. V-BLAST decodes the symbol with the highest signal-to-noise ratio (SNR) first based on ZF or MMSE criterion, and then cancels the contribution of the decoded symbol from the received signals assuming the decoding result is correct. Such process continues by decodes the symbol with the second highest SNR, and so on. Note that ZF and MMSE require that the number of receive antennas be greater than or be equal to the number of transmit antennas; however, ML does not have such constraint.

1.2. Objective and Contributions

Space-time block codes have lower encoding and decoding complexities than Space-time trellis codes. Therefore, space-time block codes are more popular in practical systems. In this thesis, we will focus on space-time block coding.

It has been proved that rate-one orthogonal space time block code for complexity signals exists only for two transmit antennas [37, 43–45]. When the number of transmit antennas is larger than two, quasi-orthogonal space-time block code [46, 47] is a good choice as it can provide full transmission rate, and full diversity can be achieved by constellation rotation [48, 49]. However, rotated QOSTBC experiences constellation expansion. In chapter 2, we propose space-time block codes from cyclic design for three and four transmit antennas for which full diversity can be achieved for real signals, i.e., pulse amplitude modulation (PAM) and complex QPSK signal. There is no constellation expansion for STBC from cyclic design.

Optimal rotation angles in the sense of maximizing coding gain [40] for QOSTBC with four antennas have been derived analytically for quadrature amplitude modulation (QAM) and triangular modulation (TRI) [49]. Phase shift

keying (PSK) is another popular modulation scheme, but the non-integer in-phase and quadrature components make it difficult to find the optimal rotation angle via an analytical approach. We propose a geometrical method [51] in Chapter 3 to find the optimal rotation angle for PSK signals based on their geometrical properties. We also prove that even-sized PSK signal has larger coding gain than odd-sized PSK signal.

Extensive amount of research has been done for rotated QOSTBC with four transmit antennas. When the number of antennas is greater than four, it is extremely difficult to design QOSTBC and derive the optimal rotation angles. In [52], Sharma and Papadias tried to find rotation angles for QOSTBC with a large number of transmit antennas; however, these results are not optimal in the sense of maximizing the coding gain. In Chapter 4, we develop a systematic method to design QOSTBC based on rate-one, real OSTBC [53]. We also find the optimal rotation angles by minimizing the number of unknown variables. A geometric method is used to find the optimal angle for QPSK; for the constellations with a larger size than QPSK, optimal rotation angles are found via computer search.

Performance analysis is a powerful tool to predict and analyze the performance of space time codes. Existing analysis on the error performance of STBC has focused on deriving error-rate upper bounds for a general system [40, 54–56] or the exact error probabilities for some special cases [59]. A general method to calculate the exact error probability for orthogonal space-time block codes that employ coherent and differential PSK over flat Rayleigh fading channels is proposed in Chapter 5 [60].

Receive diversity yields a higher SNR than transmit diversity when the total transmitted power and diversity order are the same. However, if the transmitter has complete or partial knowledge of the channel, the SNR gap between

these two schemes can be reduced. We propose an adaptive power allocation scheme for STBC to improve system performance [61] in Chapter 6. The proposed adaptive power allocation scheme improves the instantaneous SNR at the receiver. The maximum achievable SNR gain limit over the conventional scheme is also derived.

Existing space-time codes have focused on linear modulations such as QAM and PSK. Continuous phase modulation (CPM) is an attractive scheme for digital transmission because of its compact spectrum and constant envelope which is needed for power efficient transmitters. Recent research has shown that space-time coded CPM can achieve transmit diversity to improve performance while maintaining the compact spectrum of CPM signals. However, these efforts mainly combine STTC with CPM to achieve spatial diversity at the cost of a high decoding complexity. In Chapter 7, we design STBC for binary CPM with a modulation index $1/2$ [62] and develop low complexity receivers. The proposed scheme has a much lower decoding complexity than STTC CPM.

QOSTBC has a higher decoding complexity than OSTBC but lower decoding complexity than spatial multiplexing. QOSTBC for four transmit antennas can be decoded pair by pair, instead of four transmitted symbols jointly. The complexity of QOSTBC is comparable to that of SM in systems with two transmit antennas. In Chapter 8, we propose a group decoding scheme to further reduce the complexity of QOSTBC while still approach the performance of the ML decoder.

1.3. Notation Summary

Acronyms and mathematical notations are listed below.

Notation	Description
$(\cdot)^T$	Transpose
$(\cdot)^H$	Hermitian
$(\cdot)^*$	Complex Conjugate
$\ \cdot\ _F$	Frobenius Norm
BCPM0.5	Binary Continuous Phase Modulation with $h = 1/2$
BER	Bit Error Rate
BT	Bandwidth Time Product
CDF	Cumulative Distribution Function
CPM	Continuous Phase Modulation
GMSK	Gaussian Minimum Shift Keying
GSM	Global System for Mobile communications
ISI	Intersymbol Interference
MIMO	Multiple Input Multiple Output
ML	Maximum Likelihood
MMSE	Minimum Mean Square Error
NRZ	Non Return to Zero
OSTBC	Orthogonal Space Time Block Codes
PAM	Pulse Amplitude Modulation
PDF	Probability Density Function
PSD	Power Spectrum Density
PSK	Phase Shift Keying
QAM	Quadrature Amplitude Modulation
QOSTBC	Quasi-Orthogonal Space Time Block Codes
SINR	Signal-to-Interference plus Noise Ratio
SM	Spatial Multiplexing

SNR	Signal-to-Noise Ratio
STBC	Space-Time Block Codes
STTC	Space-Time Trellis Codes
V-BLAST	Vertical Bell Labs Layered Space-Time
WLAN	Wireless Local Area Network
WMAN	Wireless Metropolitan Area Network
ZF	Zero Forcing

2. SPACE-TIME BLOCK CODES FROM CYCLIC DESIGN

Linear orthogonal space-time block codes are attractive because of their inter-symbol interference (ISI) free structure and the feasibility of realizing maximum likelihood decoding using linear operations. However, in [37] Tarokh *et. al.* proved that full-rate complex orthogonal codes do not exist for systems with more than two transmit antennas. Thus the Alamouti scheme [36] is the only complex orthogonal code with full transmission rates. In order to achieve full transmission rate in systems with more than two transmit antennas, one must give up orthogonality. Therefore, in [46], Jafarkhani proposed a quasi-orthogonal code with full rate but partial diversity for systems with four transmit antennas. In [48] Sharma *et. al.* proposed a constellation-rotation scheme to improve the performance of quasi-orthogonal codes, which was subsequently extended for systems with an arbitrary number of transmit antennas in [52]. Later, He *et. al.* [63] proposed a nonlinear orthogonal code with full rate and full diversity for QPSK systems with four transmit antennas. However, the encoding and decoding complexities of this code are higher than those of quasi-orthogonal codes.

In this Chapter, we present a new space-time block coding scheme based on cyclic design. We will first analyze the determinants of real square orthogonal code matrices and propose a new real code from cyclic design. Then, we minimize ISI to design complex cyclic codes that achieve full diversity. We also study the performance of the proposed scheme and compare it with existing schemes.

2.1. System Model

Consider a system with N transmit antennas and M receive antennas. The transmission matrix is defined as

$$\mathcal{G}(\mathbf{x}) = \begin{pmatrix} c_1^1 & c_1^2 & \cdots & c_1^N \\ c_2^1 & c_2^2 & \cdots & c_2^N \\ \vdots & \vdots & \ddots & \vdots \\ c_L^1 & c_L^2 & \cdots & c_L^N \end{pmatrix} \quad (2.1)$$

where $\mathbf{c} = c_1^1 c_1^2 \cdots c_1^N c_2^1 c_2^2 \cdots c_2^N \cdots$ is a codeword, c_t^n is a combination of input constellation symbols $\{x_1, \cdots, x_P\}$, and L is the frame length. At each time slot t , signals $c_t^n, n = 1, 2, \cdots, N, t = 1, 2, \cdots, L$, are transmitted simultaneously from the N transmit antennas. The transmission rate is defined as $R = P/L$ ($R = 1$ represents full rate).

The channel is assumed to be frequency nonselective Rayleigh, and is modeled as quasi-static, allowing fading coefficients to be constant over a block of data and changes independently from one block to another. Let $h_{n,m}, n = 1, \cdots, N, m = 1, \cdots, M$, be the path gain from transmit antenna n to receive antenna m . The path gains are modeled as samples of independent zero-mean complex Gaussian random variables with variance 0.5 per real dimension.

At time t , the signal received at antenna m , r_t^m , is given by

$$r_t^m = \sum_{n=1}^N \sqrt{\frac{E_s}{N}} h_{n,m} c_t^n + \eta_t^m \quad (2.2)$$

where E_s is the average energy per symbol and $1/N$ is the power scaling factor for each transmit antenna so that the total transmission power is normalized. The received noise components $\eta_t^m, m = 1, \cdots, M$, are independent samples of zero-mean complex Gaussian random variables with variance $\mathcal{N}_0/2$ per real dimension. Assuming the availability of perfect channel state information, the maximum likelihood receiver computes the following decision metric

$$\begin{aligned}
d &= \sum_{t=1}^L \sum_{m=1}^M \left| r_t^m - \sum_{n=1}^N \sqrt{\frac{E_s}{N}} h_{n,m} \hat{c}_t^n \right|^2 \\
&= \sum_{m=1}^M \left(\mathbf{r}_m^H - \sqrt{\frac{E_s}{N}} \mathbf{h}_m^H \mathcal{G}^H(\hat{\mathbf{c}}) \right) \left(\mathbf{r}_m - \sqrt{\frac{E_s}{N}} \mathcal{G}(\hat{\mathbf{c}}) \mathbf{h}_m \right) \\
&= \sum_{m=1}^M \left(\mathbf{r}_m^H \mathbf{r}_m - \sqrt{\frac{E_s}{N}} \mathbf{h}_m^H \mathcal{G}^H(\hat{\mathbf{c}}) \mathbf{r}_m - \sqrt{\frac{E_s}{N}} \mathbf{r}_m^H \mathcal{G}(\hat{\mathbf{c}}) \mathbf{h}_m \right. \\
&\quad \left. + \frac{E_s}{N} \mathbf{h}_m^H \mathcal{G}^H(\hat{\mathbf{c}}) \mathcal{G}(\hat{\mathbf{c}}) \mathbf{h}_m \right) \tag{2.3}
\end{aligned}$$

where $(\cdot)^H$ denotes complex conjugate transpose, $\mathbf{r}_m = [r_1^m \ r_2^m \ \cdots \ r_L^m]^T$, $\mathbf{h}_m = [h_{1,m} \ h_{2,m} \ \cdots \ h_{N,m}]^T$, and $(\cdot)^T$ denotes transpose. After comparing over all possible codewords, the receiver decides in favor of the codeword that minimizes d given in Eq. (2.3).

2.2. New Codes From Cyclic Design

Cyclic codes are easy to design across time and space domains. Because of a lack of orthogonality, interference will degrade their performance. For this reason, cyclic codes are much less attractive than orthogonal codes from Hurwitz-Radon family [37] for real symbols. For full-rate complex code design, however, cyclic codes could be very attractive because inter symbol interference in these codes may not cause a loss in diversity under some conditions, and full diversity can be achieved without constellation rotation.

2.2.1. The rank criterion

Let us review the rank criterion given in [37, 40]. Let an input symbol vector be $\mathbf{y} = [y_1 \ y_2 \ \cdots \ y_P]^T$, which generates codeword $\mathbf{e} =$

$e_1^1 \cdots e_1^N e_2^1 \cdots e_2^N \cdots e_L^1 \cdots e_L^N$. In order to achieve the maximum diversity of order NM , the difference matrix between the two code matrices corresponding to distinct input symbol vector \mathbf{x} and \mathbf{y}

$$B(\mathbf{e}, \mathbf{c}) = \begin{pmatrix} e_1^1 - c_1^1 & e_1^2 - c_1^2 & \cdots & e_1^N - c_1^N \\ e_2^1 - c_2^1 & e_2^2 - c_2^2 & \cdots & e_2^N - c_2^N \\ \vdots & \vdots & \ddots & \vdots \\ e_L^1 - c_L^1 & e_L^2 - c_L^2 & \cdots & e_L^N - c_L^N \end{pmatrix}$$

must be of full rank. If $B(\mathbf{e}, \mathbf{c})$ has a minimum rank r over the set of pairs of distinct codewords, then a diversity order of rM is achieved.

2.2.2. The determinant criterion

The determinant criterion for linear space-time codes to achieve full diversity in Rayleigh fading environments: If a square code matrix $\mathcal{G}(\mathbf{x})$ is chosen to be such that $\det(\mathcal{G}(\mathbf{x})) \neq 0$ for an arbitrary non-zero input vector \mathbf{x} (the elements of \mathbf{x} are not necessary to be constellation symbols), then the code achieves full diversity.

Proof: because of linearity, we have $B(\mathbf{e}, \mathbf{c}) = \mathcal{G}(\mathbf{y}) - \mathcal{G}(\mathbf{x}) = \mathcal{G}(\mathbf{y} - \mathbf{x})$, and $\mathbf{y} \neq \mathbf{x} \Rightarrow \det(\mathcal{G}(\mathbf{y} - \mathbf{x})) \neq 0$, therefore $B(\mathbf{e}, \mathbf{c})$ is a full-rank matrix for any pair of distinct codewords \mathbf{c} and \mathbf{e} .

A non-zero determinant is a stronger condition than the full-rank criterion for achieving full diversity. It will be interesting to analyze the determinant of the linear square orthogonal transmission matrices given in [36] and [37]:

$$\mathcal{G}_2 = \begin{pmatrix} x_1 & x_2 \\ -x_2^* & x_1^* \end{pmatrix}, \quad \mathcal{G}_4 = \begin{pmatrix} x_1 & x_2 & x_3 & x_4 \\ -x_2 & x_1 & -x_4 & x_3 \\ -x_3 & x_4 & x_1 & -x_2 \\ -x_4 & -x_3 & x_2 & x_1 \end{pmatrix},$$

$$\mathcal{G}_8 = \begin{pmatrix} x_1 & x_2 & x_3 & x_4 & x_5 & x_6 & x_7 & x_8 \\ -x_2 & x_1 & x_4 & -x_3 & x_6 & -x_5 & -x_8 & x_7 \\ -x_3 & -x_4 & x_1 & x_2 & x_7 & x_8 & -x_5 & -x_6 \\ -x_4 & x_3 & -x_2 & x_1 & x_8 & -x_7 & x_6 & -x_5 \\ -x_5 & -x_6 & -x_7 & -x_8 & x_1 & x_2 & x_3 & x_4 \\ -x_6 & x_5 & -x_8 & x_7 & -x_2 & x_1 & -x_4 & x_3 \\ -x_7 & x_8 & x_5 & -x_6 & -x_3 & x_4 & x_1 & -x_2 \\ -x_8 & -x_7 & x_6 & x_5 & -x_4 & -x_3 & x_2 & x_1 \end{pmatrix}.$$

Note that \mathcal{G}_2 is a complex code whereas \mathcal{G}_4 and \mathcal{G}_8 are real codes. The determinants of \mathcal{G}_2 , \mathcal{G}_4 , and \mathcal{G}_8 can be determined to be $\det(\mathcal{G}_2) = |x_1|^2 + |x_2|^2$, $\det(\mathcal{G}_4) = (\sum_{i=1}^4 x_i^2)^2$, and $\det(\mathcal{G}_8) = (\sum_{i=1}^8 x_i^2)^4$. Obviously, all three codes achieve full diversity.

2.2.3. New full-rate full-diversity codes from cyclic design

Based on the determinant criterion, we can design the following linear real cyclic code

$$\mathcal{H}_4 = \begin{pmatrix} x_1 & x_2 & x_3 & x_4 \\ x_4 & x_1 & x_2 & -x_3 \\ -x_3 & -x_4 & x_1 & x_2 \\ -x_2 & x_3 & x_4 & x_1 \end{pmatrix}$$

whose determinant is obtained to be $\det(\mathcal{H}_4) = (x_1^2 + x_3^2)^2 + (x_2^2 + x_4^2)^2$. Thus, this code achieves full diversity for real symbols. From Eq. (2.3), it is easy to recognize that the non-zero off-diagonal elements in $\mathcal{G}^H \mathcal{G}$ represent the ISI terms. It should be mentioned that for the nonlinear codes proposed in [63], the diagonal elements, as will be shown later in this section, may cause ISI. Eq. (2.3) also explains why existing linear orthogonal codes are ISI free. Although the two codes \mathcal{H}_4 and \mathcal{G}_4 have the same diversity order, \mathcal{H}_4 has a lower signal-to-interference-plus-noise ratio (SINR) than \mathcal{G}_4 because of the ISI terms.

To design complex cyclic codes, we minimize ISI based on the structure of \mathcal{H}_4 . Equivalently, we must maximize the number of columns that are pairwise orthogonal in the code matrix. Based on this design goal, a complex cyclic code for 4 transmit antennas is obtained as

$$\mathcal{T}_4 = \begin{pmatrix} x_1 & x_2 & x_3^* & x_4^* \\ x_4 & x_1 & x_2^* & -x_3^* \\ -x_3 & -x_4 & x_1^* & x_2^* \\ -x_2 & x_3 & x_4^* & x_1^* \end{pmatrix}. \quad (2.4)$$

in matrix \mathcal{T}_4 , the 1st column is orthogonal to the 3rd column, and the 2nd column is orthogonal to the 4th column. This code satisfies the rank criterion and provides full diversity for QPSK signals.

Let us compare the code from cyclic design given in (2.4) with the quasi-orthogonal code given in [46]

$$\mathcal{A}_4 = \begin{pmatrix} x_1 & x_2 & x_3 & x_4 \\ -x_2^* & x_1^* & -x_4^* & x_3^* \\ -x_3^* & -x_4^* & x_1^* & x_2^* \\ x_4 & -x_3 & -x_2 & x_1 \end{pmatrix}.$$

It follows easily that

$$\mathcal{T}_4^H \mathcal{T}_4 = \begin{pmatrix} a & b_1 & 0 & b_2 \\ b_1^* & a & -b_2 & 0 \\ 0 & -b_2^* & a & b_1^* \\ b_2^* & 0 & b_1 & a \end{pmatrix} \quad (2.5)$$

and

$$\mathcal{A}_4^H \mathcal{A}_4 = \begin{pmatrix} a & 0 & 0 & b_3 \\ 0 & a & -b_3 & 0 \\ 0 & -b_3^* & a & 0 \\ b_3^* & 0 & 0 & a \end{pmatrix} \quad (2.6)$$

where $a = |x_1|^2 + |x_2|^2 + |x_3|^2 + |x_4|^2$, $b_1 = x_1^*x_2 + x_1x_4^* + x_3^*x_4 - x_2^*x_3$, $b_2 = x_1^*x_4^* - x_3^*x_4^* - x_2^*x_3^* - x_1^*x_2^*$, $b_3 = x_1^*x_4 + x_1x_4^* - x_2x_3^* - x_2^*x_3$. Terms b_1 and b_2 are the ISI terms for the proposed code from cyclic design, and b_3 is the ISI term for the quasi-orthogonal code. For QPSK symbols, b_1 and b_2 do not cause a loss in the diversity of the proposed cyclic code, but b_3 reduces the diversity order of the quasi-orthogonal code. Note that b_3 can be expressed as $b_3 = f(x_1, x_4) + f(x_2, x_3)$, a sum of two independent functions. Therefore, we can decode (x_1, x_4) and (x_2, x_3) independently for the quasi-orthogonal code without degrading performance. For the cyclic code, however, the decoding complexity cannot be reduced even though there is no ISI between x_1 and x_3 or between x_2 and x_4 .

2.3. Numerical Results and Discussion

In this section, we simulate the performance of the proposed cyclic code, and compare it with that of the quasi-orthogonal code and the nonlinear code given

in [63]. The nonlinear orthogonal code also provides full rate and full diversity for QPSK signals. Its code matrix is given as

$$\mathcal{O}_4 = \begin{pmatrix} x_1 & x_2 & x_3 & x_4 \\ -x_2^* & x_1^* & -x_4^* & x_3^* \\ -z_1^* & z_2 & x_1^* & -x_2 \\ -z_2^* & -z_1 & x_2^* & x_1 \end{pmatrix}$$

where $z_1 = \text{Re}\{x_3\} + j\text{Im}\{2x_1x_2x_4^*\}$ and $z_2 = x_1^{*2}x_4 + x_2^2x_4^* + x_1^*x_2x_3 - x_1^*x_2x_3^*$. The orthogonality of \mathcal{O}_4 is achieved by introducing nonlinearity. As a result, the diagonal elements of $\mathcal{O}_4^H \mathcal{O}_4$ cause ISI. The nonlinear code requires the constellation to be $(1/\sqrt{2})e^{j(\frac{\pi}{4}+k\frac{\pi}{2})}$, $k = 0, \dots, 3$. This is because with this particular choice of the constellation, y_1 and y_2 , although a function of x_1, \dots, x_4 , still belong to the same constellation. Thus, the constellation is not be expanded.

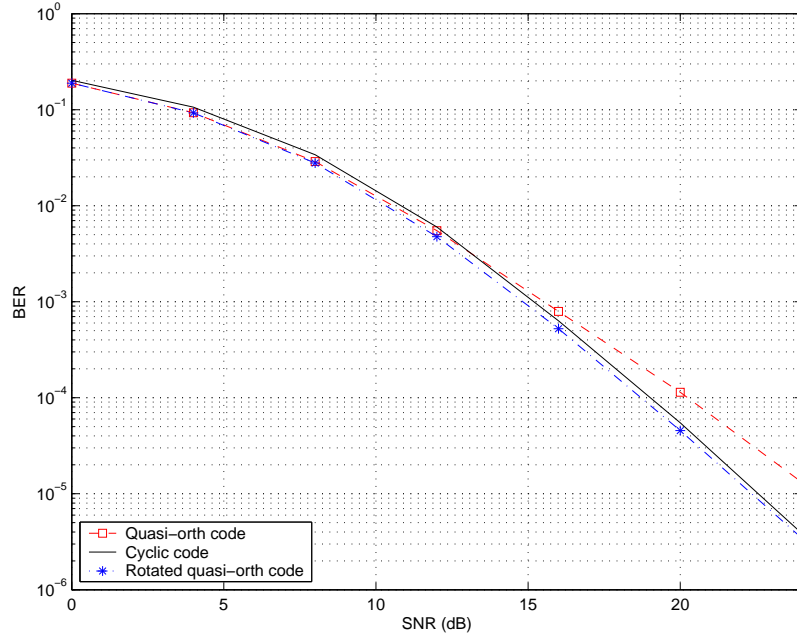


FIGURE 2.1. Error performance of cyclic code ($N = 3$, $M = 1$, QPSK)

Fig. 2.1 shows the error performance curves the proposed code, the quasi-orthogonal code, and the quasi-orthogonal code with optimal constellation rotation (optimal angle is $\pi/6$, see [48]) for a QPSK system with 3 transmit antennas and 1 receive antenna operating at 2 bits/s/Hz. Code matrices for the quasi-orthogonal design and for the cyclic design are chosen as, respectively, the first 3 columns of \mathcal{A}_4 and the first 3 columns of \mathcal{T}_4 . Error performance results of various codes including the nonlinear code proposed in [63] for a QPSK system with 4 transmit antennas and 1 receive antenna operating at 2 bits/s/Hz are shown in Fig. 2.2.

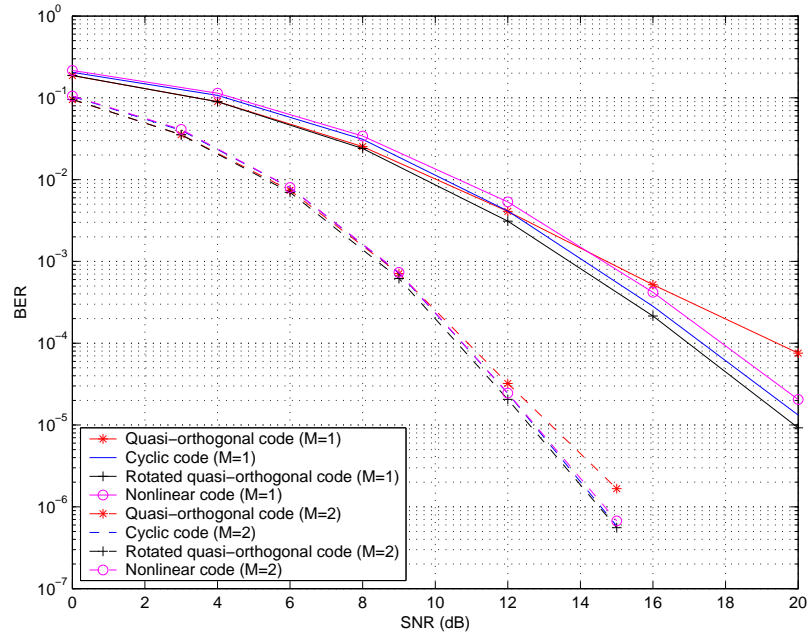


FIGURE 2.2. Error performance of cyclic code ($N = 4, M = 1, 2$, QPSK)

It is observed from Figs. 2.1 and 2.2 that the slopes of SNR versus bit-error-rate curves of the proposed cyclic code and the quasi-orthogonal code with optimal constellation rotation are the same. Therefore, both codes achieve the same diversity order. The quasi-orthogonal code without rotation is found to

provide only partial diversity. The cyclic code always provides better performance than the nonlinear code. In the low SNR region, quasi-orthogonal codes (with or without constellation rotation) perform slightly better than the cyclic code because quasi-orthogonal codes have less ISI (see Eqs. (2.5 and 2.6)). At high SNR values, the cyclic code outperforms the unrotated quasi-orthogonal code. It is also observed that the three types of codes with full diversity have comparable performance when there are two receive antennas.

2.4. Conclusion

We proposed a cyclic coding scheme for QPSK systems with three or four transmit antennas. The proposed codes achieve full rate and full diversity without requiring constellation rotation. Compared with the nonlinear code, the proposed cyclic code has a lower encoding complexity (decoding complexity is the same) and always performs better. The proposed code construction method could be applied to design rate-one, full-diversity, complex cyclic codes for systems with an arbitrary number of transmit antennas.

3. OPTIMAL ROTATION ANGLES FOR QUASI-ORTHOGONAL SPACE-TIME CODES WITH PSK MODULATION

To achieve full diversity for quasi-orthogonal codes, constellation rotation schemes were proposed in [48, 49]. Optimal rotation angles in the sense of maximizing coding gain for quadrature amplitude modulation (QAM) were addressed in [49]. In [64], optimal rotation angles for PSK with an even constellation size were derived. In this chapter, we derive, through a geometry-based approach, the optimal rotation angles for quasi-orthogonal codes with any PSK modulation. The independent work [65] also addressed the optimal rotation angles using a completely different approach. In addition to the optimal rotation angles, We also prove that coding gain for even-sized constellations is higher than that for odd-sized constellations, which was observed but not proved in [65].

3.1. Optimal constellation rotation for PSK

We focus on the scheme given in [47] for systems with four transmit antennas for which the code matrix is expressed as

$$\mathbf{C} = \begin{bmatrix} x_1 & x_2 & x_3 & x_4 \\ -x_2^* & x_1^* & -x_4^* & x_3^* \\ x_3 & x_4 & x_1 & x_2 \\ -x_4^* & x_3^* & -x_2^* & x_1^* \end{bmatrix}, \text{ and } \mathbf{C}^H \mathbf{C} = \begin{bmatrix} a & 0 & b & 0 \\ 0 & a & 0 & b \\ b & 0 & a & 0 \\ 0 & b & 0 & a \end{bmatrix}, \text{ where } (\cdot)^* \text{ denotes}$$

complex conjugate, $(\cdot)^H$ denotes conjugate transpose, $a = \sum_{i=1}^4 |x_i|^2$, and $b = x_1 x_3^* + x_3 x_1^* + x_2 x_4^* + x_4 x_2^*$. Analysis for other quasi-orthogonal codes (e.g., the code given in [46]) is similar.

The maximum likelihood decision metric for this code can be written as the sum of two independent terms $f_1(x_1, x_3) + f_2(x_2, x_4)$. Thus, the minimization

for ML decoding can be done separately on these two terms. For the code example chosen above, let us consider (x_1, x_3) and let $x_2 = x_4 = 0$ [48] in calculating the optimal rotation angles.

Let \mathcal{A} be a PSK constellation of size Q , where Q could be even ($Q = 2n$, $n > 0$ is an integer) or odd ($Q = 2n - 1$, $n > 1$), and \mathcal{B} be the rotated constellation of \mathcal{A} expressed as $\mathcal{B} = e^{j\phi}\mathcal{A}$, where ϕ represents the rotation angle. Also let $x_1, \tilde{x}_1 \in \mathcal{A}$ and $x_3, \tilde{x}_3 \in \mathcal{B}$, where $(x_1, x_3) \neq (\tilde{x}_1, \tilde{x}_3)$. Maximizing coding gain is equivalent to maximizing $|\det[\Delta_{C(x_1,0,x_3,0)}^H \Delta_{C(x_1,0,x_3,0)}]|$, where $|\cdot|$ denotes the absolute value and $\Delta_{C(x_1,0,x_3,0)}$ is the difference matrix given as $\Delta_{C(x_1,0,x_3,0)} = \mathbf{C}_{(x_1,0,x_3,0)} - \mathbf{C}_{(\tilde{x}_1,0,\tilde{x}_3,0)}$. This is also equivalent to maximizing the minimum ζ -distance between constellations \mathcal{A} and \mathcal{B} expressed as Eq. (23) in [49]

$$d_{\min,\zeta}(\mathcal{A}, \mathcal{B}) \triangleq \underbrace{\min}_{(x_1, x_3) \neq (\tilde{x}_1, \tilde{x}_3)} |(x_1 - \tilde{x}_1)^2 - (x_3 - \tilde{x}_3)^2|^{\frac{1}{2}}. \quad (3.1)$$

the set of values of $(x_1 - \tilde{x}_1)^2$ with $x_1, \tilde{x}_1 \in \mathcal{A}$ and $(x_3 - \tilde{x}_3)^2$ with $x_3, \tilde{x}_3 \in \mathcal{B}$ constitute, respectively, constellation \mathcal{X} and constellation $\mathcal{Y} = e^{j2\phi}\mathcal{X}$. Note that both \mathcal{X} and \mathcal{Y} include the origin. The optimal rotation angle in the sense of maximizing coding gain must maximize the minimum distance between any point from \mathcal{X} and any point from \mathcal{Y} , except the origin.

Before calculating the optimal rotation angles, let us examine the properties of \mathcal{X} . Examples of an even-sized constellation \mathcal{A} (16PSK) and an odd-sized constellation \mathcal{A} (7PSK) are shown in Fig. 3.1 and Fig. 3.2, respectively.

The corresponding new constellations \mathcal{X} formed by the set of values of $(x_1 - \tilde{x}_1)^2$ with $x_1, \tilde{x}_1 \in \mathcal{A}$ are shown in Fig. 3.3 and Fig. 3.4, respectively. In the following discussion, we exclude the origin in \mathcal{X} because if $x_1 - \tilde{x}_1 = 0$ or $x_3 - \tilde{x}_3 = 0$, $|(x_1 - \tilde{x}_1)^2 - (x_3 - \tilde{x}_3)^2|^{1/2}$ becomes a constant for any rotation

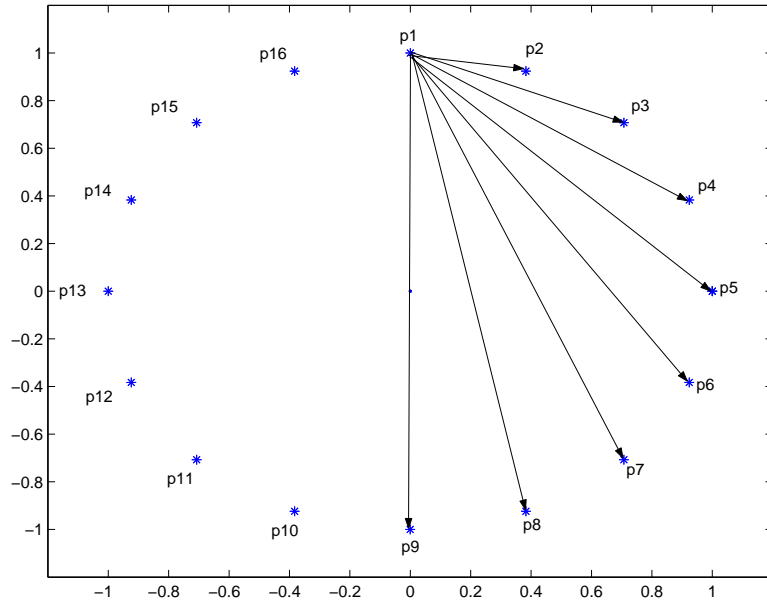


FIGURE 3.1. An example of an even-sized constellation \mathcal{A} : 16PSK.

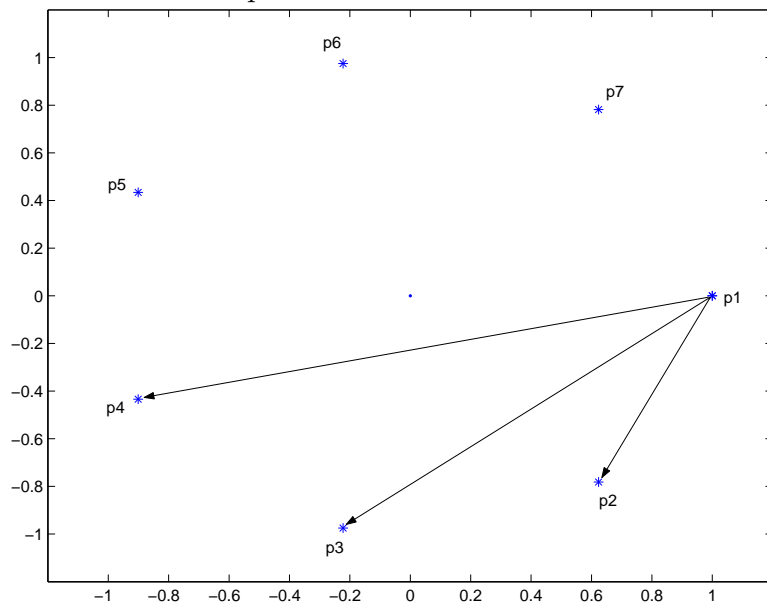


FIGURE 3.2. An example of an odd-sized constellation \mathcal{A} : 7PSK.

angle. Let $P = Q/2$ when Q is an even number and $P = (Q - 1)/2$ when Q

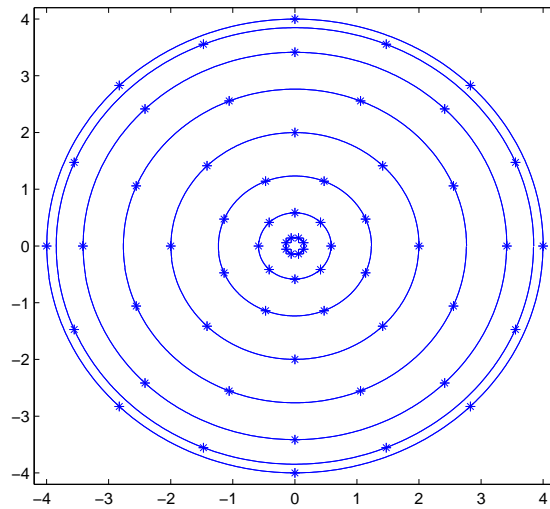


FIGURE 3.3. Constellation \mathcal{X} formed by $(x_1 - \tilde{x}_1)^2$, where $x_1, \tilde{x}_1 \in \mathcal{A}$ as shown in Fig. 3.1

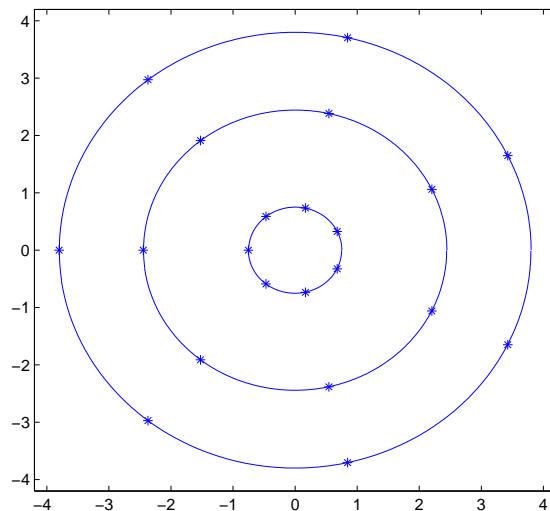


FIGURE 3.4. Constellation \mathcal{X} formed by $(x_1 - \tilde{x}_1)^2$, where $x_1, \tilde{x}_1 \in \mathcal{A}$ as shown in Fig. 3.2

($Q \geq 3$) is an odd number. In the following proofs, we focus on the case when Q is an even number. The proof when Q is an odd number is similar.

Properties of \mathcal{X} :

1. All points in \mathcal{X} can be divided into P groups, S_1, S_2, \dots, S_P , based on their relative magnitudes in ascending order as $|S_1| < |S_2| < \dots < |S_P|$.

Proof: It is easy to see from Fig. 3.1 that for all possible combinations of $x_1, \tilde{x}_1 \in \mathcal{A}$ and $x_1 \neq \tilde{x}_1$, $|x_1 - \tilde{x}_1|$ has $Q/2$ distinct values. Additionally, the group with the minimum magnitude is formed by two adjacent points in \mathcal{A} such as $x_1 = p_1$ and $\tilde{x}_1 = p_2$. The minimum magnitude is thus obtained to be $|S_1| = |p_2 - p_1|^2 = 2 - 2 \cos(2\pi/Q)$. Obviously, we have $d_{\min, \zeta}(\mathcal{A}, \mathcal{B}) \leq |S_1|^{1/2}$.

2. The distance between any two points from two different groups is greater than or equal to $|S_1|$ when Q is an even number and greater than $|S_1|$ when Q is an odd number.

Proof: Consider the worst case where two points from two adjacent groups have the same phase. The distance between these two points is $|S_i| - |S_{i-1}|$. From Fig. 3.1, it is easy to see that sides $\sqrt{|S_1|}, \sqrt{|S_{i-1}|}$, and $\sqrt{|S_i|}$ always constitute a triangle. Additionally, the angle opposite $\sqrt{|S_i|}$ is an obtuse angle or right angle (e.g., $\angle p_1 p_7 p_8$ is an obtuse angle and $\angle p_1 p_8 p_9$ is a right angle). Thus, we have $|S_i| - |S_{i-1}| \geq |S_1|$ with equality if and only if the triangle is a right triangle.

For the example shown in Fig. 3.3, the distance between the two outer circles equals the radius of the inner circle.

3. There are exactly $Q/2$ ($Q = 2n$) or Q ($Q = 2n - 1$) different points in each of the P groups, S_1, S_2, \dots, S_P , and the phases of all points in any group are uniformly distributed between 0 and 2π .

Proof: We prove using group S_1 as an example. The same method applies to other groups. All points in S_1 are listed as

$$\begin{aligned} (p_2 - p_1)^2 &= e^{j\pi}(e^{-j2\pi/Q} - 1)^2 \\ &\vdots \\ (p_Q - p_{Q-1})^2 &= e^{-j4\pi(Q-2)/Q} \cdot e^{j\pi}(e^{-j2\pi/Q} - 1)^2 \\ (p_1 - p_Q)^2 &= e^{-j4\pi(Q-1)/Q} \cdot e^{j\pi}(e^{-j2\pi/Q} - 1)^2. \end{aligned}$$

It is found that the phase difference between any two adjacent points in S_1 is $4\pi/Q$ when Q is an even number, and is $2\pi/Q$ when Q is an odd number.

3.1.1. The optimal rotation angles

According to properties 1-3 of constellation \mathcal{X} , the optimal rotation angle for quasi-orthogonal codes with PSK modulation is π/Q when Q is even and $\pi/(2Q)$ when Q is odd.

Proof: If we let $\phi = \pi/Q$, constellation \mathcal{Y} is related to constellation \mathcal{X} as $\mathcal{Y} = e^{j2\phi}\mathcal{X} = e^{j2\pi/Q}\mathcal{X}$. According to property 3 of \mathcal{X} , the minimum distance between any two points $s \in S_i$ and $\tilde{s} \in e^{j2\pi/Q}S_i$ is maximized. Additionally, from property 2 of \mathcal{X} , the minimum distance between $\alpha \in S_i$ and $\beta \in e^{j2\pi/Q}S_j$, $i \neq j$, is always greater than or equal to $|S_1|$. Therefore, the minimum ζ -distance is determined by $|S_1|$, and $\phi = \pi/Q$ is the optimal rotation angle that maximizes $d_{\min,\zeta}(\mathcal{A}, \mathcal{B})$ when Q is even. Following a similar procedure, we

can prove the conclusion for odd-sized constellations. Note that rotation with $\phi = \pi/Q$ odd-sized constellations does not even provide full diversity ([66], Theorem 2.2). This is clear from Fig. 3.4: if $\mathcal{Y} = e^{j2\pi/Q}\mathcal{X}$, then \mathcal{Y} and \mathcal{X} overlap and $|(x_1 - \tilde{x}_1)^2 - (x_3 - \tilde{x}_3)^2|^{\frac{1}{2}}$ could be zero.

The corresponding optimal minimum ζ -distance is

$$d_{\min,\zeta}(\mathcal{A}, \mathcal{B}) = \begin{cases} \min \left(\left| 2|S_1|^2(1 - \cos(\frac{2\pi}{Q})) \right|^{\frac{1}{4}}, |S_1|^{\frac{1}{2}} \right), & Q = 2n \\ \min \left(\left| 2|S_1|^2(1 - \cos(\frac{\pi}{Q})) \right|^{\frac{1}{4}}, |S_1|^{\frac{1}{2}} \right), & Q = 2n - 1 \end{cases}$$

the above expression can be simplified as

$$d_{\min,\zeta}(\mathcal{A}, \mathcal{B}) = \begin{cases} 2 \sin\left(\frac{\pi}{Q}\right), & Q = 2, 4 \\ \sqrt{8 \sin^3\left(\frac{\pi}{Q}\right)}, & Q = 2n \geq 6 \\ \sqrt{8 \sin\left(\frac{\pi}{2Q}\right) \sin^2\left(\frac{\pi}{Q}\right)}, & Q = 2n - 1 \end{cases} \quad (3.2)$$

for the specific case of 8PSK ($Q = 8$), the optimal rotation angle based on the conclusion in this letter is $\phi = \pi/8$ and the minimum ζ -distance is 0.6696, which are the same as the results obtained via computer search in [49].

3.1.2. Relative coding gain between $Q = 2n$ and $Q = 2n - 1$

Proposition 1: The cases of $Q = 2n, n \geq 3$, have larger optimal minimum ζ -distances than those of $Q = 2n - 1$. Mathematically, *Proposition 1* is expressed as

$$\sin^3\left(\frac{\pi}{2n}\right) - \sin\left(\frac{\pi}{2(2n-1)}\right) \sin^2\left(\frac{\pi}{2n-1}\right) > 0. \quad (3.3)$$

Before proving *Proposition 1*, let us prove the following inequality:

$$x > \sin(x) > x - x^3/6, \quad \text{for } x > 0. \quad (3.4)$$

Let $f_1(x) = x - \sin(x)$ and $f_2(x) = \sin(x) - x + x^3/6$. Obviously, $f_1(x)|_{x=0} = 0$ and $f_1'(x) \geq 0, \forall x > 0$, where $(\cdot)'$ denotes derivative. Thus, the left inequality of (3.4) follows. The derivative of $f_2(x)$ with respect to x is written as

$$\begin{aligned} f_2'(x) &= \cos(x) - 1 + \frac{x^2}{2} \\ &= 2 \left[\left(\frac{x}{2}\right)^2 - \sin^2\left(\frac{x}{2}\right) \right] > 0. \end{aligned} \quad (3.5)$$

Thus, the right inequality of (3.4) follows.

Let $\xi_1 = \left[\frac{\pi}{2n} - \frac{(\pi/(2n))^3}{6} \right]^3$ and $\xi_2 = \frac{\pi}{2(2n-1)} \left(\frac{\pi}{2n-1} \right)^2$. For $n \geq 3$

$$\xi_1 - \xi_2 = (n + 0.92)(n - 0.36)(n - 2.98) > 0.$$

Notice that from (3.4) we have

$$\begin{aligned} \xi_1 &< \sin^3\left(\frac{\pi}{2n}\right) \\ \xi_2 &> \sin\left(\frac{\pi}{2(2n-1)}\right) \sin^2\left(\frac{\pi}{2n-1}\right). \end{aligned}$$

Thus, *Proposition 1* expressed in (3.3) is proved.

3.2. Conclusion

We have derived, using a geometry-based method, the optimal constellation rotation angles for quasi-orthogonal space-time block codes for four-antenna systems with PSK modulation. Through constellation rotation with these rotation angles, the coding gain is maximized and full diversity of quasi-orthogonal codes is achieved. We have also proved that PSK signals with a constellation size $Q = 2n$ have larger optimal minimum ζ -distances than those with a constellation size $Q = 2n - 1$ ($n \geq 3$).

4. RATE-ONE SPACE-TIME BLOCK CODES WITH FULL DIVERSITY

Multipath fading could severely degrade the performance of wireless communication systems. As an effective method to combat the effects of fading, transmit diversity has been studied extensively in the past many years. The transmit diversity scheme proposed by Alamouti [36] is a simple and effective orthogonal space-time block code of rate one for systems with two transmit antennas. Because of its simplicity in implementation and the feasibility of having multiple antennas at the base station, this scheme has been deployed in existing mobile communications systems. In [37], Tarokh *et al.* extended the orthogonal design to systems with an arbitrary number of transmit antennas and provided a class of rate-one real orthogonal codes. It was also proved that complex orthogonal design with transmission rate one does not exist for more than two transmit antennas (see [37] and [45] for nonsquare designs). In [96] Boariu *et al.* discussed a method to construct a class of rate-one nonorthogonal space-time block codes with partial diversity. Real Hadamard matrices played a key role in the scheme proposed in [96]. A class of quasi-orthogonal space-time block codes for systems with four transmit antennas was proposed in [46, 47, 67]. These quasi-orthogonal codes provide partial diversity but transmission rate one. To achieve full diversity for quasi-orthogonal codes for four transmit antennas, constellation rotation schemes were proposed in [48, 49]. Compared with the space-time block codes in [97–99], quasi-orthogonal codes result in constant power for each transmit antenna with constant amplitude modulation, which is desirable for practical implementation. Sethuraman *et al.* proposed a family of rate one space-time block codes from division algebras [68], which also provide full diversity and constant transmit power

for any number of transmit antennas. However, division algebra codes have higher decoding complexities and lower coding gains than quasi-orthogonal codes.

In this chapter, we provide a systematic method for designing rate-one codes, real or complex, with full diversity and minimum inter-symbol interference (ISI)¹ for a general multiple-input multiple-output (MIMO) system. Through this systematic method, existing quasi-orthogonal codes for four or less transmit antennas are extended to systems with a larger number of transmit antennas. The proposed code structures are based on the real orthogonal codes given in [37] and can be used for both real and complex signals. Although the codes derived are nonorthogonal for complex signals, the orthogonality property is used in the ISI minimization process. Because of ISI, the decoder for these nonorthogonal codes is more complex than that for orthogonal codes. Thus, we provide a generalized reduced-complexity decoding algorithm for the proposed codes. This decoding method can also be applied for orthogonal codes.

4.1. System Model

We consider a wireless communication system with N transmit antennas in the base station and M receive antennas in the remote. The transmission matrix is expressed as

¹Note that ISI here refers to the mutual interference among input symbols transmitted from different antennas and different time slots within a frame.

$$\mathbf{G} = \begin{bmatrix} c_1^1 & c_1^2 & \dots & c_1^N \\ c_2^1 & c_2^2 & \dots & c_2^N \\ \vdots & \vdots & \ddots & \vdots \\ c_L^1 & c_L^2 & \dots & c_L^N \end{bmatrix} \quad (4.1)$$

where $c_l^n, l = 1, \dots, L, n = 1, \dots, N$, is the symbol transmitted from antenna n at time l . Generally, elements of \mathbf{G} are linear combinations of input symbols (s_1, s_2, \dots, s_K) and their complex conjugates. For most widely used codes, however, each element of \mathbf{G} is related to a single input symbol s_k (e.g., $s_k e^{j\phi}$, $\phi \in [0, 2\pi)$). The codes given in [36, 37, 46, 47, 67, 68] are all of this type, which is also our focus in this chapter. Note that complex conjugate and sign change of s_k are special cases of $s_k e^{j\phi}$. The code rate is defined as $R = K/L$. At time slot l , signals $\{c_l^1, \dots, c_l^N\}$ are transmitted simultaneously from the N transmit antennas, and the average power of data streams from each transmit antenna is normalized to $1/N$.

We consider a frequency-nonselective Rayleigh fading channel. Thus, the path gain from transmit antenna n to receive antenna m , denoted as $h_{n,m}$, is modeled as samples of independent complex zero-mean Gaussian random variables (RVs) with variance 0.5 per real dimension. The wireless channel is assumed to be quasi-static so that the path gains are constant over a frame of length L and change independently from one frame to another.

Let the received signal by antenna m at time l be r_l^m . The receiver model is expressed by

$$\mathbf{R} = \sqrt{\frac{\rho}{N}} \mathbf{G} \mathbf{H} + \mathbf{W} \quad (4.2)$$

where $\mathbf{R} = \{r_l^m\}_{1 \leq l \leq L, 1 \leq m \leq M}$ is the $L \times M$ received signal matrix, $\mathbf{H} = \{h_{n,m}\}_{1 \leq n \leq N, 1 \leq m \leq M}$ is the $N \times M$ channel fading coefficient matrix, $\mathbf{W} = \{w_l^m\}_{1 \leq l \leq L, 1 \leq m \leq M}$ is the $L \times M$ additive noise matrix whose elements are samples of independent zero-mean complex Gaussian RVs with variance $1/2$ per real dimension, and ρ is the signal-to-noise ratio (SNR) per receive antenna.

With perfect channel state information, the maximum likelihood (ML) receiver computes metric

$$d = \left\| \mathbf{R} - \sqrt{\frac{\rho}{N}} \mathbf{G} \mathbf{H} \right\|_{\text{F}}^2 \quad (4.3)$$

over all possible transmitted signal sets (s_1, s_2, \dots, s_K) and decides in favor of the set that minimizes d ($\|\cdot\|_{\text{F}}$ stands for Frobenius norm).

4.2. Generalized Quasi-Orthogonal Codes

4.2.1. Code construction

Since our focus is on codes for which each element of \mathbf{G} is related to a single input symbol, it is clear from (4.3) that $\mathbf{G}^H \mathbf{G}$ ($(\cdot)^H$ stands for conjugate transpose) is the only source of ISI. If all off-diagonal elements of $\mathbf{G}^H \mathbf{G}$ are zero, the transmission is ISI free. Thus, the orthogonal design (columns of \mathbf{G} are mutually orthogonal) has zero ISI, and all transmitted symbols for such design can be separated by using a maximum likelihood decoder.

To minimize ISI in rate-one design, we could maximize the number of zero off-diagonal elements, as all nonzero off-diagonal elements of $\mathbf{G}^H \mathbf{G}$ have the same statistics and therefore contributes the same amount of ISI. Quasi-orthogonal codes are constructed based on maximizing the number of orthogonal column

pairs in the code matrix. Quasi-orthogonality should hold for any complex input symbols, not just some specific complex symbols. Additionally, for real symbols the code matrix should be an orthogonal matrix so that it is suitable for both real and complex symbols. Thus, the proposed code has the same structure as the real orthogonal codes given in [37], but differs in that some elements are changed to their conjugates. Before detailing the systematic construction method for the type of codes described in the beginning of Section 4.2.1, let us prove two propositions.

Proposition 1: Any two column vectors that are both orthogonal to the third column vector must be nonorthogonal to each other.

Proof: Recall that we only consider code matrices each entry of which is related to a single input symbol. For rate-one transmission with constant power, a necessary condition to achieve full diversity without feedback is that each input symbol appears in each row and each column of the code matrix only once. Consider three column vectors \mathbf{a} , \mathbf{b} , and \mathbf{c} . If \mathbf{a} is orthogonal to \mathbf{b} and \mathbf{a} contains any input symbol s_k , then \mathbf{b} must contain s_k^* , where $(\cdot)^*$ stands for complex conjugate. For the same reason, s_k^* must appear once in \mathbf{c} . Since both \mathbf{b} and \mathbf{c} contain s_k^* , they are nonorthogonal to each other. An indirect proof is that if *Proposition 1* were assumed not true, then one should find three mutually orthogonal columns. This implies that a rate-one complex orthogonal design for 3 transmit antennas exists, which leads to a conclusion that contradicts the theorem given in [37] (Theorem 5.4.2)].

Proposition 2: The maximum number of orthogonal column pairs of a $K \times N$ code matrix is $(N/2)^2$ when N is even and $(N^2 - 1)/4$ when N is odd.

Proof: With the restrictions of the design being considered, the code matrix has a size of $K \times N$ ($K = L$ for rate-one design). Consider a complex rate-one code matrix. Without loss of generality, we assume that the first column is orthogonal

to a maximum of α other columns. To maximize the total number of orthogonal column pairs, we could let each of the remaining $N - \alpha - 1$ columns be orthogonal to all of the α columns. According to *Proposition 1*, the total number of orthogonal column pairs is $\alpha(N - \alpha)$. Let $f(\alpha) = \alpha(N - \alpha)$. It is easy to determine the maximum values of $f(\alpha)$ for integer α in the range $1 \leq \alpha \leq N - 1$. These values are found to be $(N/2)^2$ for even N and $(\frac{N-1}{2} \times \frac{N+1}{2})$ for odd N , which can be realized by dividing all columns into two groups and making any column of one group orthogonal to all columns of the other group. The number of columns in the two groups must be kept $(N - 1)/2$ and $(N + 1)/2$ for odd N , and $N/2$ for even N .

For complex codes, rate-one design can be generalized by fixing the positions and signs of the symbols in the real orthogonal design and then changing half (the top half, the bottom half, or the middle half) of all rows to their complex conjugates. Let us consider changing the top half as an example. For square rate-one real orthogonal codes when K is an integer power of 2, we can always partition

$$\mathbf{G} = \begin{bmatrix} \mathbf{G}_{-(1 \dots K/2)}^a & \mathbf{G}_{-(K/2+1 \dots K)}^a \\ \mathbf{G}_{-(K/2+1 \dots K)}^b & \mathbf{G}_{-(1 \dots K/2)}^b \end{bmatrix} \text{ for real design, and}$$

$$\mathbf{G} = \begin{bmatrix} \mathbf{G}_{-(1 \dots K/2)}^{a*} & \mathbf{G}_{-(K/2+1 \dots K)}^{a*} \\ \mathbf{G}_{-(K/2+1 \dots K)}^b & \mathbf{G}_{-(1 \dots K/2)}^b \end{bmatrix} \text{ for complex design.}$$

Consequently, any column in the left half of \mathbf{G} is orthogonal to any column in its right half. This method thus maximizes the number of orthogonal column pairs according to *Proposition 2*. Similarly, we can prove that changing the bottom half or the middle half of all rows also achieves the maximum number of orthogonal column pairs. Although different choices of these rows will affect the positions of the nonzero elements in $\mathbf{G}^H \mathbf{G}$, the total number of nonzero elements is the same. Therefore, these codes have the same performance.

We provide below a few examples of complex rate-one codes obtained by applying the proposed method. These codes are based on changing the middle rows of the real codes presented in [37] as

$$\mathbf{G}_4 = \begin{bmatrix} s_1 & s_2 & s_3 & s_4 \\ -s_2^* & s_1^* & -s_4^* & s_3^* \\ -s_3^* & s_4^* & s_1^* & -s_2^* \\ -s_4 & -s_3 & s_2 & s_1 \end{bmatrix},$$

$$\mathbf{G}_8 = \begin{bmatrix} s_1 & s_2 & s_3 & s_4 & s_5 & s_6 & s_7 & s_8 \\ -s_2 & s_1 & s_4 & -s_3 & s_6 & -s_5 & -s_8 & s_7 \\ -s_3^* & -s_4^* & s_1^* & s_2^* & s_7^* & s_8^* & -s_5^* & -s_6^* \\ -s_4^* & s_3^* & -s_2^* & s_1^* & s_8^* & -s_7^* & s_6^* & -s_5^* \\ -s_5^* & -s_6^* & -s_7^* & -s_8^* & s_1^* & s_2^* & s_3^* & s_4^* \\ -s_6^* & s_5^* & -s_8^* & s_7^* & -s_2^* & s_1^* & -s_4^* & s_3^* \\ -s_7 & s_8 & s_5 & -s_6 & -s_3 & s_4 & s_1 & -s_2 \\ -s_8 & -s_7 & s_6 & s_5 & -s_4 & -s_3 & s_2 & s_1 \end{bmatrix}.$$

The Alamouti scheme can be considered as a special case of the proposed design. By changing the last row of the real orthogonal matrix $\begin{bmatrix} s_1 & s_2 \\ -s_2 & s_1 \end{bmatrix}$, we

obtain the complex design $\mathbf{G}_2 = \begin{bmatrix} s_1 & s_2 \\ -s_2^* & s_1^* \end{bmatrix}$, which is the Alamouti scheme. Note that orthogonality still holds for this 2×2 complex code. The design \mathbf{G}_4 from the proposed method and the code matrix for four transmit antennas given in [46],

$\mathbf{A}_4 = \begin{bmatrix} s_1 & s_2 & s_3 & s_4 \\ -s_2^* & s_1^* & -s_4^* & s_3^* \\ -s_3^* & -s_4^* & s_1^* & s_2^* \\ s_4 & -s_3 & -s_2 & s_1 \end{bmatrix}$, have the same performance for complex signals as

$\mathbf{G}_4^H \mathbf{G}_4$ and $\mathbf{A}_4^H \mathbf{A}_4$ have an equal number of nonzero elements and these nonzero elements have identical statistical properties (mean and variance). However, the transmission matrix in [46] does not completely eliminate ISI for real input signals whereas the proposed design does. Additionally, the proposed design can be applied to systems with an arbitrary number of transmit antennas, whereas the Jafarkhani scheme [46] is restricted to systems with four transmit antennas.

4.2.2. Generalized fast decoding

As it is well known, orthogonal codes can be decoded symbol by symbol. In other words, other symbols do not cause any interference in the process of decoding a particular symbol. Therefore, to decode any symbol, all other symbols can be assumed to be zero in the code matrix without performance loss. For example, to decode s_1 for the Alamouti scheme, one could let $s_2 = 0$ so that the code matrix becomes $\begin{bmatrix} s_1 & 0 \\ 0 & s_1^* \end{bmatrix}$. The decision variable for s_1 is obtained as $\hat{s}_1 = \sum_{m=1}^M (h_{1,m}^* r_1^m + h_{2,m} r_2^{m*})$, which is the same as the result derived in [36]. Applying this technique to various types of orthogonal codes (e.g., rate 1, 1/2, or 3/4 codes), one can easily find the decision variable without the lengthy calculation that is otherwise needed. Similarly, for quasi-orthogonal codes such as \mathbf{G}_8 , group (s_1, s_2, s_7, s_8) can be decoded by letting $s_3 = s_4 = s_5 = s_6 = 0$. For large-size constellations, complexity even with the fast ML decoding algorithm could still be very high. In this case, the sphere decoder (lattice decoder) [69] could be applied after the generalized fast ML decoder to further lower complexity.

4.2.3. Optimal constellation rotation for quasi-orthogonal codes

Constellation rotation for 4×4 codes has been addressed in [48, 49]. Thus, we only consider \mathbf{G}_8 in this letter. Consider $\mathbf{G}_{8_{(1,2,7,8)}}$, which is formed by letting $s_3 = s_4 = s_5 = s_6 = 0$ in \mathbf{G}_8 . The minimum rank of $\mathbf{G}_{8_{(1,2,7,8)}}(\mathcal{S}) - \mathbf{G}_{8_{(1,2,7,8)}}(\tilde{\mathcal{S}})$ is 4 for some common modulation schemes such as phase-shift keying (PSK) and quadrature amplitude modulation (QAM), where $\mathcal{S} = [s_1, s_2, s_7, s_8]^T$. Therefore, \mathbf{G}_8 only provides a diversity order 4 without constellation rotation. Full diversity can be achieved by constellation rotation only if the determinant of $\mathbf{G}_{8_{(1,2,7,8)}}(\mathcal{S}) - \mathbf{G}_{8_{(1,2,7,8)}}(\tilde{\mathcal{S}})$ is always nonzero.

For quasi-static flat Rayleigh fading channels, the upper bound of the pairwise error probability is given as [49, 40]

$$P(\mathbf{G} \rightarrow \tilde{\mathbf{G}}) \leq \frac{1}{2} \left(\prod_{i=1}^r \lambda_i \right)^{-M} \left(\frac{\rho}{4N} \right)^{-rM} \quad (4.4)$$

where \mathbf{G} and $\tilde{\mathbf{G}}$ are two different but arbitrarily chosen code matrices, $r = \min(\text{rank}(\mathbf{G} - \tilde{\mathbf{G}}))$ is the diversity order, and $\lambda_1, \lambda_2, \dots, \lambda_r$ are the nonzero eigenvalues of $(\mathbf{G} - \tilde{\mathbf{G}})(\mathbf{G} - \tilde{\mathbf{G}})^H$. The minimum value of the product $\lambda_1 \lambda_2 \dots \lambda_r$ over all pairs of distinct code matrices is defined as the coding gain. For \mathbf{G}_8 with full diversity, $\det[\mathbf{G} - \tilde{\mathbf{G}}] = \left(\det[(\mathbf{G} - \tilde{\mathbf{G}})^H] \right)^* \neq 0$. Maximizing the coding gain is equivalent to maximizing the minimum absolute value of the determinant of $(\mathbf{G} - \tilde{\mathbf{G}})$.

Consider the group (s_1, s_2, s_7, s_8) with

$$b = \left| \det[\mathbf{G}_{8_{(1,2,7,8)}} - \tilde{\mathbf{G}}_{8_{(1,2,7,8)}}] \right| = \left| (s_1 - \tilde{s}_1)^2 + (s_2 - \tilde{s}_2)^2 + (s_7 - \tilde{s}_7)^2 + (s_8 - \tilde{s}_8)^2 \right|^4. \quad (4.5)$$

Let s_1 be the reference symbol with a rotation angle 0 (without rotation) and rotation angles for s_2 , s_7 , and s_8 be θ_1 , θ_2 , and θ_3 , respectively. Eq. (4.5) can then be re-written as

$$b = \left| (s_1 - \tilde{s}_1)^2 + e^{j2\theta_1}(s_2 - \tilde{s}_2)^2 + e^{j2\theta_2}(s_7 - \tilde{s}_7)^2 + e^{j2\theta_3}(s_8 - \tilde{s}_8)^2 \right|^4. \quad (4.6)$$

It is very difficult to determine the optimal values of the three variables $(\theta_1, \theta_2, \theta_3)$ simultaneously via an analytical approach. Moreover, the optimal rotation angles are constellation dependent. Through exhaustive numerical search and careful inspection, it is found that when the minimum value of b is maximized Eq. (4.6) can always be written as

$$b = \left| \left[(s_1 - \tilde{s}_1)^2 + e^{j2\theta'}(s_2 - \tilde{s}_2)^2 \right] + e^{j2\theta} \left[(s_7 - \tilde{s}_7)^2 + e^{j2\theta'}(s_8 - \tilde{s}_8)^2 \right] \right|^4. \quad (4.7)$$

where $\theta' = \pi/4$ for QAM and $\theta' = \pi/Q$ for even-sized PSK with constellation size of Q . Note that θ' is the optimal rotation angle for quasi-orthogonal codes with four transmit antennas [49, 51]. This leaves θ the only variable to be determined. In other words, if we let \mathcal{X} be the new constellation formed by $(s_1 - \tilde{s}_1)^2 + e^{j2\theta'}(s_2 - \tilde{s}_2)^2$, then maximizing the minimum value of b is equivalent to maximizing the minimum distance between any point in \mathcal{X} and any point in $\mathcal{Y} = e^{j2\theta}\mathcal{X}$. If the minimum distance is nonzero (except between the origins of constellations \mathcal{X} and \mathcal{Y}), then full diversity is achieved.

For 4QAM symbols $\{\frac{\sqrt{2}}{2} \pm \frac{\sqrt{2}}{2}j, -\frac{\sqrt{2}}{2} \pm \frac{\sqrt{2}}{2}j\}$, the optimal value of θ and the corresponding b can be determined by using the geometric method given in [51]. Fig. 4.1 shows five circles with radii $\{2, 2\sqrt{2}, 4, 4\sqrt{2}, 6\}$. For constellation \mathcal{X} , there are four points uniformly distributed on each circle. The angles of the four

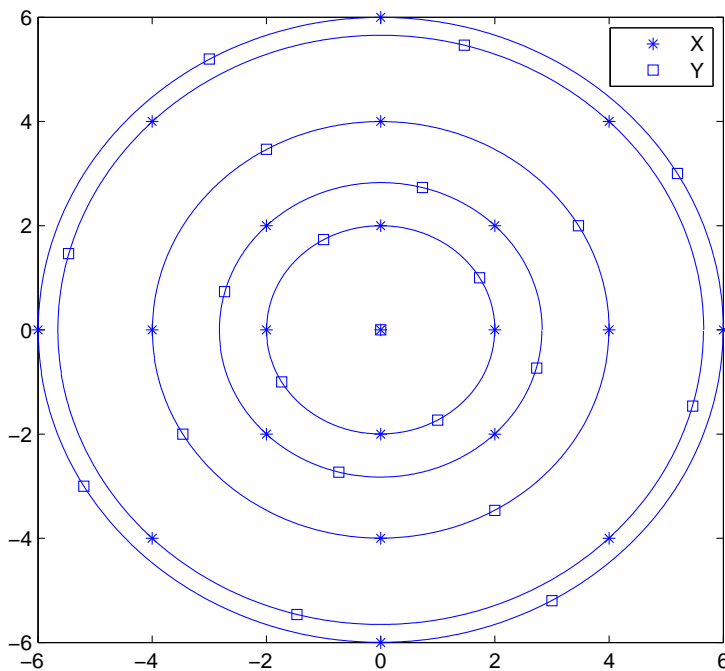


FIGURE 4.1. Constellation \mathcal{X} and $\mathcal{Y} = e^{j\pi/6}\mathcal{X}$.

points on the same circle are $\{0, \pi/2, \pi, 3\pi/2\}$ or $\{\pi/4, 3\pi/4, 5\pi/4, 7\pi/4\}$. The optimal value of θ is found to maximize the distance between (x_1, y_1) and the distance between (x_2, y_1) simultaneously. It is found that for 4QAM $\theta = \pi/12$ and the minimum value of b is maximized to be $(8 - 8 \cos \frac{\pi}{6})^2$.

The conclusion that $\theta = \pi/12$ is optimal is briefly proved as follows.

1. Consider the four points on the same circle. It is straightforward that after constellation rotation by $2\theta = \pi/6$, the distance between any point in \mathcal{X} and any point in \mathcal{Y} is greater than or equal to the distance between (x_1, y_1) .

2. Consider a pair of points (x, y) on the different circles. First, let us not consider the middle circle and the two outer circles. It is easily found from Fig. 4.1 that $2\theta = \pi/6$ is optimal and distances $\text{dist}_{(x_1, y_1)} = \text{dist}_{(x_2, y_1)} = \sqrt{8 - 8 \cos \frac{\pi}{6}} = 1.0353$. It is also easy to find that the distances between middle circle and its adjacent circles are greater than 1.0353. Finally, we need to check point pair (x, y) on the two outer circles, for which it is determined that the distance between (x, y) on the two outer circles is always greater than 1.0353. Therefore, $2\theta = \pi/6$ is the optimal rotation angle ($\theta = \pi/12$) for 4QAM.

Because of the symmetry of \mathcal{X} , the minimum value of b is a periodic function of θ with a period of $\pi/4$ for QAM and π/Q for even-sized PSK with a constellation size Q . There are two optimal rotation angles for any modulation within one period (e.g., $\pi/6$ is another optimal rotation angle for 4QAM). For higher order modulation schemes, analysis via an analytical approach is difficult. Through exhaustive numerical search, we determined the optimal rotation angles in the sense of maximizing coding gain for some commonly used constellations and listed them in Table 1.

Constellation	θ (radians, within one period)
4QAM (QPSK)	$\pi/12, \pi/6$
8PSK	0.165, 0.227
16QAM	0.322, 0.464
16PSK	0.0825, 0.1138

Table 1: Optimal rotation angles for some commonly used constellations.

Unlike \mathbf{G}_4 given in [48, 49], for which all QAM constellations have the same optimal rotation angles, the optimal rotation angles of 4QAM and 16QAM are different for \mathbf{G}_8 .

4.3. Simulation Results

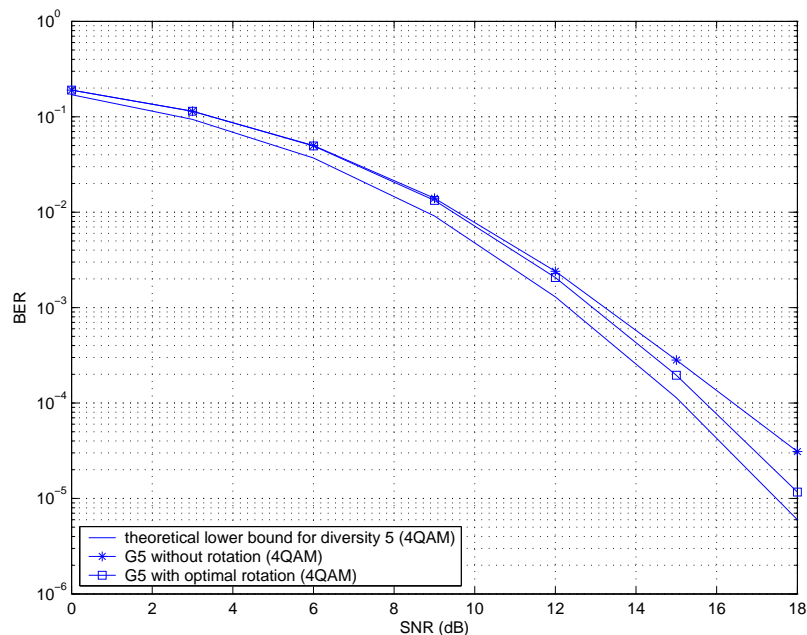


FIGURE 4.2. Performance comparison between \mathbf{G}_5 and theoretical lower bound ($N = 5$, $M = 1$, 2 bits/s/Hz).

Error performance of the codes derived using the proposed method is simulated and compared with the theoretical lower bound. The theoretical lower bound is obtained based on a model with one transmit antenna and NM receive antennas that provides full receive diversity. To make it a fair comparison, the average transmission power for this model is normalized to $1/N$, the same as the space-time block coded system with N transmit antennas. The decision variable for any symbol is expressed as

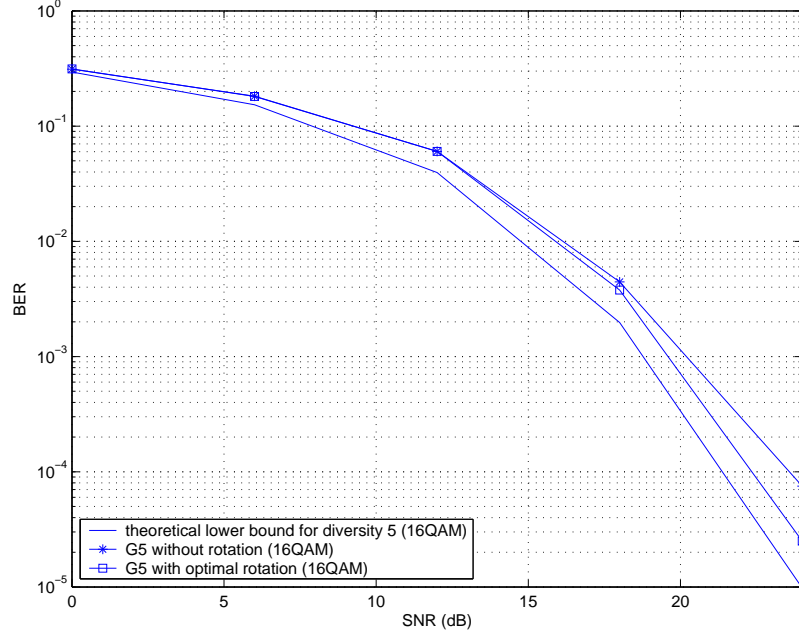


FIGURE 4.3. Performance comparison between \mathbf{G}_5 and theoretical lower bound ($N = 5$, $M = 1$, 4 bits/s/Hz).

$$\hat{s} = \sum_{i=1}^{NM} \left(\sqrt{\frac{\rho}{N}} |h_i|^2 s + h_i^* \eta_i \right) \quad (4.8)$$

where η_i , $i = 1, \dots, NM$, are samples of independent zero-mean complex Gaussian random variables with variance $1/2$ per real dimension, h_i is the fading coefficient for the i^{th} receive antenna, and s is a symbol. Rate-one ISI-free codes (i.e., orthogonal codes) such as the Alamouti code achieves this bound.

Fig. 4.2 and Fig. 4.3 show, respectively, the simulated bit error rate (BER) versus SNR curves for 4QAM and 16QAM systems with five transmit antennas and one receive antenna. Code matrix \mathbf{G}_5 is the taken as the first five columns of \mathbf{G}_8 . The codes obtained using the proposed method with the optimal

constellation rotation angles were found to have the same BER-SNR slope as the theoretical BER lower bound. This verifies that the codes derived in this letter achieve full diversity. Without rotation, these codes suffer from performance degradation at the high SNR region because of a loss in diversity. Performance of the code proposed in [68] is also shown in Fig. 4.2. Its code matrix is given as

$$\begin{bmatrix} s_1 & e^{j\omega} s_5 & e^{j\omega} s_4 & e^{j\omega} s_3 & e^{j\omega} s_2 \\ s_2 & s_1 & e^{j\omega} s_5 & e^{j\omega} s_4 & e^{j\omega} s_3 \\ s_3 & s_2 & s_1 & e^{j\omega} s_5 & e^{j\omega} s_4 \\ s_4 & s_3 & s_2 & s_1 & e^{j\omega} s_5 \\ s_5 & s_4 & s_3 & s_2 & s_1 \end{bmatrix}. \text{ Through computer search, the optimal value of } \omega$$

in the sense of maximizing coding gain is obtained to be 5.38 radians for 4QAM. Compared with quasi-orthogonal codes, this code suffers from performance loss due to higher ISI.

4.4. Conclusion

We have provided a systematic design method of rate-one space-time block codes with full diversity for systems with an arbitrary number of transmit antennas. Our code structures are based on the real orthogonal codes and can be applied to real as well as complex signals. Full diversity is achieved by constellation rotation. A decoding method has been provided to lower the decoding complexity of these codes when applied to a MIMO system. Simulation results verified these properties of the codes derived.

5. EXACT ERROR PROBABILITY FOR SPACE-TIME BLOCK-CODED MIMO SYSTEMS OVER RAYLEIGH FADING CHANNELS

Most existing analysis on the performance of STBC has focused on error rate upper bounds [40, 54–58], whereas in [59] an exact error probability for coherent and differentially coherent schemes proposed by Alamouti for two transmit antenna systems [36, 72] was derived. The major purpose of this chapter is to extend the results in [59] and derive the analytical error performance expressions of coherent and differentially coherent orthogonal STBCs for systems with an arbitrary number of transmit and receive antennas.

5.1. Performance Analysis

In this chapter, we consider phase shift keying signals only. Recall that the transmission matrix is

$$\mathcal{G}_c = \begin{bmatrix} c_1^1 & c_1^2 & \dots & c_1^N \\ c_2^1 & c_2^2 & \dots & c_2^N \\ \vdots & \vdots & \ddots & \vdots \\ c_L^1 & c_L^2 & \dots & c_L^N \end{bmatrix} \quad (5.1)$$

by applying the orthogonality property of the transmission matrix \mathcal{G}_c , we have $\mathcal{G}_c^H \mathcal{G}_c = \alpha I_N$, where $(\cdot)^H$ denotes complex conjugate transpose, α is a scalar, and I_N is the $N \times N$ identity matrix. Decoding can be done using only linear operations on the received signals and channel fading coefficients. We apply the decision variables given in [36, 37, 70, 71] and derive the closed-form error probability expressions for systems with different transmission rates based on the method introduced in [74, 75].

5.1.1. Rate 1 codes

The decision variable for rate 1 codes with PSK modulation is given as [36, 70]

$$\hat{s} = \sum_{m=1}^M \sum_{n=1}^N \left(\sqrt{\frac{E_s}{N}} |h_{n,m}|^2 s + V_{n,m} \right) \quad (5.2)$$

where $V_{n,m}$ is the noise component associated with channel coefficient $h_{n,m}$ and is given as $V_{n,m} \in \{\pm h_{n,m}^* v_{n,m}, \pm h_{n,m} v_{n,m}^*\}$, and $v_{n,m}, n = 1, \dots, N, m = 1, \dots, M$, are independent samples of zero-mean complex Gaussian random variables with variance $\frac{N_0}{2}$ per real dimension. For example, with the real transmission matrix

$$[37] \mathcal{G}_3 = \begin{bmatrix} s_1 & s_2 & s_3 \\ -s_2 & s_1 & -s_4 \\ -s_3 & s_4 & s_1 \\ -s_4 & -s_3 & s_2 \end{bmatrix}, \text{ the decision variable for } s_2 \text{ is given as}$$

$$\begin{aligned} \hat{s}_2 &= \sum_{m=1}^M (h_{2,m}^* r_1^m - h_{1,m} r_2^{m*} + h_{3,m} r_4^{m*}) \\ &= \sum_{m=1}^M \left[\sum_{n=1}^3 \sqrt{\frac{E_s}{3}} |h_{n,m}|^2 s_2 + \sqrt{\frac{E_s}{3}} (h_{1,m} h_{3,m}^* - \right. \\ &\quad \left. h_{1,m}^* h_{3,m}) s_4 + h_{2,m}^* \eta_1^m - h_{1,m} \eta_2^{m*} + h_{3,m} \eta_4^{m*} \right]. \end{aligned} \quad (5.3)$$

note that only the real part of above equation is of our concern because $s_p, p = 1, \dots, 4$, are real numbers. The interference term is $\Re \left\{ \sqrt{\frac{E_s}{3}} (h_{1,m} h_{3,m}^* - h_{1,m}^* h_{3,m}) s_4 \right\} = 0$, where $\Re\{\cdot\}$ denotes the real part. In this case $v_{1,m} = \eta_2^m, v_{2,m} = \eta_1^m, v_{3,m} = \eta_4^m$, and signal-to-noise ratio (SNR) is determined to be $\frac{\sum_{m=1}^M \sum_{n=1}^N |h_{n,m}|^2 E_s}{N N_0}$.

Let $X_k = h_{n,m}^*, Y_k = \sqrt{\frac{E_s}{N}} h_{n,m} s \pm v_{n,m}$ if $V_{n,m} = \pm h_{n,m}^* v_{n,m}$, and $X_k = h_{n,m}, Y_k = \sqrt{\frac{E_s}{N}} h_{n,m}^* s \pm v_{n,m}^*$ if $V_{n,m} = \pm h_{n,m} v_{n,m}^*$. The decision variable in (5.2)

can then be written in a general form as $\hat{s} = \sum_{k=1}^{NM} (X_k Y_k) = \hat{s}_r + j\hat{s}_i$ for an $(NM)^{th}$ -order diversity system, where $\hat{s}_r = \Re\{\hat{s}\}$, the real part of \hat{s} , and $\hat{s}_i = \Im\{\hat{s}\}$, the imaginary part of \hat{s} . Although each pair of the complex zero-mean Gaussian random variables (X_k, Y_k) are correlated, the NM pairs (X_k, Y_k) are independent and identically distributed. Let the magnitude of \hat{s} be $r = \sqrt{\hat{s}_r^2 + \hat{s}_i^2}$. The decision variable for space-time block coded MPSK signals is expressed as $\theta = \tan^{-1}(\hat{s}_i/\hat{s}_r)$.

Based on the assumption that all signaling waveforms are equally likely, we assume, without loss of generality, that symbol s has a zero phase (i.e., $s = 1$). The joint characteristic function of random variables \hat{s}_r and \hat{s}_i can be expressed in the form [75]

$$\Psi(j\xi_1, j\xi_2) = \left[\frac{\frac{4}{\Lambda_{xx}\Lambda_{yy}(1-\mu^2)}}{\left(\xi_1 - j\frac{2\mu}{\sqrt{\Lambda_{xx}\Lambda_{yy}(1-\mu^2)}}\right)^2 + \xi_2^2 + \frac{4}{\Lambda_{xx}\Lambda_{yy}(1-\mu^2)^2}} \right]^{NM} \quad (5.4)$$

where $\Lambda_{xx} = E(|X_k|^2) = 1$, $\Lambda_{yy} = E(|Y_k|^2) = \frac{E_s}{N} + \mathcal{N}_0$, $\Lambda_{xy} = E(X_k Y_k) = \sqrt{\frac{E_s}{N}}$ are identical for all values of k , and $\mu = \frac{\Lambda_{xy}}{\sqrt{\Lambda_{xx}\Lambda_{yy}}} = \sqrt{\frac{E_s/\mathcal{N}_0}{E_s/\mathcal{N}_0 + N}}$. Note that a real-valued parameter μ implies that the signals have a symmetric spectrum.

The Fourier transform of function $\Psi(j\xi_1, j\xi_2)$ with respect to variables ξ_1 and ξ_2 is given as

$$p(\hat{s}_r, \hat{s}_i) = \frac{(1-\mu^2)^{NM}}{(NM-1)!\pi 2^{NM}} \left(\sqrt{\hat{s}_r^2 + \hat{s}_i^2}\right)^{NM-1} \times \exp(\mu\hat{s}_r) K_{NM-1} \left(\sqrt{\hat{s}_r^2 + \hat{s}_i^2}\right) \quad (5.5)$$

where $K_{NM-1}(\cdot)$ is the modified Hankel function of order $NM-1$. The joint probability density function (PDF) of r and θ is expressed as

$$p(r, \theta) = \frac{(1-\mu^2)^{NM}}{(NM-1)!\pi 2^{NM}} r^{NM-1} \exp[\mu r \cos(\theta)] K_{NM-1}(r). \quad (5.6)$$

The marginal PDF of θ is obtained by integrating $p(r, \theta)$ over r as

$$p(\theta) = \frac{(-1)^{NM-1}(1-\mu^2)^{NM}}{2\pi(NM-1)!} \left\{ \frac{\partial^{NM-1}}{\partial b^{NM-1}} \left[\frac{1}{b-\mu^2 \cos^2 \theta} + \frac{\mu \cos \theta}{[b-\mu^2 \cos^2 \theta]^{3/2}} \right. \right. \\ \left. \left. \cos^{-1} \left(-\frac{\mu \cos \theta}{b^{1/2}} \right) \right] \right\} \Big|_{b=1}. \quad (5.7)$$

note that in the special case of no diversity (i.e., $NM = 1$), the expression given in Eq. (5.7) reduces to the well-known case of single-antenna systems with PSK signaling over frequency-nonselctive Rayleigh fading channels.

Because $p(\theta)$ is an even function of θ , we only need to consider the range of $0 \leq \theta \leq \pi$. Furthermore, the continuity of the integrand and its derivatives, together with the fact that the limits θ_1 and θ_2 are independent of b , allow us to interchange the sequence of integration and differentiation. Thus, we have

$$\int_{\theta_1}^{\theta_2} p(\theta) d\theta = \frac{(-1)^{NM-1}(1-\mu^2)^{NM}}{2\pi(NM-1)!} \frac{\partial^{NM-1}}{\partial b^{NM-1}} \left\{ \frac{1}{b-\mu^2} \left[\frac{\mu \sqrt{1-(b/\mu^2-1)x^2}}{b^{1/2}} \cot^{-1} x - \right. \right. \\ \left. \left. \cot^{-1} \left(\frac{xb^{1/2}/\mu}{\sqrt{1-(b/\mu^2-1)x^2}} \right) \right] \right\} \Big|_{x_1}^{x_2} \Big|_{b=1} \quad (5.8)$$

where $x_i = \frac{-\mu \cos \theta_i}{\sqrt{b-\mu^2 \cos^2 \theta_i}}$, $i = 1, 2$.

It is easy to verify that $\theta_1 = \pi/2$ implies $x_1 = 0$ and $\theta_2 = \pi$ implies $x_2 = \mu/\sqrt{b-\mu^2}$. Therefore, for BPSK signals the bit error rate (BER) expression is given as

$$P_{2b} = 2 \int_{\pi/2}^{\pi} p(\theta) d\theta \\ = \frac{(-1)^{NM-1}(1-\mu^2)^{NM}}{2(NM-1)!} \frac{\partial^{NM-1}}{\partial b^{NM-1}} \left[\frac{1}{b-\mu^2} - \frac{\mu}{b^{1/2}(b-\mu^2)} \right] \Big|_{b=1}. \quad (5.9)$$

this integration can be obtained in closed form as

$$P_{2b} = \frac{1}{2} \left[1 - \mu \sum_{k=0}^{NM-1} \binom{2k}{k} \left(\frac{1-\mu^2}{4} \right)^k \right]. \quad (5.10)$$

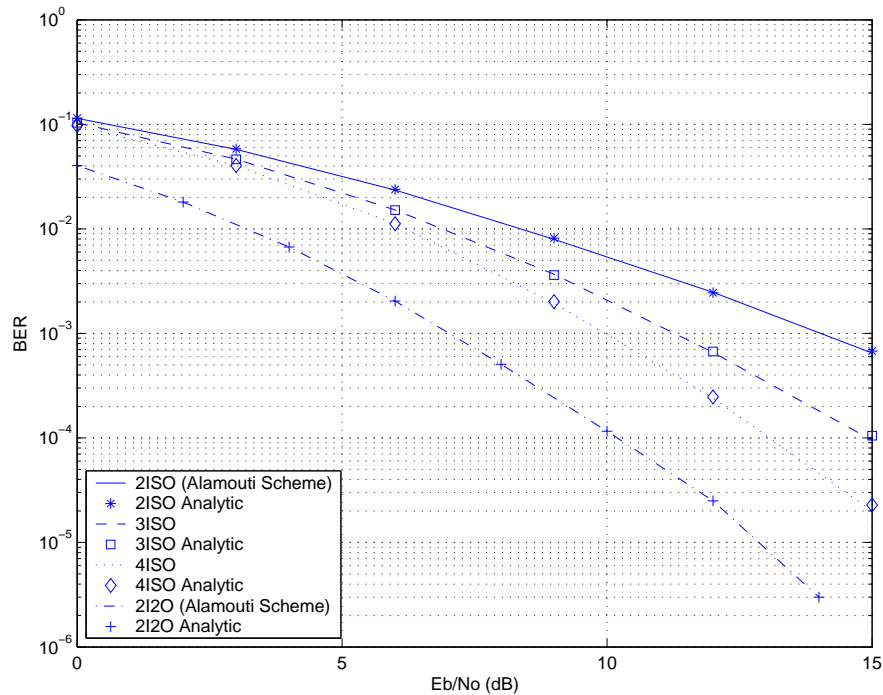


FIGURE 5.1. Rate 1 codes with BPSK modulation.

The simulated and analytical error performance curves of rate 1 codes with different system parameters are shown in Fig. 5.1.

5.1.2. Rate 3/4 complex codes

The decision variable for rate 3/4 codes with PSK modulation can be expressed as [71]

$$\hat{s} = \sum_{m=1}^M \sum_{n=1}^N \left[\sqrt{\frac{E_s}{N}} |h_{n,m}|^2 s + V_{n,m} \right] \quad (5.11)$$

where the noise component $V_{n,m} \in [\pm h_{n,m}^* v_{n,m}, \pm h_{n,m} v_{n,m}^*, \Xi]$ and Ξ is a complex random variable with a zero mean and variance \mathcal{N}_0 . For example, with the trans-

mission matrix [71] $\mathcal{H}_3 = \begin{bmatrix} s_1 & s_2 & \frac{s_3}{\sqrt{2}} \\ -s_2^* & s_1^* & \frac{s_3}{\sqrt{2}} \\ \frac{s_3^*}{\sqrt{2}} & \frac{s_3^*}{\sqrt{2}} & \frac{-s_1 - s_1^* + s_2 - s_2^*}{2} \\ \frac{s_3^*}{\sqrt{2}} & -\frac{s_3^*}{\sqrt{2}} & \frac{s_2 + s_2^* + s_1 - s_1^*}{2} \end{bmatrix}$, the decision variable for s_1 is expressed as [71]

$$\begin{aligned} \hat{s}_1 &= \sum_{m=1}^M \left[h_{1,m}^* r_1^m + h_{2,m} r_2^{m*} + \frac{h_{3,m}^* (r_4^m - r_3^m)}{2} - \frac{h_{3,m} (r_3^m + r_4^m)^*}{2} \right] \\ &= \sum_{m=1}^M \left[\sum_{n=1}^3 \sqrt{\frac{E_s}{3}} |h_{n,m}|^2 s_1 + h_{1,m}^* \eta_1^m + h_{2,m} \eta_2^{m*} + \right. \\ &\quad \left. \frac{1}{2} (h_{3,m}^* \eta_4^m - h_{3,m}^* \eta_3^m - h_{3,m} \eta_4^{m*} - h_{3,m} \eta_3^{m*}) \right]. \end{aligned} \quad (5.12)$$

For this case $v_{1,m} = \eta_1^m$, $v_{2,m} = \eta_2^m$, and $V_{3,m} = \frac{1}{2} (h_{3,m}^* \eta_4^m - h_{3,m}^* \eta_3^m - h_{3,m} \eta_4^{m*} - h_{3,m} \eta_3^{m*})$. Obviously, $V_{3,m}$ has a zero mean and variance \mathcal{N}_0 , and all noise components ($V_{1,m}$, $V_{2,m}$, and $V_{3,m}$) are mutually independent. The SNR is obtained to be $\frac{\sum_{m=1}^M \sum_{n=1}^3 |h_{n,m}|^2 E_s}{N \mathcal{N}_0}$, which is the same as rate 1 codes. Comparing Eq.(5.2) and Eq.(5.11), we find that the method used for rate 1 codes is also suitable for rate 3/4 codes. The symbol error probability (SEP) for MPSK (assuming Q constellation points) signaling is

$$\begin{aligned} P_Q &= 2 \int_{\pi/Q}^{\pi} p(\theta) d\theta \\ &= \frac{(-1)^{NM-1} (1 - \mu^2)^{NM}}{\pi (NM - 1)!} \frac{\partial^{NM-1}}{\partial b^{NM-1}} \left\{ \frac{1}{b - \mu^2} \left[\frac{\pi}{Q} (Q - 1) - \right. \right. \\ &\quad \left. \left. \frac{\mu \sin(\pi/Q)}{\sqrt{b - \mu^2 \cos^2(\pi/Q)}} \cot^{-1} \left(\frac{-\mu \cos(\pi/Q)}{\sqrt{b - \mu^2 \cos^2(\pi/Q)}} \right) \right] \right\} \Big|_{b=1}. \end{aligned} \quad (5.13)$$

For QPSK signaling with Gray code mapping, it is obvious that a single-bit error occurs if the received phase is in the range of $\pi/4 < \theta < 3\pi/4$, and a double-bit error occurs if the received phase is in the range of $3\pi/4 < \theta < \pi$. Therefore, the probability of bit error is obtained as

$$\begin{aligned}
P_{4b} &= \int_{\pi/4}^{3\pi/4} p(\theta)d\theta + 2 \int_{3\pi/4}^{\pi} p(\theta)d\theta \\
&= \frac{(-1)^{NM-1}(1-\mu^2)^{NM}}{2(NM-1)!} \frac{\partial^{NM-1}}{\partial b^{NM-1}} \left[\frac{1}{b-\mu^2} - \frac{\mu}{(b-\mu^2)(2b-\mu^2)^{1/2}} \right] \Big|_{b=1}. \quad (5.14)
\end{aligned}$$

The BER expression given in Eq. (5.14) can be obtained in closed form as

$$P_{4b} = \frac{1}{2} \left[1 - \frac{\mu}{\sqrt{2-\mu^2}} \sum_{k=0}^{NM-1} \binom{2k}{k} \left(\frac{1-\mu^2}{4-2\mu^2} \right)^k \right]. \quad (5.15)$$

As another example, the BER for 8PSK signaling with Gray code mapping is obtained as

$$\begin{aligned}
P_{8b} &= \frac{1}{3} \left[2 \int_{\pi/8}^{3\pi/8} p(\theta)d\theta + 4 \int_{3\pi/8}^{5\pi/8} p(\theta)d\theta + 4 \int_{5\pi/8}^{7\pi/8} p(\theta)d\theta + 4 \int_{7\pi/8}^{\pi} p(\theta)d\theta \right] \\
&= \frac{(-1)^{NM-1}(1-\mu^2)^{NM}}{3\pi(NM-1)!} \left\{ \frac{\partial^{NM-1}}{\partial b^{NM-1}} \left[\frac{1}{b-\mu^2} \left(\frac{3\pi}{2} - \frac{\mu\sqrt{1-1/\sqrt{2}}}{\sqrt{2b-\mu^2(1+1/\sqrt{2})}} \right. \right. \right. \\
&\quad \times \cot^{-1} \frac{-\mu\sqrt{1+1/\sqrt{2}}}{\sqrt{2b-\mu^2(1+1/\sqrt{2})}} - \frac{\mu\sqrt{1+1/\sqrt{2}}}{\sqrt{2b-\mu^2(1-1/\sqrt{2})}} \\
&\quad \left. \left. \left. \times \cot^{-1} \frac{-\mu\sqrt{1-1/\sqrt{2}}}{\sqrt{2b-\mu^2(1-1/\sqrt{2})}} \right) \right] \right\} \Big|_{b=1}. \quad (5.16)
\end{aligned}$$

Following the same procedure, we can obtain the bit error rate expressions for other higher-order PSK schemes (e.g., 16PSK and 32PSK) from Eq. (5.8). However, a simple closed-form expression exists only for P_{2b} and P_{4b} .

The simulated and analytical error performance curves of rate 3/4 codes with various system parameters are shown in Fig. 5.2.

5.1.3. Rate 1/2 complex codes

The decision variable for rate 1/2 codes with PSK modulation can be expressed as [71]

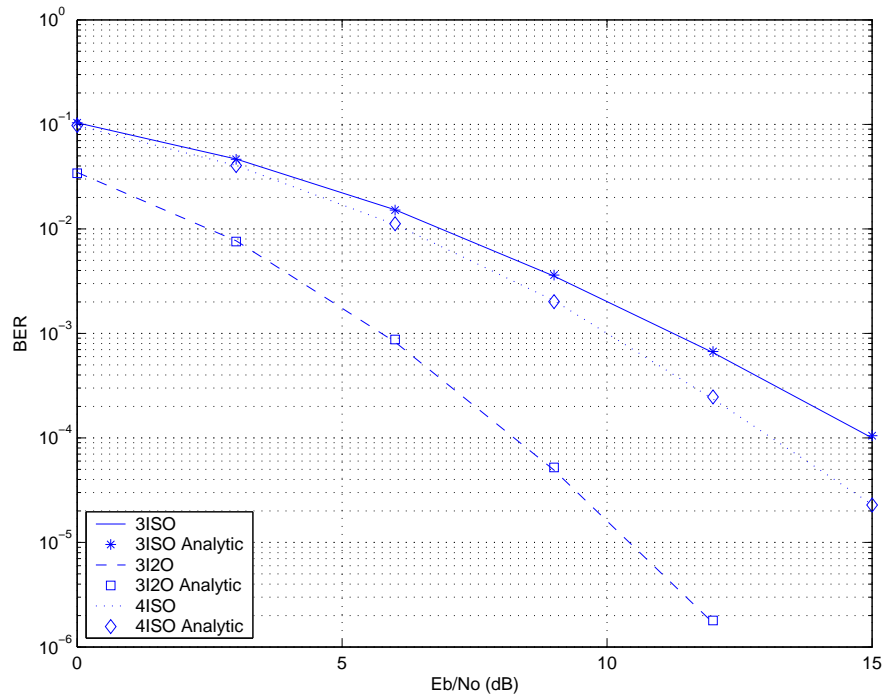


FIGURE 5.2. Rate 3/4 codes with QPSK modulation.

$$\hat{s} = \sum_{m=1}^M \sum_{n=1}^N \left[2\sqrt{\frac{E_s}{N}} |h_{n,m}|^2 s + V_{n,m} \right] \quad (5.17)$$

where $V_{n,m}$ has a variance $2\mathcal{N}_0$, instead of \mathcal{N}_0 .

For example, with the transmission matrix [71] $\mathcal{A}_4 =$

$$\begin{bmatrix} s_1 & s_2 & s_3 & s_4 \\ -s_2 & s_1 & -s_4 & s_3 \\ -s_3 & s_4 & s_1 & -s_2 \\ -s_4 & -s_3 & s_2 & s_1 \\ s_1^* & s_2^* & s_3^* & s_4^* \\ -s_2^* & s_1^* & -s_4^* & s_3^* \\ -s_3^* & s_4^* & s_1^* & -s_2^* \\ -s_4^* & -s_3^* & s_2^* & s_1^* \end{bmatrix},$$

the decision variable for s_1 is given

as [71]

$$\begin{aligned} \hat{s}_1 &= \sum_{m=1}^M (h_{1,m}^* r_1^m + h_{2,m}^* r_2^m + h_{3,m}^* r_3^m + h_{4,m}^* r_4^m + h_{1,m} r_5^{m*} + h_{2,m} r_6^{m*} + h_{3,m} r_7^{m*} + h_{4,m} r_8^{m*}) \\ &= \sum_{m=1}^M \left[\sum_{n=1}^4 2\sqrt{\frac{E_s}{4}} |h_{n,m}|^2 s_1 + (h_{1,m}^* \eta_1^m + h_{1,m} \eta_5^{m*}) + (h_{2,m}^* \eta_2^m + h_{2,m} \eta_6^{m*}) + (h_{3,m}^* \eta_3^m + \right. \\ &\quad \left. h_{3,m} \eta_7^{m*}) + (h_{4,m}^* \eta_4^m + h_{4,m} \eta_8^{m*}) \right]. \end{aligned} \quad (5.18)$$

The signal-to-noise ratio is obtained to be $\frac{2 \sum_{m=1}^M \sum_{n=1}^4 |h_{n,m}|^2 E_s}{N \mathcal{N}_0}$. Obviously, rate 1/2 codes provide full diversity as rate 3/4 codes but have an additional 3dB SNR advantage when compared with rate 1 and rate 3/4 codes. As a result, in a BER vs SNR plot, the curve for rate 1/2 code must be parallel to that for rate 3/4 code and the latter performs 3 dB worse if we use the same modulation scheme for both codes. So the error probability of rate 1/2 codes has the same form as that of rate 3/4 codes. The only difference is that the parameter μ must be modified to $\mu = \sqrt{\frac{2E_s/\mathcal{N}_0}{2E_s/\mathcal{N}_0+N}} = \sqrt{\frac{E_s/\mathcal{N}_0}{E_s/\mathcal{N}_0+N/2}}$ for rate 1/2 complex codes.

The simulated and analytical error performance curves of rate 1/2 codes with various system parameters are shown in Fig. 5.3. By comparing Fig. 5.1 with

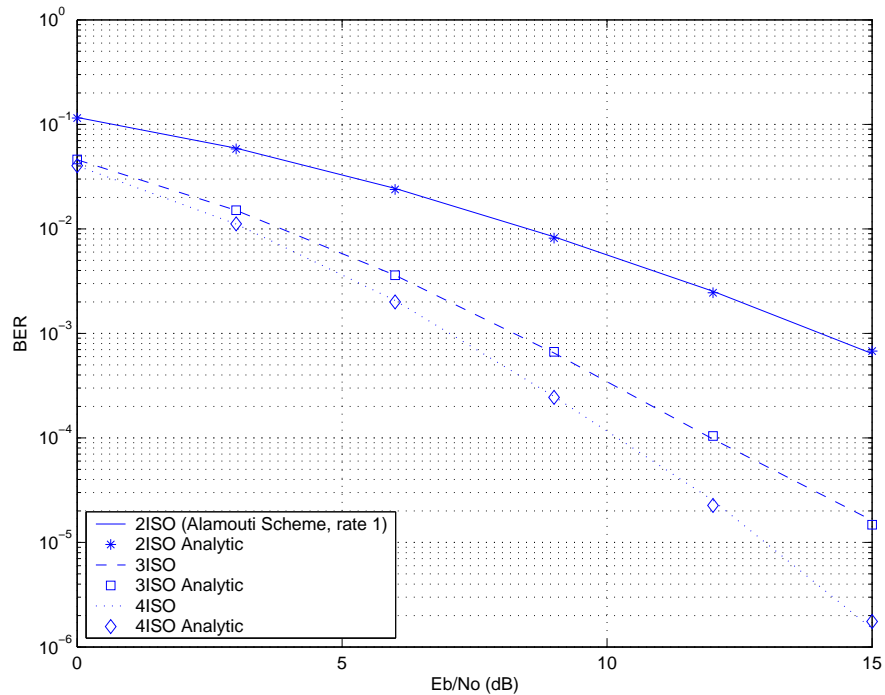


FIGURE 5.3. Rate 1/2 codes with QPSK modulation.

Fig. 5.3, we found that 1/2 rate codes have an additional 3dB SNR advantage compared with rate 1 codes¹, and the diversity order for both cases are the same.

5.1.4. Differential space-time block codes

To calculate the decision metric of maximum likelihood decoding, a receiver that employs the maximum likelihood decoding method needs the estimates of the channel coefficients. When neither the receiver nor the transmitter has the knowl-

¹Note that there is no interference between the inphase and quadrature components for QPSK symbols.

edge of the channel, full-diversity differential coding schemes could be employed. In [72], the Alamouti scheme (2 transmit antennas system) was extended to differential coding. In [73] the differential orthogonal space-time coding scheme was further extended to MIMO systems. The encoding and decoding details for differential space-time codes can be found in [72, 73]. Because the orthogonality property of the transmission matrices is still maintained in the differential scheme, the decoding procedure also has a linear computational complexity. However, signals transmitted from two adjacent blocks are correlated with the differential scheme, whereas signals in two adjacent blocks are independent with the coherent scheme. It has been shown [72, 73] that performance of the differential scheme is 3dB worse than the coherent scheme at high SNR values. In the low SNR region, there is a slight bias due to the second-order noise terms with the differential schemes. Thus, the error rates with high SNR values can be easily obtained using the same method applied for the coherent schemes, except that parameter μ must be modified as $\mu = \sqrt{\frac{E_s/2\mathcal{N}_0}{E_s/2\mathcal{N}_0+N}} = \sqrt{\frac{E_s/\mathcal{N}_0}{E_s/\mathcal{N}_0+2N}}$. For a system with two transmit antennas, this yields the result as given in [76].

The simulated and analytical error performance curves of differential codes with various system parameters are shown in Fig. 5.4. As we expect, there is a slight mismatch between analytical and simulation results at low SNR values due to the second order noise terms.

5.2. Conclusion

We have derived the closed-form expressions of the error probability for coherent and differentially coherent STBC schemes over slowly fading, flat Rayleigh channels. These results can be applied for performance evaluation of space-time

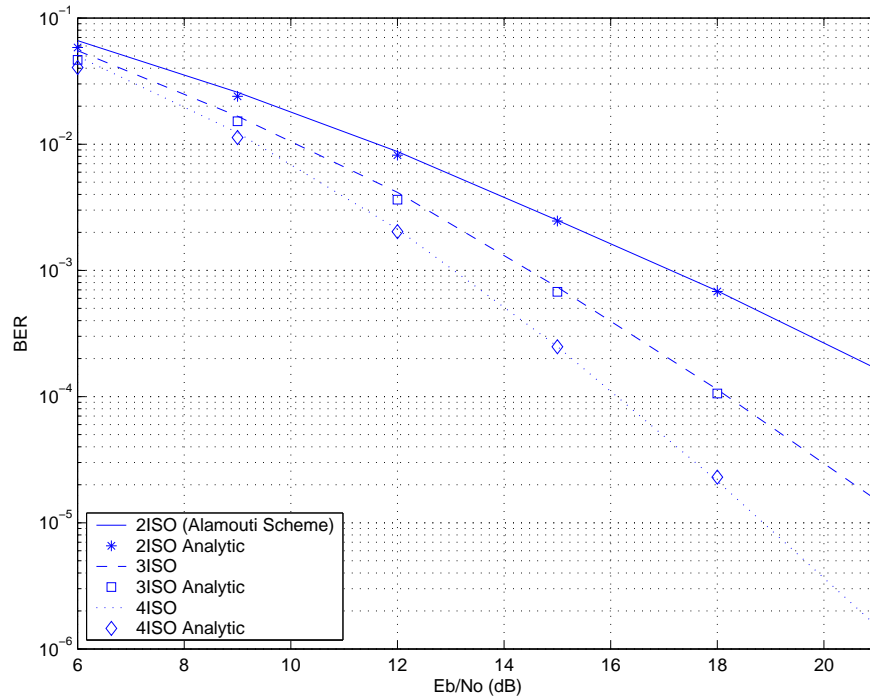


FIGURE 5.4. Differential codes with BPSK modulation, full rate.

block coded systems with different coding rates and an arbitrary number of transmit and receive antennas. Simulation results match well with the analytical results derived.

6. AN ADAPTIVE POWER ALLOCATION SCHEME FOR SPACE-TIME BLOCK CODED MIMO SYSTEMS

Space-time block codes provide transmit diversity over fading channels. In a commonly used STBC, transmit power is equally divided among all transmit antennas. However, if the transmitter has full or partial knowledge of the channel, adaptive transmit power allocation that allocates more power to the transmit antenna with a better fading condition will improve the received signal-to-noise ratio. In [77–80], several adaptive power allocation methods for systems with two transmit antennas were introduced. These schemes can be considered as a variation of the Alamouti scheme [36]. In [81], a method to transmit the Alamouti block code based on selecting two out of three transmit antennas was proposed. When the transmitter does not have perfect knowledge of the fading coefficients, none of the methods mentioned above can guarantee the maximum SNR at the receiver.

In this chapter, we derive the maximum SNR gain limit achievable by adaptive power allocation for STBC designed for multiple-input multiple-output systems when perfect feedback is available. Then, an adaptive power allocation scheme with imperfect feedback is proposed and analyzed. A design parameter u is introduced to control the power scaling factors. SNR gain of the proposed scheme over the conventional scheme in which power is equally distributed among all transmit antennas is provided. The conventional STBC scheme and the adaptive scheme analyzed in [77] are special cases of the proposed scheme with specific choices of a design parameter u .

6.1. System model

Consider a wireless communications system with M transmit antennas and N receive antennas, denoted as an (M, N) system in this chapter (note that we use (N, M) in the previous chapters). Each receive antenna responds to each transmit antenna through a statistically independent fading coefficient. The received signals are further corrupted by additive white Gaussian noise that is statistically independent among different receive antennas and different symbol periods. Let the $P \times M$ transmission matrix be

$$\mathcal{G} = \begin{bmatrix} g_{1,1} & g_{1,2} & \cdots & g_{1,M} \\ g_{2,1} & g_{2,2} & \cdots & g_{2,M} \\ \vdots & \ddots & \ddots & \vdots \\ g_{P,1} & g_{P,2} & \cdots & g_{P,M} \end{bmatrix} \quad (6.1)$$

and the transmitted symbol vector be $\mathbf{s} = [s_1, s_2, \cdots, s_K]^T$, where $[\cdot]^T$ denotes transpose. Each element of \mathcal{G} is a linear combination of symbols s_1, s_2, \cdots, s_K and their complex conjugates. The (p, m) th entry of \mathcal{G} , $g_{p,m}$, will be transmitted at time slot p from transmit antenna m . The code rate, as defined in [37], is given as K/P , where P is the number of time slots used to transmit K symbols. The total average transmit power is normalized to 1. Average energy of each symbol is E_s . Thus, the transmitted signal at time slot p from transmit antenna m is expressed as $x_{p,m} = \alpha_m \sqrt{E_s} g_{p,m}$, where α_m is a real power scaling factor determined by feedback information. In order to maintain the same total average power after power scaling, it is required that

$$\sum_{m=1}^M \alpha_m^2 = 1. \quad (6.2)$$

for the conventional STBC scheme, $\alpha_m = \sqrt{1/M}$, $m = 1, \dots, M$.

The channel is assumed to be quasi-static, allowing it to be constant over a frame of symbols and change independently from one frame to another. Let $h_{m,n}$ denote the fading coefficient from the m th transmit antenna to the n th receive antenna of an (M, N) system. Rayleigh fading is considered so that $h_{m,n}$ is a zero-mean complex Gaussian random variable. The average power of the channel is also normalized so that $h_{m,n}$ has a unit variance.

The received signal at time p by receive antenna n , $r_{p,n}$, is given as

$$r_{p,n} = \sum_{m=1}^M h_{m,n} x_{p,m} + \nu_{p,n} \quad (6.3)$$

where $\nu_{p,n}$ is the additive zero-mean white Gaussian noise component with variance \mathcal{N}_0 . The maximum likelihood (ML) decoder calculates the following decision metric

$$d = \sum_{p=1}^P \sum_{n=1}^N \left| r_{p,n} - \sum_{m=1}^M \alpha_m \sqrt{E_s} \hat{g}_{p,m} \right|^2 \quad (6.4)$$

and the codeword $(\hat{s}_1, \dots, \hat{s}_K)$ that minimizes d will be the decoder output.

6.2. SNR Analysis

Assuming a full-diversity system coded with orthogonal space-time block codes, ML decoding can be achieved using linear operations on $r_{p,n}$, α_m , and $h_{m,n}$. In a system with a rate-1 transmission matrix or with a rate-3/4 transmission matrix, the decision variable for the k th element of \mathbf{s} , \hat{s}_k , is expressed as [36, 37, 71, 70]

$$\hat{s}_k = \sqrt{E_s} \sum_{n=1}^N \sum_{m=1}^M \alpha_m^2 |h_{m,n}|^2 s_k + \xi_k \quad (6.5)$$

where ξ_k is the complex zero-mean Gaussian noise component whose variance is given as $\sigma_{\xi_k}^2 = \mathcal{N}_0 \sum_{n=1}^N \sum_{m=1}^M \alpha_m^2 |h_{m,n}|^2$. As an example, in a (2,1) system ($M = 2, N = 1$) with the Alamouti code [36], the received signals are expressed as

$$r_{1,1} = \sqrt{E_s} (\alpha_1 h_{1,1} s_1 + \alpha_2 h_{2,1} s_2) + \nu_{1,1} \quad (6.6a)$$

$$r_{2,1} = \sqrt{E_s} (-\alpha_1 h_{1,1} s_2^* + \alpha_2 h_{2,1} s_1^*) + \nu_{2,1} \quad (6.6b)$$

and the decision variables are given as

$$\begin{aligned} \hat{s}_1 &= \alpha_1 h_{1,1}^* r_{1,1} + \alpha_2 h_{2,1}^* r_{2,1} \\ &= \sqrt{E_s} (\alpha_1^2 |h_{1,1}|^2 + \alpha_2^2 |h_{2,1}|^2) s_1 + \alpha_1 h_{1,1}^* \nu_{1,1} + \alpha_2 h_{2,1}^* \nu_{2,1} \\ \hat{s}_2 &= \alpha_2 h_{2,1}^* r_{1,1} - \alpha_1 h_{1,1}^* r_{2,1} \\ &= \sqrt{E_s} (\alpha_1^2 |h_{1,1}|^2 + \alpha_2^2 |h_{2,1}|^2) s_2 + \alpha_2 h_{2,1}^* \nu_{1,1} - \alpha_1 h_{1,1}^* \nu_{2,1}. \end{aligned}$$

In a system with rate-1/2 transmission matrix for complex signals, the decision variable is given as [71]

$$\hat{s}_k = 2\sqrt{E_s} \sum_{n=1}^N \sum_{m=1}^M \alpha_m^2 |h_{m,n}|^2 s_k + \eta_k \quad (6.8)$$

where η_k is the complex zero-mean Gaussian noise component whose variance is given as $\sigma_{\eta_k}^2 = 2\mathcal{N}_0 \sum_{n=1}^N \sum_{m=1}^M \alpha_m^2 |h_{m,n}|^2$. Obviously, the SNR for rate-1/2 codes is doubled compared with rate-1 and rate-3/4 codes. With adaptive power allocation, however, the SNR gain will be the same for codes of rate 1, 3/4, and 1/2. Specifically, let SNR_a be the SNR with adaptive power allocation and SNR_c

be the SNR with the conventional equal-power scheme. The ratio $\frac{SNR_a}{SNR_c}$ will be the same for codes of rate 1, 3/4, and 1/2. Thus, in the following discussion, we will only focus on rate 1 and rate 3/4 codes. The received instantaneous SNR is obtained as

$$\gamma = \frac{E_s}{\mathcal{N}_0} \sum_{m=1}^M \left[\alpha_m^2 \sum_{n=1}^N |h_{m,n}|^2 \right]. \quad (6.9)$$

6.3. Adaptive power allocation

6.3.1. Minimum Feedback Allocation Scheme (Antenna Selection)

Let $\beta_m = \sum_{n=1}^N |h_{m,n}|^2$. Without loss of generality, we assume that $\beta_1 \geq \beta_2 \geq \dots \geq \beta_M$. Thus, we can write $\beta_{M-1} = \beta_M + \delta_1$, $\beta_{M-2} = \beta_M + \delta_1 + \delta_2$, ..., $\beta_1 = \beta_M + \delta_1 + \dots + \delta_{M-1}$, where β_i and δ_j are nonnegative real numbers. The instantaneous SNR is then expressed as

$$\gamma = \frac{E_s}{\mathcal{N}_0} \left[\beta_M + \delta_1 \sum_{i=1}^{M-1} \alpha_i^2 + \delta_2 \sum_{i=1}^{M-2} \alpha_i^2 + \dots + \delta_{M-1} \alpha_1^2 \right]. \quad (6.10)$$

obviously, when $\alpha_1 = 1$ (note that $\sum_{m=1}^M \alpha_m^2 = 1$), γ is maximized to be $\frac{E_s}{\mathcal{N}_0} \beta_1$. This means that if $\beta_1 \geq \dots \geq \beta_M$ holds, the system should allocate all its power to transmit antenna 1 for best performance.

The feedback required for this scheme is minimum; only $\lceil \log_2(M) \rceil$ bits for each transmission, where $\lceil \cdot \rceil$ denotes the nearest integer towards infinity. For simplicity, we will refer to this scheme as the minimum-feedback-allocation scheme (MFAS). Note that this scheme results in antenna selection (one out of M). Other advantages of the MFAS include that there are no quantization errors for the

feedback. Because there is no inter-symbol interference, it is easy to realize a rate-1 transmission for complex signals with full diversity, which is a challenging issue for MIMO systems with STBCs. However, this scheme, as will be seen from simulation results in Section V, is more sensitive to feedback errors than other power allocation schemes.

6.3.2. A New Adaptive Power Allocation Scheme

In practice when feedbacks are imperfect (channel coefficients obtained by the transmitter through feedback contain errors), a very simple scheme with $\alpha_1 > \dots > \alpha_M$ will improve the system performance if $\beta_1 > \dots > \beta_M$. In this case there are $M - 1$ variables, $\alpha_1, \dots, \alpha_{M-1}$ ($\alpha_M = \sqrt{1 - \sum_{m=1}^{M-1} \alpha_m^2}$), to be solved, and it is rather difficult to determine which set of combinations of α_m give the best performance. Thus, we propose a new scheme with only one parameter that can be easily controlled to maximize SNR at the receiver. Additionally, this scheme is robust to feedback errors. In the proposed adaptive power allocation scheme, the real scaling factor for the m th transmit antenna is given as

$$\alpha_m = \sqrt{\frac{\beta_m^u}{\sum_{m=1}^M \beta_m^u}} \quad (6.11)$$

where for a given set of channel coefficients, $h_{m,n}$, parameter u controls the power scaling factor α_m . It is easy to verify that α_m given in (6.11) satisfies the requirement given in (6.2).

It is worth of mentioning two special cases, $u = 0$ and $u = 2$, which correspond to, respectively, the conventional STBC scheme in which power is equally distributed among all transmit antennas and the adaptive scheme proposed in [77]

for a system with two transmit antennas. By applying the power scaling factor α_m given in (6.11) to the instantaneous SNR given in (6.9), we obtain

$$\gamma_u = \frac{E_s}{\mathcal{N}_0} \frac{\sum_{m=1}^M \beta_m^{u+1}}{\sum_{m=1}^M \beta_m^u}. \quad (6.12)$$

It will be interesting to examine the relationship between SNR and parameter u for the adaptive power allocation scheme. The difference between γ_{u+1} and γ_u is obtained to be

$$\begin{aligned} \gamma_{u+1} - \gamma_u &= \frac{E_s}{\mathcal{N}_0} \left(\frac{\sum_{m=1}^M \beta_m^{u+2}}{\sum_{m=1}^M \beta_m^{u+1}} - \frac{\sum_{m=1}^M \beta_m^{u+1}}{\sum_{m=1}^M \beta_m^u} \right) \\ &= \frac{E_s}{\mathcal{N}_0} \frac{\left(\sum_{i=1}^M \beta_i^u \right) \left(\sum_{j=1}^M \beta_j^{u+2} \right) - \left(\sum_{j=1}^M \beta_j^{u+1} \right)^2}{\left(\sum_{i=1}^M \beta_i^u \right) \left(\sum_{j=1}^M \beta_j^{u+1} \right)} \\ &= \frac{E_s}{\mathcal{N}_0} \frac{\sum_{1 \leq i < j \leq M} \beta_i^u \beta_j^u (\beta_i - \beta_j)^2}{\sum_{i=1}^M \sum_{j=1}^M \beta_i^u \beta_j^{u+1}}. \end{aligned} \quad (6.13)$$

It can be seen from Eq. (6.13) that $\gamma_{u+1} - \gamma_u$ is always greater than or equal to 0 with equality only if $\beta_1 = \beta_2 = \dots = \beta_M$. If this condition does not hold, which is true for any practical scenario, SNR increases monotonically with parameter u (note that u does not necessarily need to be an integer). However, performance improvement with the proposed adaptive power allocation scheme will saturate as u increases. This is proved as follows. Without loss of generality, we assume that $\beta_1 = \beta_2 = \dots = \beta_w = \max\{\beta_1, \dots, \beta_M\}$, where $1 \leq w < M$. The ratio γ_{u+1}/γ_u can be written as

$$\begin{aligned} \frac{\gamma_{u+1}}{\gamma_u} &= \frac{\beta_1^{-2u-2} (\beta_1^{u+2} + \dots + \beta_M^{u+2}) (\beta_1^u + \dots + \beta_M^u)}{\beta_1^{-2u-2} (\beta_1^{u+1} + \dots + \beta_M^{u+1})^2} \\ &= \frac{w^2 + \epsilon_1}{w^2 + \epsilon_2}. \end{aligned}$$

it can be easily determined that $\lim_{u \rightarrow +\infty} \epsilon_1 = \lim_{u \rightarrow +\infty} \epsilon_2 = 0$, which implies

$$\lim_{u \rightarrow +\infty} \gamma_{u+1}/\gamma_u = 1. \quad (6.14)$$

additionally, let us consider the limit of γ_u :

$$\begin{aligned} \lim_{u \rightarrow +\infty} \gamma_u &= \frac{E_s}{\mathcal{N}_0} \lim_{u \rightarrow +\infty} \frac{\beta_1^{u+1} + \beta_2^{u+1} + \dots + \beta_M^{u+1}}{\beta_1^u + \beta_2^u + \dots + \beta_M^u} \\ &= \frac{E_s}{\mathcal{N}_0} \lim_{u \rightarrow +\infty} \frac{\beta_1 + \beta_2 \left(\frac{\beta_2}{\beta_1}\right)^u + \dots + \beta_M \left(\frac{\beta_M}{\beta_1}\right)^u}{1 + \left(\frac{\beta_2}{\beta_1}\right)^u + \dots + \left(\frac{\beta_M}{\beta_1}\right)^u} \\ &= \frac{E_s}{\mathcal{N}_0} \beta_1. \end{aligned} \quad (6.15)$$

Eq. (6.15) gives the ultimately achievable maximum SNR at receiver with the proposed adaptive power allocation scheme, which is the same as the SNR achieved by antenna selection. Based on Eq. (6.15) and the fact that γ_u is a continuous function of u , an appropriate u could results in the maximum achievable SNR. This reduces the multidimensional problem to a one-dimensional problem.

We define the average SNR gain as the ratio of the average SNR with the adaptive power allocation scheme to the average SNR with the equal-power scheme. This ratio is expressed as $10 \log_{10} \left[\frac{E\{\gamma_u\}}{E\{\gamma_0\}} \right]$ dB, where $E\{\cdot\}$ denotes expectation. Recall that the average SNR for the traditional equal-power scheme is given as

$$E\{\gamma_0\} = \frac{E_s}{M\mathcal{N}_0} E \left\{ \sum_{m=1}^M \left[\sum_{n=1}^N |h_{m,n}|^2 \right] \right\} = \frac{NE_s}{\mathcal{N}_0}. \quad (6.16)$$

the maximum average SNR gain in dB can be obtained as

$$10 \log_{10} \left(\frac{E\{\gamma_{+\infty}\}}{E\{\gamma_0\}} \right) = 10 \log_{10} \left(\frac{E\{\max(\beta_1, \dots, \beta_M)\}}{N} \right) \quad (6.17)$$

where β_i , $i = 1, \dots, M$, are central chi-square-distributed random variables with freedom $2N$ in a Rayleigh fading environment. The cumulative distribution function (CDF) of β_i can be found in closed form as [74]

$$F_Y(y) = 1 - e^{-y/2\sigma^2} \sum_{k=0}^{N-1} \frac{1}{k!} \left(\frac{y}{2\sigma^2} \right)^k, \quad y \geq 0 \quad (6.18)$$

where $\sigma = \sqrt{2}/2$. The CDF of $\max(\beta_1, \dots, \beta_M)$ is given as

$$\begin{aligned} F_Y^{\max}(y) &= \left[1 - e^{-y/2\sigma^2} \sum_{k=0}^{N-1} \frac{1}{k!} \left(\frac{y}{2\sigma^2} \right)^k \right]^M \\ &= \left[1 - e^{-y} \sum_{k=0}^{N-1} \frac{1}{k!} y^k \right]^M, \quad y \geq 0. \end{aligned} \quad (6.19)$$

The probability density function (PDF) of $\max(\beta_1, \dots, \beta_M)$, $p_Y^{\max}(y)$, can be calculated by differentiating $F_Y^{\max}(y)$. The expected value of $\max(\beta_1, \dots, \beta_M)$ is obtained as

$$E\{\max(\beta_1, \dots, \beta_M)\} = \int_0^{\infty} y p_Y^{\max}(y) dy. \quad (6.20)$$

as an example, let us consider a (2,1) system:

$$\begin{aligned} F_Y(y) &= 1 - e^{-y}, \quad y \geq 0 \Rightarrow \\ F_Y^{\max}(y) &= (1 - e^{-y})^2, \quad y \geq 0 \Rightarrow \\ p_Y^{\max}(y) &= 2e^{-y}(1 - e^{-y}) \Rightarrow \\ E\{\max(\beta_1, \beta_2)\} &= \int_0^{\infty} 2ye^{-y}(1 - e^{-y}) dy = \frac{3}{2}. \end{aligned}$$

therefore, the maximum average SNR gain for a (2,1) system is $10 \log_{10}(\frac{3}{2}) = 1.76$ dB. Values of the maximum average SNR gains for various combinations of M and N of a MIMO system are evaluated numerically and summarized in Table 6.1.

Gain (dB)	$M=2$	$M=3$	$M=4$	$M=5$	$M=6$
$N = 1$	1.7609	2.6323	3.1875	3.5856	3.8917
$N = 2$	1.383	2.0588	2.4886	2.797	3.0344
$N = 3$	1.181	1.7567	2.1232	2.3866	2.5897
$N = 4$	1.0498	1.5615	1.8876	2.1223	2.3033
$N = 5$	0.9555	1.4215	1.7188	1.9329	2.0983

Table 6.1: The maximum gains in the average SNR for MIMO systems.

Examining Table 6.1, we find that the maximum gain in the average SNR due to the proposed adaptive power allocation increases as the number of transmit antennas increases, and decreases as the number of receive antenna increases. This can be intuitively explained as follows. As M increases with N fixed, $E\{\max(\beta_1, \dots, \beta_M)\}$ has more dimensions to provide a gain. On the other hand, when N increases with M fixed, the difference between $\max(\beta_1, \dots, \beta_M)$ and the average value of β_i decreases.

6.3.3. The New Scheme with Imperfect Feedback

In a practical system, channel coefficients will not be perfectly known. Even if channel coefficients were perfectly known, there will be quantization errors in the feedback. In order to resolve the problem of imperfect feedback and lower the number of feedback bits required, we pre-determine a finite set of values for α_m . The receiver only needs to inform the transmitter that which pre-determined power scaling factor should be assigned to antenna m . For example, in a system with two transmit antennas, we pre-determine a fixed set of values for α_m as $\alpha_m \in (0.8, 0.6)$. If the receiver finds out that $\beta_1 > \beta_2$, it then needs only 1 bit to

instruct the transmitter to allocate 0.8 to antenna 1. For a general system with M transmit antennas, $\lceil \log_2(M!) \rceil$ feedback bits are needed.

For simplicity, we assume that the feedback system is a SISO system with the same constellation as the information channel. The average energy of feedback symbols is also E_s . The pre-determined power scaling factors $\alpha_m, m = 1, \dots, M$ for a particular choice of parameter u can be determined using the method as follows. As defined earlier, β_m is a function of fading coefficients $h_{m,1}, \dots, h_{m,N}$. For each realization of the channel coefficients, let $\beta_{max} = \max\{\beta_1, \dots, \beta_M\}$. The pre-determined largest power scaling factor α_{max} can be set as $\alpha_{max} = E \left\{ \sqrt{\frac{\beta_{max}^u}{\sum_{m=1}^M \beta_m^u}} \right\}$. In the same manner, let β_{sec} be the second largest value among β_1, \dots, β_M , for each realization of the channel. The second largest power scaling factor α_{sec} is calculated to be $\alpha_{sec} = E \left\{ \sqrt{\frac{\beta_{sec}^u}{\sum_{m=1}^M \beta_m^u}} \right\}$. This method can be continued until the smallest scaling factor α_{min} is determined as $\alpha_{min} = \sqrt{1 - \alpha_{max}^2 - \alpha_{sec}^2 - \dots}$. As an example, if u is chosen to be $u = 1$ for a system with $M = 3$, then the pre-determined power scaling factors can be calculated to be $(\alpha_1, \alpha_2, \alpha_3) \approx (0.7765, 0.5158, 0.3620)$. If u is chosen to be $u = 2$, then $(\alpha_1, \alpha_2, \alpha_3) \approx (0.8602, 0.4144, 0.2973)$.

For 3 transmit antennas, we have to use $\lceil \log_2(3!) \rceil = 3$ bits to feed back $3! = 6$ possible groups $(\alpha_{max}, \alpha_{sec}, \alpha_{min})$. However, the 3 bits could represent 8 unique groups, yielding two invalid groups. The transmission power allocation strategy for this case is that if feedback symbols are erroneously decoded as one of two invalid groups, equal power allocation will be used in next transmission.

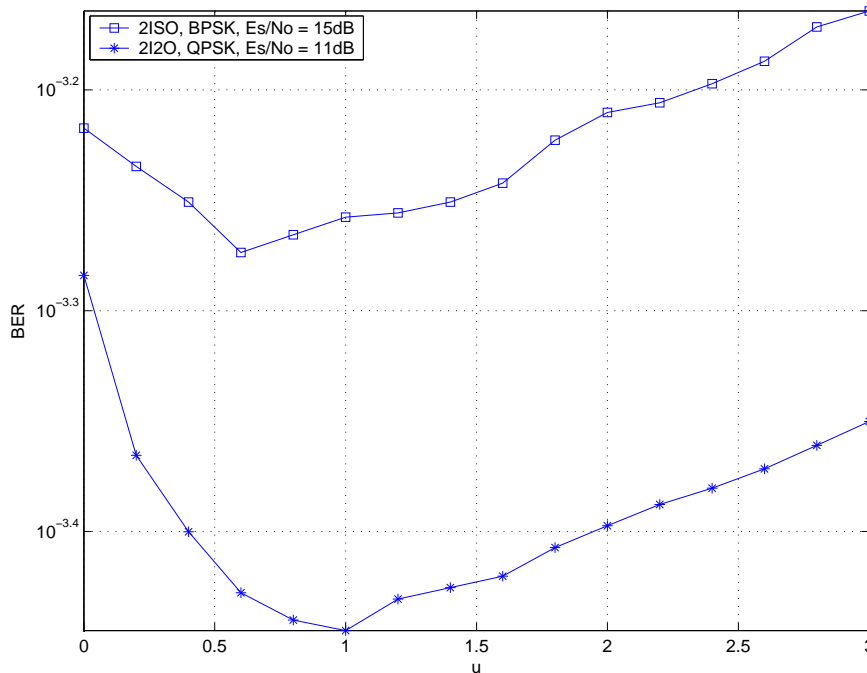


FIGURE 6.1. BER versus parameter u ($M = 2, N = 1, 2$)

6.4. Numerical Examples and Discussion

Simulated results demonstrating the performance of the proposed adaptive power allocation schemes are obtained in this section. Fig. 6.1 shows the error probability of different systems as a function of parameter u . It is found that for a (2,1) system with BPSK modulation operating at $E_s/\mathcal{N}_0 = 15\text{dB}$, the optimum value of u is 0.6. The corresponding power scaling factors for the proposed adaptive scheme with imperfect feedbacks can be determined to be $(\alpha_{max}, \alpha_{min}) \approx (0.8196, 0.57293)$. For a (2,2) system with QPSK modulation operating at $E_s/\mathcal{N}_0 = 11\text{dB}$, the optimum value of u is found to be 1. The corresponding power scaling factors for the two transmit antennas are determined to be $(\alpha_{max}, \alpha_{min}) \approx (0.88452, 0.4665)$.

It is usually not easy to determine the optimum value of u by an analytical approach since it depends on E_s/\mathcal{N}_0 in the information channel, the power of feedback symbols, the number of transmit and receiver antennas (M, N), and the modulation scheme. With the feedback model and PSK modulation, the optimum u in the sense of minimizing error probabilities can be calculated numerically using the procedure described below.

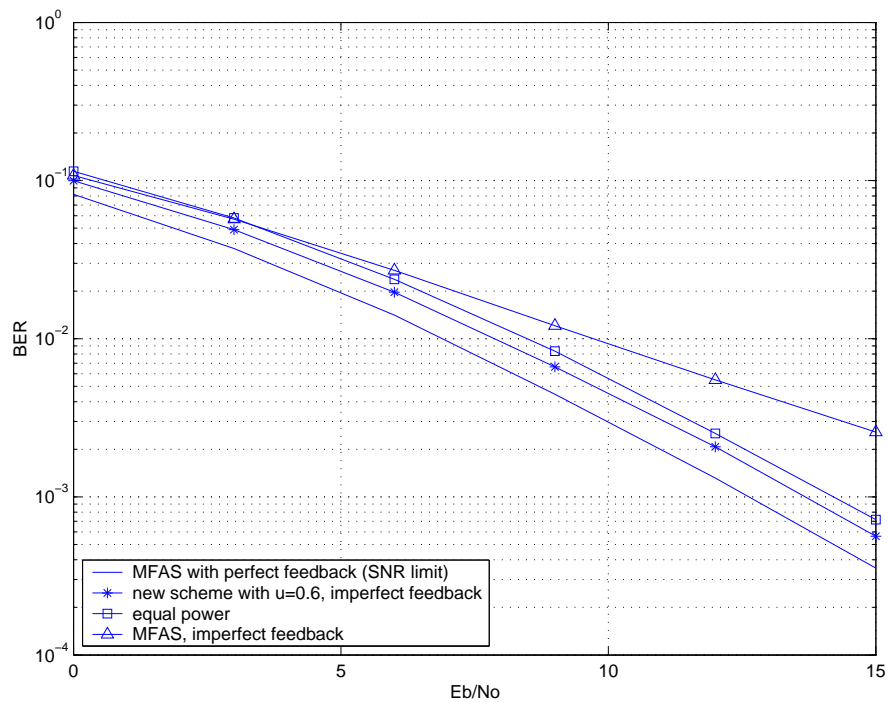


FIGURE 6.2. BER versus E_b/\mathcal{N}_0 curves for different schemes ($M = 2, N = 1$, BPSK)

According to Eq. (6.5), orthogonal space-time block codes in an (M, N) system have the same performance as a $(1, MN)$ system (a diversity-reception only system) using maximal ratio combining, provided that the transmit power per antenna is the same in both systems to make the comparison fair. Therefore, the optimum value of u can be found by using the exact error probabil-

ity for multichannel PSK signals given in ([74], Appendix C). As an example, let us consider the Alamouti scheme using BPSK in a (2, 1) system. We can easily compute the error probability in the feedback channel P_{feedback} and the error probability in the information channel for equal power allocation $P_{\text{i,equal}}$ (no adaptive power allocation), where $P_{\text{i,equal}} = f(\frac{E_s}{N_0})$ is a function of the received signal-to-noise ratio. Additionally, we have $E\{\beta^{\text{max}}\} = 1.5$ from Table 6.1. Thus, $E\{\beta^{\text{min}}\} = 2 - 1.5 = 0.5$. The average error probability for the information channel with adaptive power allocation under imperfect feedback is given by $P_{\text{i,adp}} = (1 - P_{\text{feedback}})f(1.5\alpha_{\text{max}}^2 \frac{E_s}{N_0}) + P_{\text{feedback}}f(0.5(1 - \alpha_{\text{max}}^2) \frac{E_s}{N_0})$, where $\alpha_{\text{max}} \in (0, 1)$ is a variable that depends on u . If we fix $\frac{E_s}{N_0}$, then $P_{\text{i,adp}}$ is a function of u . The optimal value of u can be found by minimizing $P_{\text{i,adp}}$.

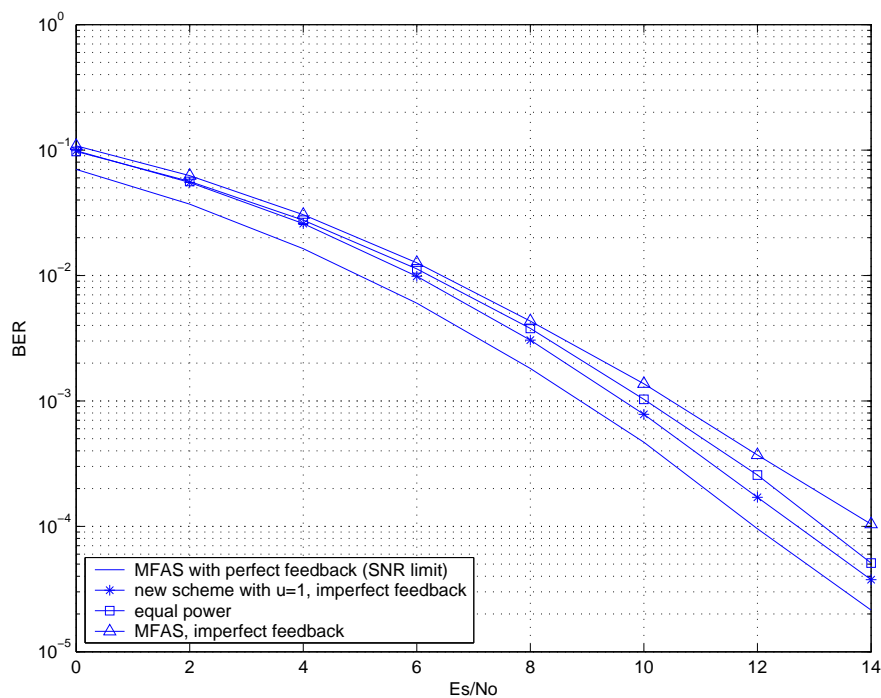


FIGURE 6.3. BER versus E_s/N_0 curves for different schemes ($M = 2, N = 2$, QPSK)

Figs. 6.2 and 6.3 compare the error performances of the MFAS, the equal-power scheme, and the adaptive power allocation scheme which applies the optimum u . Although the optimum u depends on E_s/\mathcal{N}_0 , for simplicity the values of u obtained in Fig. 6.1 are used for any E_s/\mathcal{N}_0 in Figs. 6.2 and 6.3. It is found that when perfect feedback symbols are assumed, the antenna-selection scheme works the best. However, when there are feedback symbol errors, the antenna-selection scheme suffers from diversity loss.

6.5. Conclusion

We have proposed a new power allocation scheme for space-time block coded MIMO systems. If the channel coefficients are known, the power scaling factors for all transmit antennas are controlled by a single parameter u which, for some special cases, can be predetermined numerically. Different choices of parameter u yields different SNR gains. The maximum achievable SNR gain can be achieved by choosing an appropriate value of u . Some special choices of parameter u with the proposed adaptive power allocation scheme reduce to some existing STBC power allocation schemes (i.e. [77, 36]). A much simpler power allocation scheme (single antenna selection) that needs significantly less number of feedback bits is also proposed. Performance gains of the proposed schemes over the conventional equal-power STBC scheme are simulated for systems with different number of antennas and modulation schemes.

7. SIMPLIFIED RECEIVER DESIGN FOR STBC BINARY CPM WITH MODULATION INDEX $H = 1/2$

CPM is a very attractive modulation scheme for wireless communications because of its constant envelope, compact spectrum, and flexible bandwidth-performance tradeoffs. Binary CPM with modulation index $1/2$ (for brevity, we call it as BCPM0.5 in this paper) is widely used in wireless communications. For example, minimum shift keying (MSK) and Gaussian minimum shift keying (GMSK) which is used in the global system for mobile communications (GSM). The duration LT of the pre-modulation filter is one of the parameters that controls the signal spectrum, where T is the bit period; increasing the L results in a more compact spectrum at the expense of a higher bit-error rate for the same bit-energy-to-noise-density ratio E_b/\mathcal{N}_0 due to the increased level of ISI. These properties make BCPM0.5 an attractive scheme to use, especially in power-constrained applications. Combining space-time codes with it adds diversity while having constant envelope properties and low complexity.

In the literature, space-time code design criteria for general CPM were developed by Zhang and Fitz [82], and a reduced-complexity receiver for multi-antenna layered space-time systems with binary CPM was described by Zhao and Giannakis [83]. Space-time coded MSK was analyzed by Cavers [84]. In particular, the relationship between offset and non-offset modulation formats and the effect of pulse shape was explored. Orthogonal space-time coding with CPM for systems with two transmit antennas was introduced in [85, 86] to reduce decoding complexity. However, Viterbi decoders were used to recover transmitted symbols in these papers and decoding complexity is still relatively high. Additionally, the power spectrum density (PSD) of the transmitted signal is affected because of the introduction of an additional phase shift.

In this chapter, we focus on designing orthogonal space-time block codes [36, 37] for BCPM0.5 to achieve spatial diversity. The orthogonal code design is based on Laurent decomposition of BCPM0.5 signals combined with differential precoding. We then derive a simplified decoder with a linear finite impulse response (FIR) filter to reduce ISI inherent in BCPM0.5 signals with two transmit antennas, and thus significantly improve the error performance. For STBC BCPM0.5 with three and more transmit antennas, decoding based on FIR filtering becomes inefficient; therefore, we derive a soft decision feedback decoding scheme to simplify the receiver while guaranteeing a satisfactory performance. The STBC BCPM0.5 designed in this paper has a lower decoding complexity than space-time trellis coded BCPM0.5, while their performances are similar. We will briefly discuss the signal model in Section 7.1. Section 7.2 presents details of the design of STBC with BCPM0.5 based on Laurent decomposition. Two low-complexity, ISI-resistant decoding schemes for STBC BCPM0.5 are presented in Section 7.3. Finally, we provide performance analysis and numerical results to assess the diversity performance of the proposed code and the effect of various system parameters.

7.1. System Model

The baseband model of a binary CPM signal can be expressed as [82, 87]

$$s(t) = \sqrt{\frac{E_b}{T}} e^{j\theta(t)}, \quad t \geq 0 \quad (7.1)$$

where E_b is the energy per bit. The phase of the transmitted signal is expressed as

$$\theta(t) = 2\pi h \int_0^t \sum_{i=0}^{N-1} \alpha_i g(\tau - iT) d\tau, \quad t \geq 0 \quad (7.2)$$

where $h = 0.5$ is the modulation index in this paper, $\alpha_i \in \{+1, -1\}$ with equal probability are the transmitted bits, N is the number of consecutive bits, and $g(t)$ is the frequency pulse and is nonzero in the interval $[0, LT]$, $g(t)$ has area equal to $1/2$ and is symmetric about $LT/2$. For instance, $g(t)$ of GMSK is expressed as

$$g(t) = \frac{1}{2T} \left[Q\left(\beta \frac{BT}{T} \left(t - \frac{(L+1)T}{2}\right)\right) - Q\left(\beta \frac{BT}{T} \left(t - \frac{(L-1)T}{2}\right)\right) \right], \quad t \in [0, LT]$$

where $\beta = 2\pi/\sqrt{\ln(2)}$, B is 3-dB bandwidth and $Q(\cdot)$ is the Gaussian Q -function defined as

$$Q(t) = \int_t^\infty \frac{1}{\sqrt{2\pi}} e^{-\tau^2/2} d\tau \quad (7.3)$$

L depends on the system time-bandwidth product BT ; the smaller the BT product, the larger the impulse length.

Let us define the integral of the frequency pulse as

$$q(t) = \int_0^t g(\tau) d\tau. \quad (7.4)$$

then, $\theta(t)$ in Eq. (7.2) can be written as

$$\theta(t) = \pi h \sum_{i=0}^{N-1} \alpha_i q(t - iT), \quad t \geq 0. \quad (7.5)$$

We consider systems with M transmit antennas and one receive antenna in this paper, but the results can be easily extended to systems with multiple receive antennas. The received signal is given as

$$r(t) = \sqrt{\frac{1}{M}} \mathbf{h}^T(t) \mathbf{s}(t) + n(t) \quad (7.6)$$

where $(\cdot)^T$ denotes transpose, $\sqrt{\frac{1}{M}}$ is used to normalize the total transmit power, $n(t)$ is a complex Gaussian noise with variance \mathcal{N}_0 , and $\mathbf{h}(t)$ is the channel fading-coefficient vector expressed as

$$\mathbf{h}(t) = [h_1(t), h_2(t), \dots, h_M(t)]^T \quad (7.7)$$

with $h_i(t)$ being the fading coefficient from transmit antenna i to the receive antenna. The transmitted signal vector is expressed as

$$\mathbf{s}(t) = [s_1(t), s_2(t), \dots, s_M(t)]^T \quad (7.8)$$

where $s_i(t)$ is the signal from transmit antenna i . As typically accepted in space-time codes, we adopt a quasistatic fading model in this paper. Thus, $h_i(t)$ is constant over a frame of transmitted data and changes independently from frame to frame.

7.2. Code Design Based on Laurent Decomposition

The complex baseband binary CPM signal in Eq. (7.1) can be exactly expressed as the sum of $K = 2^{L-1}$ pulse-amplitude modulation (PAM) signals as [87–89]

$$s(t) = \sqrt{\frac{E_b}{T}} \sum_{k=0}^{K-1} \sum_{n=0}^{N-1} e^{j\pi h a_{k,n}} c_k(t - nT), \quad t \in [LT, NT] \quad (7.9)$$

where the pseudo-symbols $\{a_{k,n}\}$ are related to the transmitted bits as

$$a_{k,n} = \sum_{i=0}^n \alpha_i - \sum_{j=1}^{L-1} \alpha_{n-j} \beta_{k,j}. \quad (7.10)$$

In Eq. (7.10), $\beta_{k,j} \in \{0, 1\}$ is used in the binary representation of the index k as

$$k = \sum_{j=1}^{L-1} 2^{j-1} \beta_{k,j}, \quad k \in [0, K-1]. \quad (7.11)$$

function $c_k(t)$ in Eq. (7.9) is expressed as

$$c_k(t) = f_0(t) \prod_{j=1}^{L-1} f_{j+L\beta_{k,j}}(t), \quad k \in [0, K-1] \quad (7.12)$$

where

$$f_j(t) = \frac{\sin(\phi(t+jT))}{\sin(\pi h)} = f_0(t+jT) \quad (7.13)$$

$$\phi(t) = \begin{cases} 2\pi h \int_0^t g(\tau) d\tau, & t \in [0, LT) \\ \pi h - 2\pi h \int_0^{t-LT} g(\tau) d\tau, & t \in [LT, 2LT) \\ 0, & \text{otherwise.} \end{cases}$$

among the K terms of PAM signals in Eq. (7.9), the first term $c_0(t-nT)$ usually contains the bulk of the total signal energy [88], and the length of $c_0(t)$ is $(L+1)T$ [89]. Therefore, considering only the first term $c_0(t-nT)$ will significantly reduce the decoding complexity with a negligible performance loss. By keeping only the major term, the binary CPM signal can be approximated as

$$s(t) \approx \sqrt{\frac{E_b}{T}} \sum_{n=0}^{N-1} e^{j\pi h a_{0,n}} c_0(t-nT). \quad (7.14)$$

For example, for MSK signals with $BT = \infty$, $L = 1$, $K = 2^{L-1} = 1$, the frequency impulse is

$$g(t) = \begin{cases} \frac{1}{2T}, & t \in [0, T) \\ 0, & \text{otherwise} \end{cases} \quad (7.15)$$

and Laurent decomposition consists of only the $c_0(t)$ term, which is expressed as

$$c_0(t) = \begin{cases} \sin(\frac{\pi t}{2T}), & t \in [0, 2T) \\ 0, & \text{otherwise.} \end{cases} \quad (7.16)$$

this also leads to the well-known interpretation of MSK as offset-QPSK in which the pulse shape is a half-cycle sinusoid with period $4T$ [87].

Suppose that the receiver has perfect knowledge of the channel fading coefficients. The maximum likelihood (ML) receiver calculates

$$\mathcal{E} = \int_{LT}^{NT} \left| r(t) - \sqrt{\frac{1}{M}} \mathbf{h}^T(t) \hat{\mathbf{s}}(t) \right|^2 dt \quad (7.17)$$

under all possible combinations of the transmitted bit sequence and the one which minimizes \mathcal{E} is the estimated sequence $\hat{\mathbf{a}} = [\hat{a}_{0,L}, \hat{a}_{0,L+1}, \dots, \hat{a}_{0,N}]$, where we assume that $[\hat{a}_{0,0}, \hat{a}_{0,1}, \dots, \hat{a}_{0,L-1}]$ are known, since, as observed in [87], Laurent decomposition is accurate only for $t \geq LT$ in Eq. (7.9).

Then, $\hat{\alpha}_n$ can be decoded by differential decoding of the pseudo-symbols $\hat{a}_{0,n}$ and $\hat{a}_{0,n-1}$. Note that $\hat{a}_{0,n} = \sum_{i=0}^n \hat{\alpha}_i$ [87, 88]. In this case, the Viterbi algorithm can be applied because of the memory structure of CPM signals. However, there is a performance loss due to differential detection. Fortunately, this loss can be eliminated by a data precoding algorithm applied to the non-return-to-zero (NRZ) source data symbols prior to BCPM0.5 modulation [90]. The precoding scheme is described as follows.

Let $d_k, d_k \in \{\pm 1\}, k \geq 0$, denote the equally probable source data symbols at time $t = kT$. The output of the precoder α_k , which is the input to the BCPM0.5 modulator, is formed as

$$\alpha_k = (-1)^k d_k d_{k-1} \quad (7.18)$$

where d_{-1} could be chosen as $d_{-1} = 1$. Since symbols d_k and α_k have identical statistics, BCPM0.5 signals with and without precoding have the same power spectrum.

When precoding is applied to the source data symbols d_k , we have

$$e^{j\pi h a_{0,n}} = e^{j\frac{\pi}{2} a_{0,n}} = \begin{cases} jd_n, & n = 0, 2, 4, \dots \\ d_n, & n = 1, 3, 5, \dots \end{cases} \quad (7.19)$$

with precoding, the memory in BCPM0.5 is eliminated; thus we can use a linear receiver, rather than a Viterbi decoder, to decode the precoded BCPM0.5 signals. Now, we can readily apply OSTBC for BCPM0.5 with precoding. The transmission matrix is given by

$$\mathbf{G} = \begin{bmatrix} g_{11} & g_{12} & \cdots & g_{1M} \\ g_{21} & g_{22} & \ddots & g_{2M} \\ \vdots & \ddots & \ddots & \vdots \\ g_{p1} & g_{p2} & \cdots & g_{pM} \end{bmatrix} \quad (7.20)$$

where g_{ij} is information bit or its negative transmitted from antenna j within bit interval i and p is the block size.

For example, the modified Alamouti scheme (the transpose of the original Alamouti code, because we want to keep the transmitted signal from the first antenna the same as transmitted signal in single input single output (SISO))

with transmission matrix $\begin{bmatrix} x_1 & -x_2 \\ x_2 & x_1 \end{bmatrix}$ can be used for 2 transmit antennas with BCPM0.5. From the first transmit antenna, we transmit $d_0, d_1, d_2, d_3, \dots$; therefore, the transmitted signal is exactly the same as the single-antenna case. For the second transmit antenna, we transmit $-d_1, d_0, -d_3, d_2, \dots$. Obviously, signals from the two transmit antennas have the same spectrum. The modified Alamouti

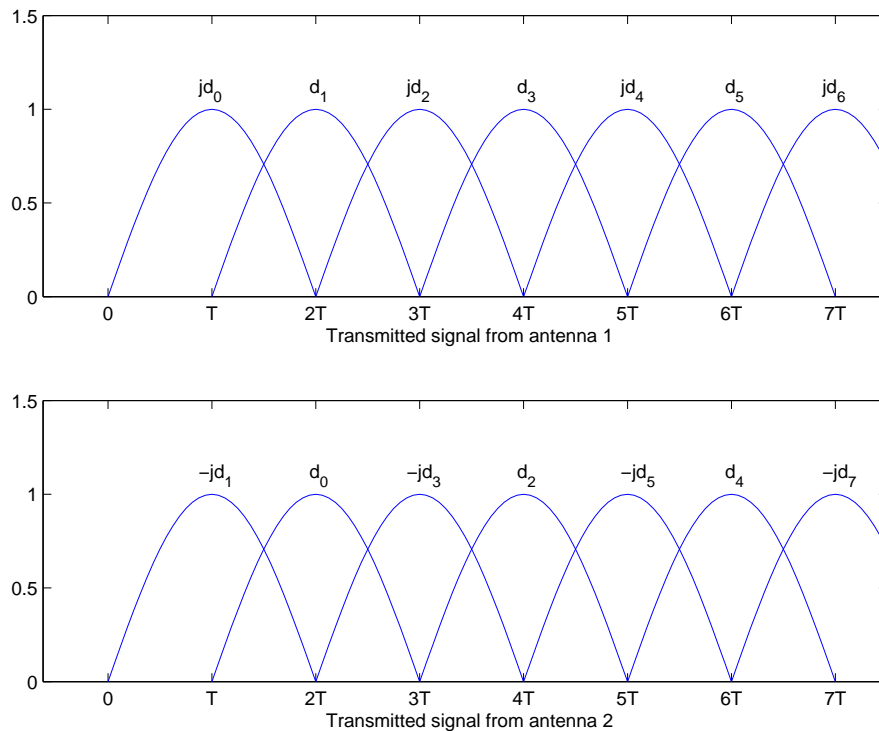


FIGURE 7.1. The modified Alamouti scheme ($M = 2$) for MSK with precoding based on Laurent decomposition.

scheme for MSK signals based on Laurent decomposition with precoding is shown in Fig. 7.1.

7.3. Low-Complexity Decoding

7.3.1. The receiver without FIR

After passing through a matched filter $c_0(-t)$, the received signal is sampled at time $t = kT$. The output of the sampler is expressed as $r_i = \int_{iT}^{(i+L+1)T} r(t)c_0(t-iT)dt$, which is a sufficient statistic of the transmitted signal. Space-time decoding for linear modulations can also be applied on r_i .

Neglecting ISI in detecting BCPM0.5 signals leads to the simplest receiver whose decoding complexity is the same as that of linear modulations. However, ISI increases as the number of transmit antennas and L increase, which will result in performance degradation. Note that, for MSK, there is no ISI for single transmit antenna as adjacent pulses are orthogonal (in-phase and quadrature are orthogonal). In this case, the decision variables are formed by multiplying the complex conjugate of fading coefficients with the received signal r_i . For multiple transmit antennas, however, ISI cannot be eliminated after space-time decoding because transmitted signals from different transmit antennas experience independent fading.

We illustrate the decoding scheme by using the following example. Let us consider MSK with the Alamouti space-time coding scheme. To decode symbols d_{2n} and d_{2n+1} , we use the outputs of the sampler after the matched filter (r_{2n} and r_{2n+1}). With the assumption of a quasistatic fading, we can write $h_i(t) = h_i$. Therefore, we have

$$r_{2n} = \sqrt{\frac{E_b}{MT}} [h_1 (jd_{2n}c_{\text{full}} + (d_{2n-1} + d_{2n+1})c_{\text{half}}) + h_2 (-jd_{2n+1}c_{\text{full}} + (d_{2n-2} + d_{2n})c_{\text{half}})] + n_{2n} \quad (7.21a)$$

$$r_{2n+1} = \sqrt{\frac{E_b}{MT}} [h_1 (d_{2n+1}c_{\text{full}} + j(d_{2n} + d_{2n+2})c_{\text{half}}) + h_2 (d_{2n}c_{\text{full}} - j(d_{2n+1} + d_{2n+3})c_{\text{half}})] + n_{2n+1} \quad (7.21b)$$

where

$$c_{\text{full}} = \int_0^{(L+1)T} c_0^2(t) dt = \int_0^{2T} \sin^2\left(\frac{\pi t}{2T}\right) dt = T \quad (7.22a)$$

$$c_{\text{half}} = \int_0^{(L+1)T} c_0(t)c_0(t-T) dt = T/\pi \quad (7.22b)$$

$$n_{2n} = \int_{2nT}^{(2n+L+1)T} n(t)c_0(t-2nT) dt \quad (7.22c)$$

$$n_{2n+1} = \int_{(2n+1)T}^{(2n+L+2)T} n(t)c_0(t-(2n+1)T) dt. \quad (7.22d)$$

by applying the space-time decoding algorithm described by Alamouti [36], we have

$$\begin{aligned} d'_{2n} &= \Re \left\{ h_1^* r_{2n} / j + h_2 r_{2n+1}^* \right\} \\ &= \Re \left\{ \sqrt{\frac{E_b}{MT}} \left[(|h_1|^2 + |h_2|^2) d_{2n} c_{\text{full}} - j h_1^* h_2 c_{\text{half}} (2d_{2n} + d_{2n-2} + d_{2n+2}) \right] - \right. \\ &\quad \left. j h_1^* n_{2n} + h_2 n_{2n+1}^* \right\} \\ &= \Re \left\{ \sqrt{\frac{E_b T}{M}} \left[(|h_1|^2 + |h_2|^2) d_{2n} - \frac{j h_1^* h_2}{\pi} (2d_{2n} + d_{2n-2} + d_{2n+2}) \right] - \right. \\ &\quad \left. j h_1^* n_{2n} + h_2 n_{2n+1}^* \right\} \end{aligned} \quad (7.23a)$$

$$\begin{aligned} d'_{2n+1} &= \Re \left\{ -h_2^* r_{2n} / j + h_1 r_{2n+1}^* \right\} \\ &= \Re \left\{ \sqrt{\frac{E_b}{MT}} \left[(|h_1|^2 + |h_2|^2) d_{2n+1} c_{\text{full}} + j h_1 h_2^* c_{\text{half}} (2d_{2n+1} + d_{2n-1} + d_{2n+3}) \right] + \right. \\ &\quad \left. j h_2^* n_{2n} + h_1 n_{2n+1}^* \right\} \\ &= \Re \left\{ \sqrt{\frac{E_b T}{M}} \left[(|h_1|^2 + |h_2|^2) d_{2n+1} + \frac{j h_1 h_2^*}{\pi} (2d_{2n+1} + d_{2n-1} + d_{2n+3}) + \right. \right. \\ &\quad \left. \left. j h_2^* n_{2n} + h_1 n_{2n+1}^* \right] \right\} \end{aligned} \quad (7.23b)$$

where $\Re\{\cdot\}$ denotes the real part.

The decision variables can be written as

$$\hat{d}_{2n} = \text{sgn}\{d'_{2n}\} \quad (7.24a)$$

$$\hat{d}_{2n+1} = \text{sgn}\{d'_{2n+1}\} \quad (7.24b)$$

where $\text{sgn}\{\cdot\}$ denotes signum function. Note that the nonzero terms $2d_{2n} + d_{2n-2} + d_{2n+2}$ and $2d_{2n+1} + d_{2n-1} + d_{2n+3}$ in Eqs. (7.23a) and (7.23b) cause ISI. If ISI is completely canceled, space-time coded MSK has the same error performance as space-time coded BPSK.

7.3.2. The receiver with FIR

Examining Eqs. (7.23a) and (7.23b) and noting that $\Re\{-jh_1^*h_2/\pi\} = \Re\{jh_1h_2^*/\pi\}$, we found that d'_{2n} and d'_{2n+1} are equivalent to the outputs when the input information sequence $d_0, d_1, d_2, d_3, \dots$ is passed through a pseudo-channel modeled as a 5-tap symmetric FIR filter with an impulse response

$$\mathbf{h}_{\text{imp}} = \sqrt{\frac{E_b T}{M}} \Re \left\{ \left[-\frac{jh_1^*h_2}{\pi}, 0, (|h_1|^2 + |h_2|^2) - \frac{2jh_1^*h_2}{\pi}, 0, -\frac{jh_1^*h_2}{\pi} \right] \right\}. \quad (7.25)$$

the output of the pseudo-channel is further corrupted by additive Gaussian noise.

To design the optimum linear receiver in the sense of minimum mean-square error (MMSE), we apply the method in Chapter 6 of [91]. The optimum FIR filter to recover the original information bit sequence is obtained to be

$$\mathbf{c}_{\text{mmse}} = \mathbf{R}^{-1} \mathbf{d} \quad (7.26)$$

where $\mathbf{R} = E\{\mathbf{x}(n)\mathbf{x}^T(n)\}$ ($x(n) = d'_n, n = 0, 1, \dots$) is the autocorrelation matrix of d'_n , the output of the pseudo-channel which can be calculated by using Eqs.

(7.23a) and (7.23b), and $E\{\cdot\}$ denotes expectation. $\mathbf{d} = E\{d_n \mathbf{x}(n)\}$ is the cross-correlation vector between the input and the output of the pseudo-channel. Note that the information bit sequence is assumed to be white with zero mean and power $P_d = E\{|d_n|^2\} = 1$.

The autocorrelation matrix \mathbf{R} is Toeplitz, symmetric, and real, and is expressed as

$$\mathbf{R} = \begin{bmatrix} r_x(0) & r_x(1) & r_x(2) & r_x(3) & r_x(4) \\ r_x(-1) & r_x(0) & r_x(1) & r_x(2) & r_x(3) \\ r_x(-2) & r_x(-1) & r_x(0) & r_x(1) & r_x(2) \\ r_x(-3) & r_x(-2) & r_x(-1) & r_x(0) & r_x(1) \\ r_x(-4) & r_x(-3) & r_x(-2) & r_x(-1) & r_x(0) \end{bmatrix}. \quad (7.27)$$

the autocorrelation of $x(n)$, $r_x(l)$, is obtained as

$$\begin{aligned} r_x(0) &= \mathbf{h}_{\text{imp}}^2(1) + \mathbf{h}_{\text{imp}}^2(2) + \cdots + \mathbf{h}_{\text{imp}}^2(5) + \sigma_v^2 \\ r_x(\pm 1) &= \mathbf{h}_{\text{imp}}(1)\mathbf{h}_{\text{imp}}(2) + \cdots + \mathbf{h}_{\text{imp}}(4)\mathbf{h}_{\text{imp}}(5) \\ r_x(\pm 2) &= \mathbf{h}_{\text{imp}}(1)\mathbf{h}_{\text{imp}}(3) + \cdots + \mathbf{h}_{\text{imp}}(3)\mathbf{h}_{\text{imp}}(5) \\ r_x(\pm 3) &= \mathbf{h}_{\text{imp}}(1)\mathbf{h}_{\text{imp}}(4) + \mathbf{h}_{\text{imp}}(2)\mathbf{h}_{\text{imp}}(5) \\ r_x(\pm 4) &= \mathbf{h}_{\text{imp}}(1)\mathbf{h}_{\text{imp}}(5) \\ r_x(l) &= 0, \quad |l| \geq 5 \end{aligned} \quad (7.28)$$

where σ_v^2 is the power of the noise term of d'_n given in Eqs. (7.23a) and (7.23b).

The minimum order of \mathbf{c}_{mmse} is the number of taps of \mathbf{h}_{imp} . Note that although a higher order of \mathbf{c}_{mmse} usually results in a better performance, we still choose the minimum order in this paper to achieve the best performance-complexity tradeoff. The cross-correlation vector is found to be

$$\mathbf{d} = [\mathbf{h}_{\text{imp}}(5), \mathbf{h}_{\text{imp}}(4), \dots, \mathbf{h}_{\text{imp}}(1)]^T. \quad (7.29)$$

consequently, the optimum FIR filter $\mathbf{c}_{\text{mmse}} = \mathbf{R}^{-1}\mathbf{d}$ must be an adaptive filter whose impulse response depends on the estimates of the channel coefficients. In fact, \mathbf{c}_{mmse} is essentially the inverse filter of \mathbf{h}_{imp} with the noise effect taken into consideration. In practice, if noise power σ_v^2 is unknown, we can design a zero-forcing filter \mathbf{c}_{zf} based on similar procedures; the only changes needed is to let $r_x(0) = \mathbf{h}_{\text{imp}}^2(1) + \mathbf{h}_{\text{imp}}^2(2) + \dots + \mathbf{h}_{\text{imp}}^2(5)$ in Eq. (7.28).

The most complex part of the linear receiver designed in this paper comes from inverting the correlation matrix \mathbf{R} . Since \mathbf{R} is a Toeplitz and symmetric matrix, the Levinson-Durbin recursion algorithm could be applied to efficiently calculate the inversion. More details of such algorithms can be found in [92]. Moreover, the inversion can be further simplified by considering the zero elements in \mathbf{R} . Overall, the proposed linear receiver has a much lower computational complexity than existing schemes that employ the Viterbi decoder.

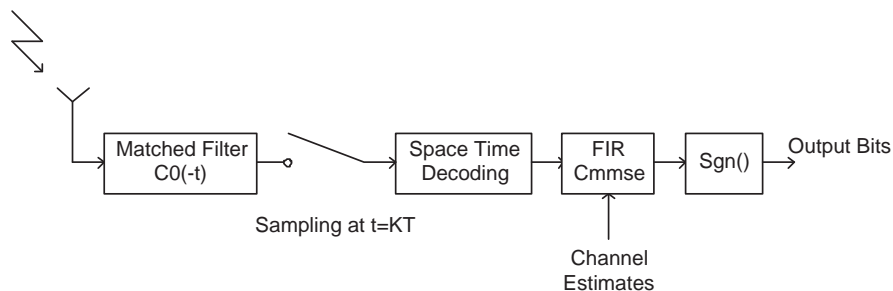


FIGURE 7.2. Receiver structure of space-time block coded BCPM0.5 with 2 transmit antennas.

The structure of the proposed linear receiver is shown in Fig. 7.2. As mentioned earlier, the FIR filter is an adaptive filter whose taps are dependent on channel estimates. CPM with $L = 1$ is called full response CPM, i.e. MSK.

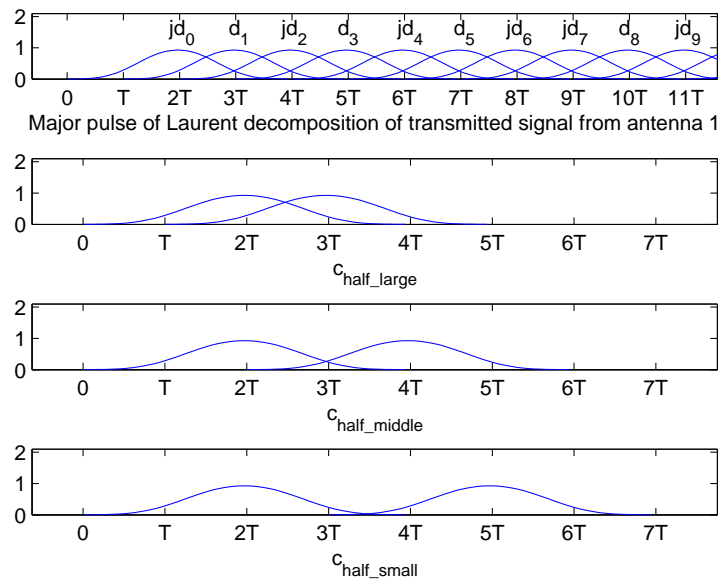


FIGURE 7.3. GMSK with $BT = 0.3$, $L = 3$

For partial response BCPM0.5 ($L > 1$), the design method of FIR receiver is the same, the only difference is the order of \mathbf{h}_{imp} . For example, \mathbf{h}_{imp} for GMSK with $BT = 0.5, L = 2$ has five taps (three nonzero taps); \mathbf{h}_{imp} for GMSK with $BT = 0.3, L = 3$ has nine taps (five nonzero taps). However, the smallest two among five nonzero taps can be ignored to reduce the order to five. The details are shown in Fig. 7.3.

There are three overlap terms among $c_0(t)$ and its time-shifted copies which, as seen clearly from Eq. (7.23), cause ISI. These terms are expressed as

$$\begin{aligned}
c_{\text{half_large}} &= \int_0^{(L+1)T} c_0(t)c_0(t-T) \approx 0.52T \\
c_{\text{half_middle}} &= \int_0^{(L+1)T} c_0(t)c_0(t-2T) \approx 0.06T \\
c_{\text{half_small}} &= \int_0^{(L+1)T} c_0(t)c_0(t-3T) \approx 0.0008T.
\end{aligned} \tag{7.30}$$

it found that $c_{\text{half_small}}$ causes only about 0.1% of the total interference energy; thus we may ignore its contribution to lower decoding complexity, two among five nonzero taps are contributed by $c_{\text{half_small}}$ only, so we can reduce the order of \mathbf{h}_{imp} from nine to five. As a result, GMSK with $L = 3$ has the same decoding complexity as that with $L = 1, 2$. Similarly, for $L > 3$ GMSK or non-GMSK BCPM0.5, keeping the pulses that contribute the largest amount of ISI could significantly decrease the decoding complexity with a negligible performance loss.

7.3.3. The receiver with decision feedback

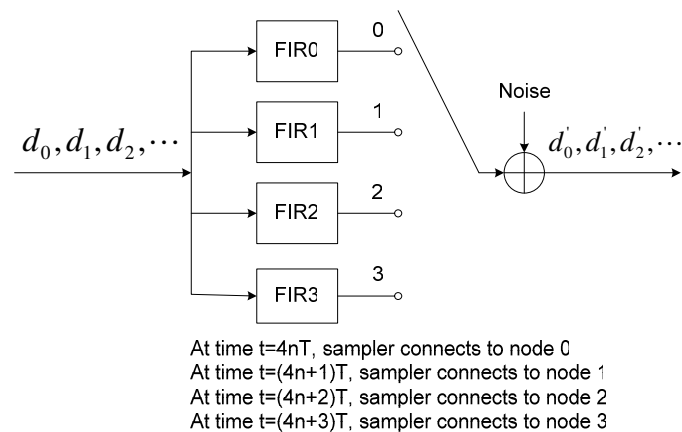


FIGURE 7.4. Equivalent system model for space-time block coded GMSK with 4 antennas.

When the number of transmit antennas is greater than two, the symmetry property of \mathbf{h}_{imp} does not hold anymore. As an example, let us consider orthogonal

space time block coded BCPM0.5 for 4 transmit antennas, we apply the transpose of code matrix (4) in [37] as our transmission matrix in this paper. By apply the decoding algorithm for linear modulations, we obtain similar results as given Eq. (7.23) for $d'_{4n}, d'_{4n+1}, d'_{4n+2}, d'_{4n+3}$. If we treat information bits $d_0, d_1, d_2, d_3, \dots$ as the system input and $d'_0, d'_1, d'_2, d'_3, \dots$ as the output, the equivalent model of this system is illustrated in Fig. 7.4.

The equivalent system model includes four FIR filters with different coefficient and a sampler. Unfortunately, the overall system is no longer linear, and linear receivers will suffer from an irreducible error floor especially when the value of L is small. Therefore, for more than 2 transmit antennas, we apply a decision-feedback receiver with soft decisions to achieve a good performance.

Generally speaking, d'_n is a linear combination of d_n corrupted by noise. At each iteration of the decision-feedback process, soft decisions for d_n are derived first based on d'_n , which is then followed by ISI suppression. A common method is to use the tanh function [93]; however, in practice, tanh function is difficult to realize because of its nonlinearity. We will apply a linear function to obtain optimum soft decisions in the sense of minimum mean-square error.

The output of the space-time decoder is the information bit sequence interrupted by ISI and additive noise, which can be expressed as $r = \delta_0 s_0 + \sum_{i=1}^l \delta_i s_i + \delta_n n$, where $s_i, i = 0, \dots, l$, are independent bits with equal probability to take on the values of -1 and 1, l equals the number of taps of the FIR filter minus one in the equivalent system model shown in Fig. 7.4, n is the real Gaussian noise, $\delta_i, i = 0, \dots, l$, are the power of s_i , which are essentially the taps of the FIR filter in Fig. 7.4, and δ_n is the noise power. The optimal scaler x used to approximate s_0 should minimize mean-square error as

$$\underbrace{\operatorname{argmin}}_x E \left\{ \left(\frac{\delta_0 s_0 + \sum_{i=1}^l \delta_i s_i + \delta_n n}{x} - s_0 \right)^2 \right\}. \quad (7.31)$$

with some simplifications, we obtain

$$x = \frac{\sum_{i=0}^l \delta_i^2 + \delta_n^2}{\delta_0} \quad (7.32)$$

Strictly speaking, x in Eq. (7.32) is optimal only for the first iteration, as the signal-to-interference-plus-noise ratio (SINR) will be slightly different after the first iteration. However, considering the slight variation of SINR for each iteration will increase the hardware complexity without significant performance improvements. Therefore, we keep x constant in the iterative process. The magnitude of r/x should be further bounded, i.e., soft decisions for s_0 should satisfy $\operatorname{sgn}\{r/x\}$ if $|r/x| > \eta$ [94]. We may set $\eta = 1$ for any number of transmit antennas and any frequency impulse length L . Compared with the optimal η values, which can be found by exhaustive searching, $\eta = 1$ suffers from only negligible performance loss.

To obtain x , we must calculate the power of the FIR filter in the equivalent system model, which implies that we need to compute the power of four FIR filters for all the four transmit antennas shown in Fig. 7.4. Fortunately, the major taps δ_0 of these four filters are very close to one another while the weight magnitudes for the minor taps $\delta_i, i = 1, \dots, l$, are from the same set but with different permutations. Therefore, we can use any of the four filters to compute x , rather than calculating x four times.

Let us again use the system with two transmit antennas to illustrate the details of the decoding. In Eq. (7.23), the value of d'_{2n} is dependent on d_{2n-2} and d_{2n+2} . In order to suppress ISI caused by d_{2n-2} and d_{2n+2} , we can eliminate the

effects of d_{2n-2}, d_{2n+2} by using soft decisions of d_{2n-2} and d_{2n+2} from Eq. (7.23).

The soft decision for the first iteration is

$$d_n^{(1)} = \begin{cases} \frac{\mathbf{h}_{\text{imp}(3)}d'_n}{\sum_{i=1}^5 |\mathbf{h}_{\text{imp}(i)}|^2 + \delta_n^2}, & \left| \frac{\mathbf{h}_{\text{imp}(3)}d'_n}{\sum_{i=1}^5 |\mathbf{h}_{\text{imp}(i)}|^2 + \delta_n^2} \right| < 1 \\ \text{sgn} \left(\frac{\mathbf{h}_{\text{imp}(3)}d'_n}{\sum_{i=1}^5 |\mathbf{h}_{\text{imp}(i)}|^2 + \delta_n^2} \right), & \left| \frac{\mathbf{h}_{\text{imp}(3)}d'_n}{\sum_{i=1}^5 |\mathbf{h}_{\text{imp}(i)}|^2 + \delta_n^2} \right| \geq 1. \end{cases} \quad (7.33)$$

The soft decision $d_n^{(j)}$ for the j -th iteration is computed by substituting d'_n in Eq. (7.33) with $d_n^{(j-1)}$. After j iterations, the signum function is applied to obtain the final estimate of d_n . The complexity of the decision-feedback receiver with soft decisions depends on the number of iterations and the number of taps of the FIR filters. The number of iterations is dependent on mainly L . However, the number of taps of the FIR filters depends on L and the number of antennas. When L is large, which is equivalent to a small BT , the number of taps of the FIR filters increases, and the complexity of the decision-feedback receiver with soft decisions increases accordingly. When we allow a small amount of ISI which causes a negligible performance loss, the decoding complexity could be significantly reduced as what we mentioned in 7.3.2.

7.4. Performance Analysis

Performance of the proposed linear decoder for two transmit antennas can be analyzed by considering the major Laurent PAM component only. Based on the linear system model, the decision variable is given by

$$\hat{d}_n = \mathbf{c}_{\text{mmse}} \star (\mathbf{h}_{\text{imp}} \star d_n + n_n) \quad (7.34)$$

where \star stands for convolution and n_n is the colored Gaussian noise term. n_{2n} and n_{2n+1} have a zero mean and variance \mathcal{N}_0T , which can be easily calculated from Eq. (7.22). Therefore, for each realization of the channel, n_n is the noise term

in Eq. (7.23), which has zero-mean and variance $(|h_1|^2 + |h_2|^2)\mathcal{N}_0T$. The major term of \mathbf{h}_{imp} , δ_0 , is usually much greater than other terms $\delta_i, i = 1, \dots, l$, based on the statistical properties of the channel. Thus it is reasonable to assume that \mathbf{c}_{mmse} is the inverse filter of \mathbf{h}_{imp} . Consequently, $\mathbf{c}_{\text{mmse}} \star \mathbf{h}_{\text{imp}} \approx \delta(n)$, where $\delta(n)$ is kroneckner delta function, and Eq. (7.34) simplifies to

$$\hat{d}_n = d_n + \mathbf{c}_{\text{mmse}} \star n_n. \quad (7.35)$$

The instantaneous signal-to-noise ratio (SNR) is written as

$$\rho_{\text{in}} = \frac{1}{(|h_1|^2 + |h_2|^2)\mathcal{N}_0T \|\mathbf{c}_{\text{mmse}}\|^2} \quad (7.36)$$

where $\|\cdot\|$ denotes Frobenius norm. Assuming that the noise term in Eq. (7.35) is independent for each realization of the channel, we can calculate the average error probability by averaging the conditional error probability (conditioned on each channel realization). Let $h_1 = \lambda_1 + j\lambda_2$ and $h_2 = \lambda_3 + j\lambda_4$, where $\lambda_1, \lambda_2, \lambda_3, \lambda_4$ are independent Gaussian random variables with zero mean and variance $1/2$. The average error probability is given as

$$P_e^{(\text{fir})} = \int \int \int \int Q(2\rho_{\text{in}})\gamma(\lambda_1)\gamma(\lambda_2)\gamma(\lambda_3)\gamma(\lambda_4)d\lambda_1d\lambda_2d\lambda_3d\lambda_4 \quad (7.37)$$

where $\gamma(\lambda)$ is probability density function (pdf) of the Gaussian random variable λ .

The performance with soft decision feedback depends on the SINR received. SINR values will approach the upper limit as the number of iterations increases. As the sum of interference and noise terms can be approximated as a Gaussian random variable when the number of independent interference sources is large, the error probability could be approximated as [93]

$$P_e^{(\text{soft})} \approx Q \left(\sqrt{d_{\min}^2 \frac{E_b}{\mathcal{N}_0}} \right) \quad (7.38)$$

where d_{\min}^2 is normalized minimum squared Euclidean distance which is dependent on SINR. Generally speaking, increasing the number of iterations in the decision-feedback process will result in a higher SINR until it saturates at the upper limit. Thus, a natural question that needs to be answered is the necessary number of iterations. Such answer can be found by calculating the SINR upper limit and the SINR for each iteration. When the difference between the SINR limit and the SINR achieved after a certain number of iterations is smaller than a predefined threshold, the iteration process can stop. In practice, the SINR difference between two adjacent iterations is also a good measure which can be used to determine when to stop the iteration after considering performance-complexity tradeoffs.

7.5. Simulation Results

Error performances of orthogonal space-time block coded BCPM0.5 (we use GMSK as examples) with two transmit antennas over frequency-flat Rayleigh fading channels are shown in Figs. 7.5, 7.6, and 7.7, which correspond to GMSK $BT = \infty$ ($L = 1$), $BT = 0.5$ ($L = 2$), $BT = 0.3$ ($L = 3$), respectively. The size of a frame over which the quasistatic channel coefficients remain constant is 200 data bits. Signal waveforms over one bit interval T are represented by 16 samples in the waveform-based simulation.

BER curves of BPSK systems with the Alamouti code is used as the baseline performance. The exact error probability of BPSK with full diversity employing the Alamouti code can be found in [74]. It is found that the linear receiver with an MMSE FIR filter is very robust to ISI. By examining the slopes of the BER

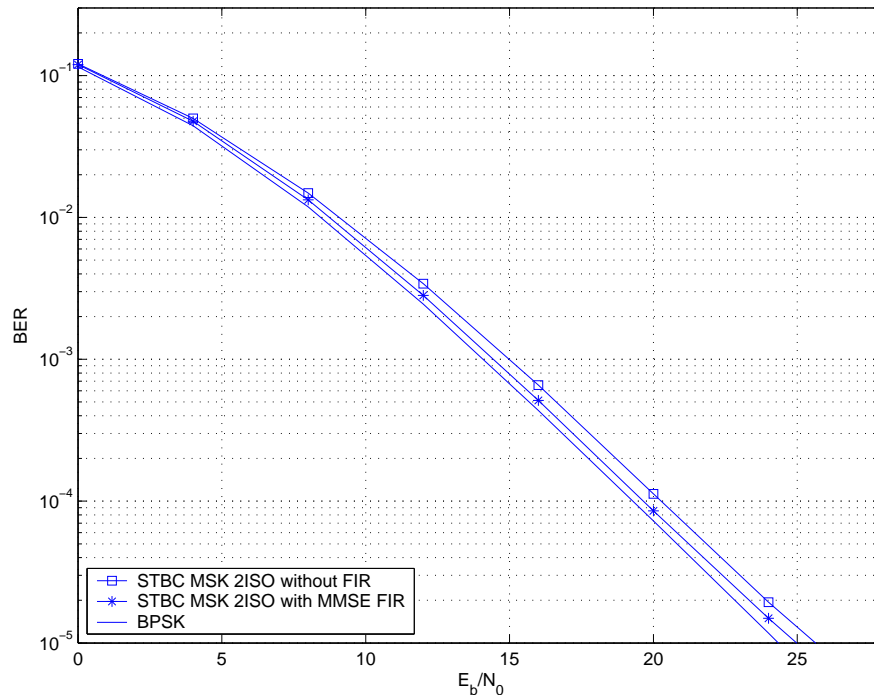


FIGURE 7.5. Performance of space-time block coded GMSK ($BT = \infty$, $L = 1$, $M = 2$).

curves, we found that the proposed STBC BCPM0.5 system with linear receiver achieves full diversity. Comparing the performances of the linear receiver with and without an FIR filter, we found that at a BER of 10^{-4} the FIR filter achieves about 0.6 dB, 1.5 dB and 4.5 dB gains for $L = 1, 2$, and 3, respectively. With $BT = 0.3$, the proposed STBC for GMSK with an FIR filter performs about 1.3 dB worse than BPSK with the Alamouti code at a BER of 10^{-4} ; with $BT = 0.5$, the gap is within half a dB.

Performance of systems with three and four antennas are shown in Fig. 7.8 and Fig. 7.9, respectively. Soft decision feedback is found achieving full diversity

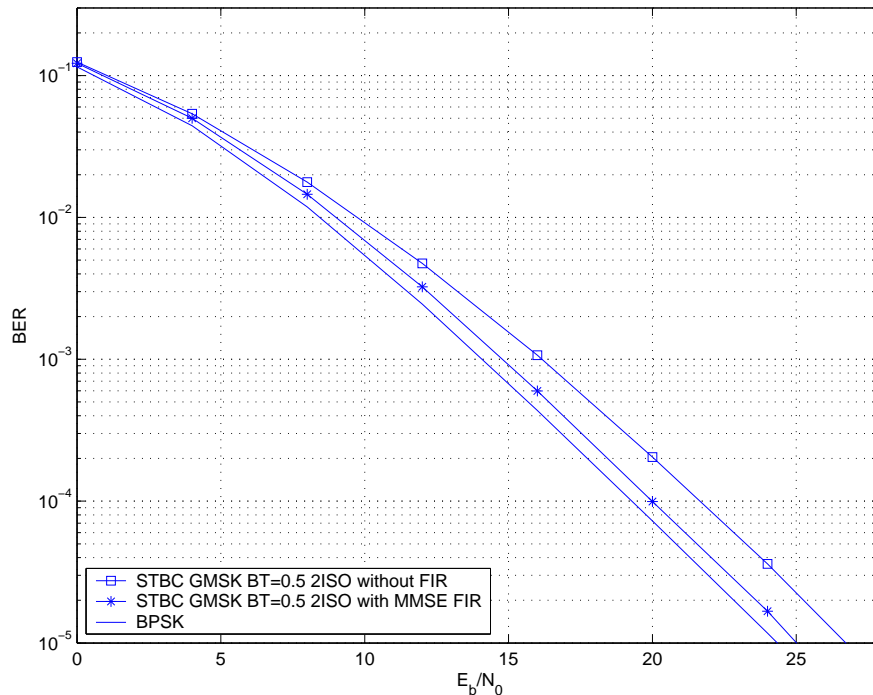


FIGURE 7.6. Performance of space-time block coded GMSK ($BT = 0.5$, $L = 2$, $M = 2$).

for both cases. Without decision feedback, GMSK with $BT = 0.3$ for 4 antennas suffers from irreducible error floor due to large ISI.

Comparing our simulation results with the results in [84], we find that the proposed simplified receiver achieves almost the same performance as an ML receiver for MSK signals. The complexity of the proposed receiver is lower than existing algorithms, especially for BCPM0.5 with large L values.

7.6. Conclusion

We have proposed a space-time block code for BCPM0.5 signals. This scheme is based on Laurent decomposition combined with data precoding, which

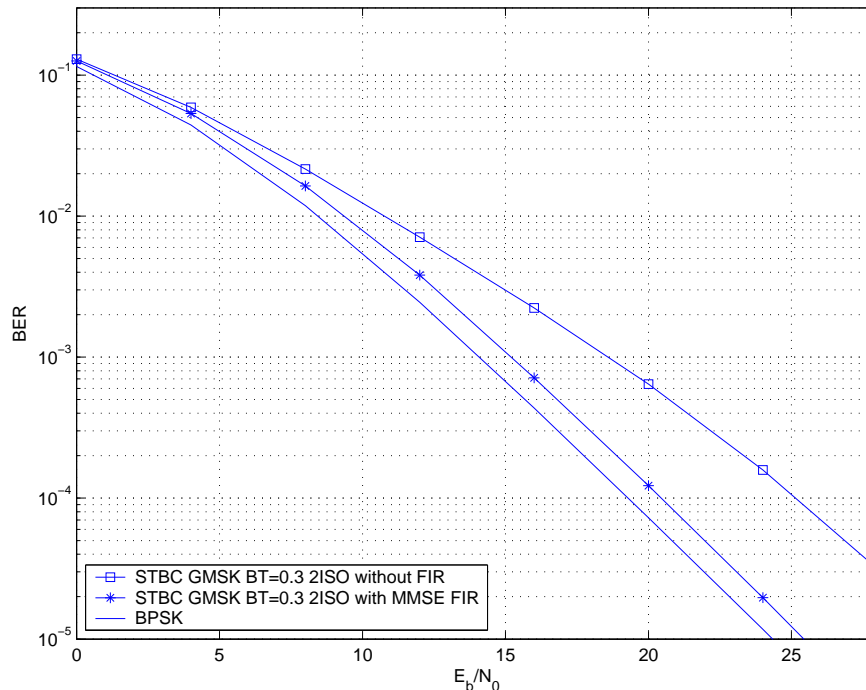


FIGURE 7.7. Performance of space-time block coded GMSK ($BT = 0.3$, $L = 3$, $M = 2$).

allows us to apply the orthogonal code structure. We have also derived a linear MMSE receiver for the proposed space-time block coded BCPM0.5 with two transmit antennas, and a nonlinear MMSE receiver for systems with more than two antennas. The simplified receiver is very robust to ISI inherent in BCPM0.5 signals. The combination of the proposed orthogonal code and the simplified receiver achieves full diversity for BCPM0.5 systems, and the decoding complexity is lower than existing STTC schemes. The performance gap between the proposed scheme and the baseline scheme - BPSK over frequency-flat Rayleigh fading channels depends on frequency pulse length L and the number of transmit antennas.

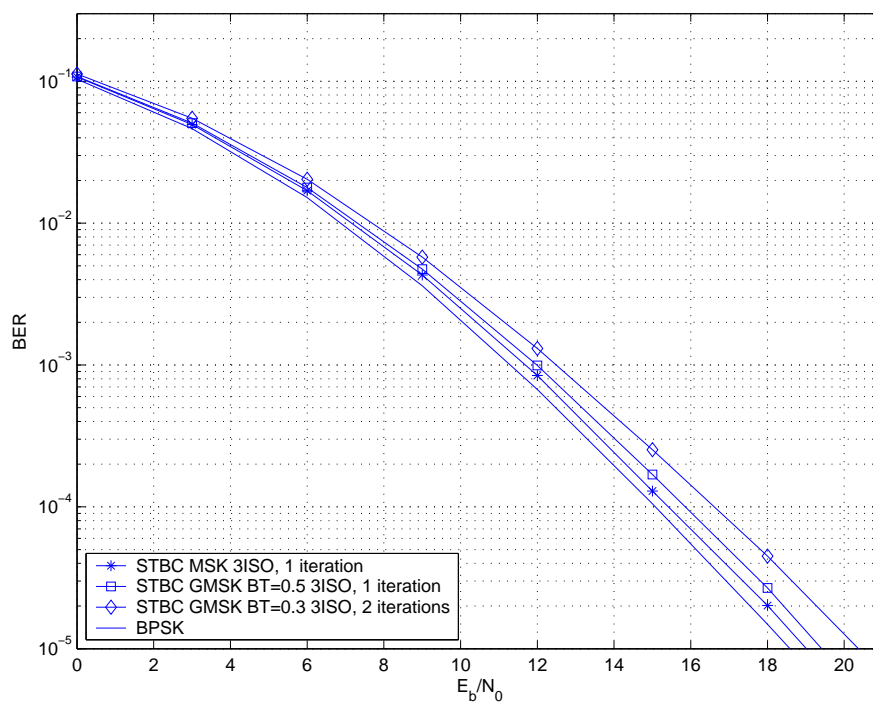


FIGURE 7.8. Performance of space-time block coded GMSK with 3 transmit antennas

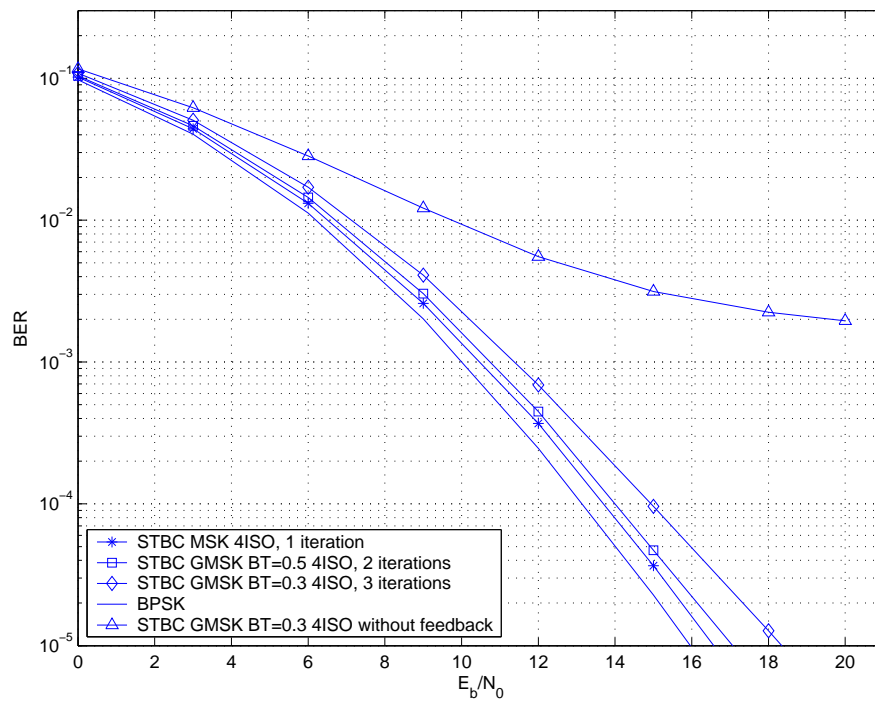


FIGURE 7.9. Performance of space-time block coded GMSK with 4 transmit antennas

8. LOW-COMPLEXITY MAXIMUM LIKELIHOOD DECODING FOR QUASI-ORTHOGONAL SPACE-TIME CODES

8.1. Low-Complexity ML Decoding and Simulation Results

The proposed scheme is based on an effective constellation-reduction procedure that consists of two main steps. In the first stage, we *assume* that the transmitted symbols belong to a lower-size constellation, called the “virtual constellation”, rather than the actual constellation. Once the choice of the virtual constellation has been made, metrics $f_{14}(x_1, x_4)$ and $f_{23}(x_2, x_3)$ [46] are applied to find the most likely points for all transmitted symbols in the virtual constellation, where x_i , $i = 1, \dots, 4$ are transmitted symbols from the same constellation. In the second stage, the receiver moves back to actual constellation, and checks *only* those points near the temporary symbol decision made in the first stage. As a result, the complexity will be significantly reduced when the size of the actual constellation is large.

As described in [46], decoding of (x_2, x_3) is similar to decoding of (x_1, x_4) . Thus, let us consider decoding (x_1, x_4) only. For 8PSK with actual constellation points $\{e^{jk\pi/4}, k = 0, \dots, 7\}$, the fast ML decoder must check $8^2 = 64$ possible combinations. In the proposed scheme, the receiver first assumes that the transmitted signals belong to a QPSK virtual constellation with points $\{e^{jk\pi/2}, k = 0, \dots, 3\}$. If, for example, ‘ x ’ is the decision made in stage 1, then in stage 2 the receiver checks its five nearby points $\{xe^{jk\pi/4}, k = -2, \dots, 2\}$, which include ‘ x ’. The number of comparisons to decode all codewords (including virtual codewords) is $4^2 + 5^2 = 39$, representing a 35.9% reduction when compared to fast ML decoding. For 16PSK signals the virtual constellation could be chosen as QPSK. If a point in the virtual constellation is decided, the receiver then checks the

nearest seven points in the actual constellation. The complexity is $4^2 + 7^2 = 65$, which equals 25.4% of 16^2 comparisons required in fast ML decoding. For both 32PSK and 64PSK, the virtual constellation could be chosen as 8PSK for decoding in stage 1. In stage 2, the receiver checks seven points for 32PSK and thirteen points for 64PSK. Complexity of the proposed scheme is reduced to 11% and 5.7% of that of fast ML decoding for 32PSK and 64PSK, respectively.

For 16QAM signals, the virtual constellation can be chosen as 4QAM which includes the four points having the largest amplitude in the actual constellation. In stage 2, the receiver checks the nearest nine points, and complexity is reduced to 37.9%.

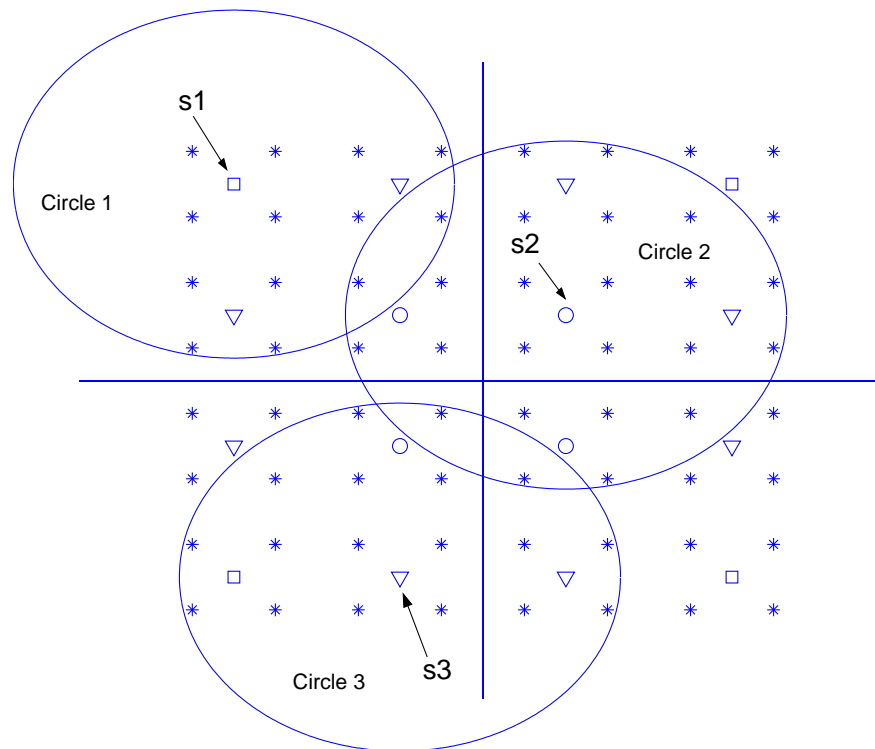


FIGURE 8.1. The virtual constellation and actual constellation for 64QAM.

For 64QAM, however, a good choice of the virtual constellation is not formed by a subset of the actual constellation points. This is illustrated in Fig. 8.1 where the actual constellation is represented by stars and the virtual constellation is 16QAM. Points in the 16QAM are divided, according to their geometric properties, into three groups: group 1 - four squares, group 2 - four circles, and group 3 - eight triangles. For example, if a point in group 1 (e.g., ‘s1’ as shown in Fig. 8.1) is the stage-1 decision, the receiver then checks the nearest thirteen points within circle 1 as illustrated in Fig. 8.1. Similarly a stage-1 decision in group 2 and 3 (e.g., ‘s2’ and ‘s3’ as shown in Fig. 8.1) causes the receiver to check the nearest twenty four and eighteen points within circle 2 and circle 3, respectively. Strictly speaking, the virtual-constellation points in different groups may have different probabilities to be chosen as the decision in stage 1. For simplicity in estimating the complexity reduction, we assume that they have equal probabilities. With this assumption, decoding complexity of the proposed scheme is about $16^2 + \frac{(24 \times 4 + 18 \times 8 + 13 \times 4)}{16} = 589$, which equals 14.4% of that of fast ML decoding.

Our proposed scheme is nonlinear, but its performance depends on the linearity of ML decoding. If ML decoding is fully linear (e.g, orthogonal codes for which a decision variable exists), the proposed scheme always achieves exactly the same performance as ML decoding regardless of the choices of the virtual constellation. For QOC, however, a decision variable for ML decoding does not exist, so linear ML decoding does not exist either. The proposed scheme can still achieve the same performance as ML decoding with appropriate choices of the virtual constellation in stage 1 and a sufficient number of nearby points in stage 2. Poor choices of these two parameters will cause an error floor at high SNR.

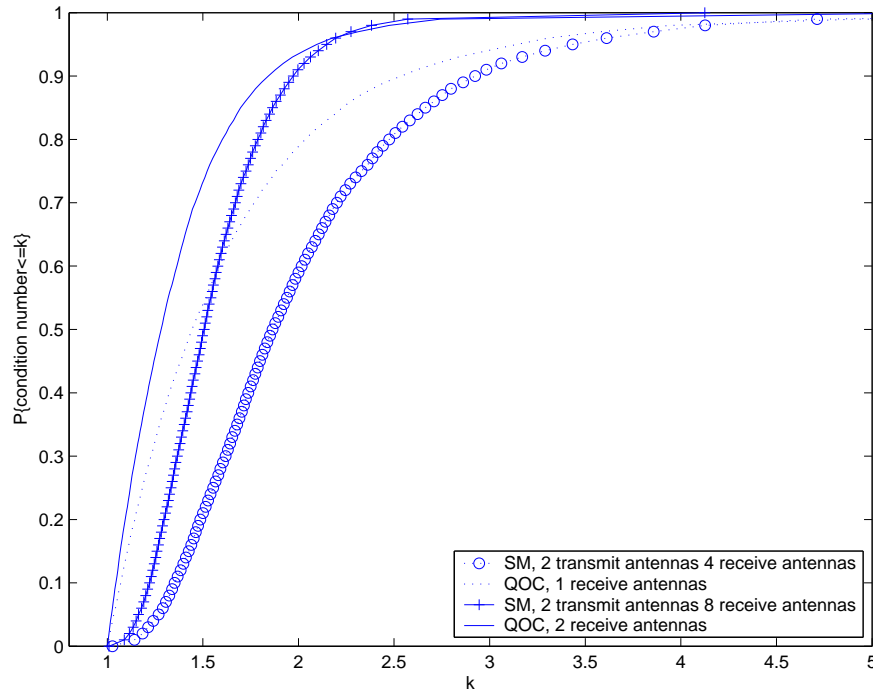


FIGURE 8.2. CDF of condition numbers of channel matrices for QOC and SM.

Linearity can be measured by cumulative distribution function (CDF) of condition number (the ratio between maximum singular value and minimum singular value) of channel matrix [95]. For orthogonal codes, condition number is always one (full linearity). For QOC and spatial multiplexing (SM) or V-BLAST [41], CDF of condition numbers of their channel matrices are illustrated in Fig.8.2. Note that QOC has comparable decoding complexity with 2 transmit antennas SM. Rotated QOC has full diversity $4N$, where N is the number of receive antennas, it is required for SM to have $4N$ receive antennas to get the same diversity order. Obviously, channel matrix for SM is more ill-conditioned than that for QOC. Performance of proposed scheme suffers from ill-conditioned channel matrix when this scheme is applied to SM. However, it is interesting to see linearities

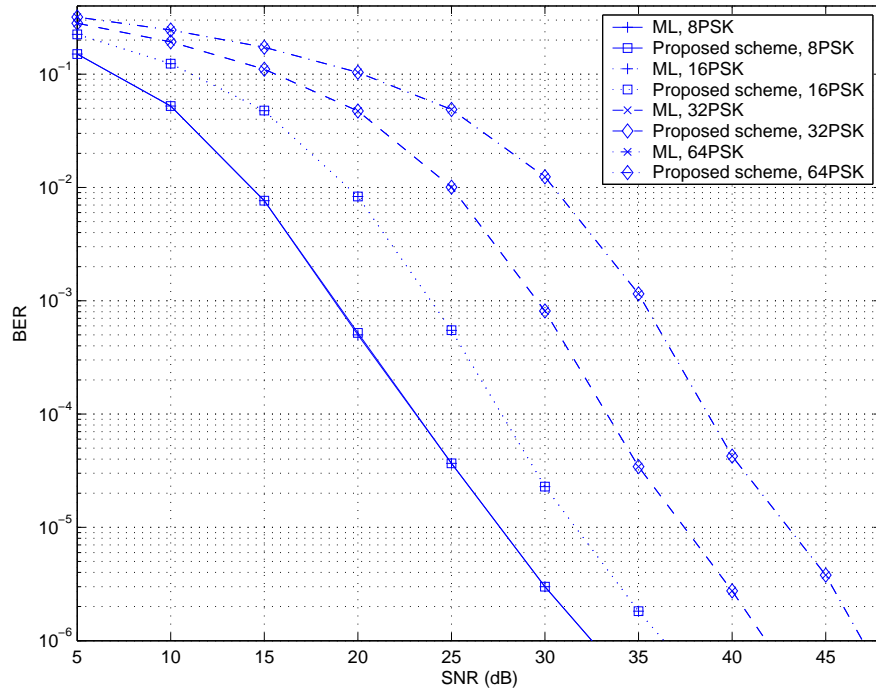


FIGURE 8.3. Performance comparison of maximum likelihood and the proposed decoding schemes for PSK signals.

of QOC and SM increase with increase of the number of receive antennas. Therefore, our scheme can achieve good performance for SM when the number of receive antennas is large. Or complexity of our scheme can be reduced further (i.e. decrease searching range in stage 2) for QOC with large number of receive antennas.

Simulation results are obtained to demonstrate the performance of the proposed low-complexity decoding scheme for QOC and how it compares with ML decoding. For all simulations, $M = 1$, $N = 4$ and Gray mapping are adopted. Simulated bit error rate (BER) versus received signal-noise ratio (SNR) of ML decoding and the proposed scheme for PSK and QAM signals are shown in Fig. 8.3 and Fig. 8.4, respectively. It is clearly seen that the proposed scheme achieves

the same performance as ML decoding when BER is as low as 10^{-6} , for practical wireless system, simulated BER is low enough.

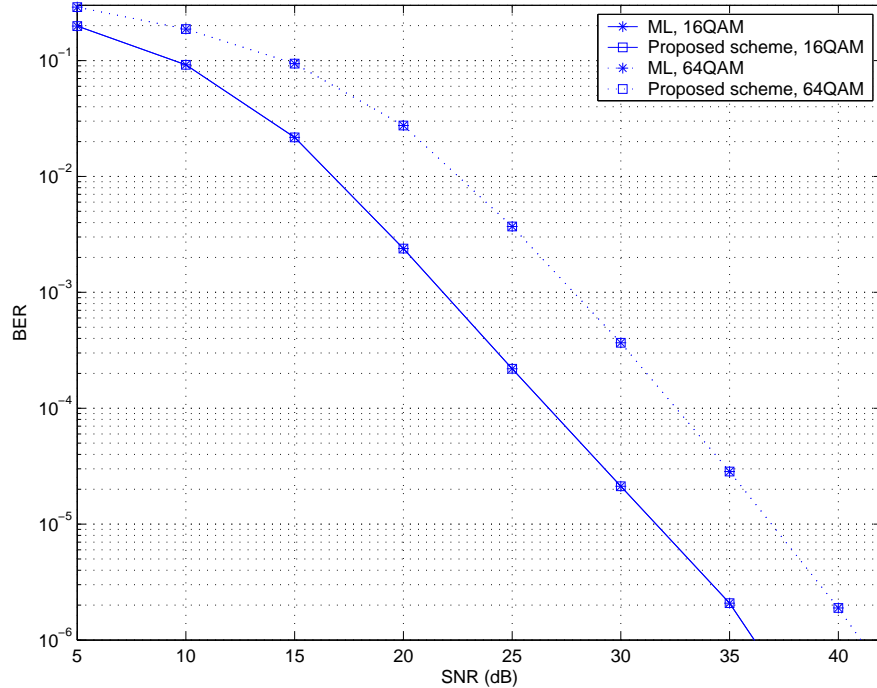


FIGURE 8.4. Performance comparison of maximum likelihood and the proposed decoding schemes for QAM signals.

8.2. Conclusion

We have proposed a low-complexity decoding scheme for quasi-orthogonal space-time block codes, mainly for systems with a large constellation size. The proposed scheme is based on a two-stage procedure. The first stage reduces the searching range for possible codewords and the second stage determines the final decoded symbols. Compared to fast ML decoding, such a procedure results in significant reduction of computational complexity. Performance of the proposed scheme depends on the linearity of ML decoding.

9. SUMMARY

In this thesis, I have proposed a new STC design from cyclic design which achieves full diversity without constellation rotation for four transmit antennas. I then proposed a systematic method to design QOSTBC for an arbitrary number of transmit antennas, and derived the optimal constellation rotation angles to achieve full diversity. I also proposed an analytical method to derive the exact error probabilities of OSTBC, which can be used to predict the performance of OSTBC. In order to improve the error performance, I introduced an adaptive power allocation scheme for OSTBC which can guarantee maximum achievable SNR. I also applied OSTBC to binary CPM with modulation index $h = 0.5$, and developed a simplified receiver for such scheme. Binary CPM with $h = 0.5$ is widely used in practical systems, i.e. GSM mobile communications, my proposed simplified receiver could be used to increase the transmission rate or extend the coverage range. Finally, I presented a decoding method to reduce the complexity of QOSTBC without degrading its error performance which also has a high practical value.

BIBLIOGRAPHY

- [1] G. J. Foschini and M. J. Gans, "On limits of wireless communications in a fading environment when using multiple antennas," *Wireless Personal Communications*, vol. 6, pp. 311-335, Mar. 1998.
- [2] D. Gesbert, M. Shafi, D. Shiu, P. J. Smith and A. Naguib, "From theory to practice: an overview of MIMO space-time coded wireless systems," *IEEE Journal on Selected Areas in Communications*, vol. 21, pp. 281-302, Apr. 2003.
- [3] S. Sandu and A. Paulraj, "Space-time block codes: a capacity perspective," *IEEE Communications Letters*, vol. 4, pp. 384-386, Dec. 2000.
- [4] A. J. Paulraj, D. A. Gore, R. U. Nabar and H. Bölcskei, "An overview of MIMO communications—a key to gigabit wireless," *Proceedings of the IEEE*, vol. 92, pp. 198-218, Feb. 2004.
- [5] J. Guey, M. P. Fitz, M. R. Bell and W. Kuo, "Signal design for transmitter diversity wireless communication systems over Rayleigh fading channels," *Proc. IEEE VTC*, 1996, pp. 136-140.
- [6] G. J. Foschini, "Layered space-time architecture for wireless communication in a fading environment when using multi-element antennas," *Bell Labs Tech. J.*, vol. 1, pp. 41-59, 1996.
- [7] I. E. Telatar, "Capacity of multi-antenna Gaussian channels," *Eur. Trans. Tel.*, vol. 10, pp. 585-595, Nov./Dec. 1999.
- [8] D. Gesbert, H. Bölcskei, D. A. Gore and A. J. Paulraj, "Outdoor MIMO wireless channels: models and performance prediction," *IEEE Transactions on Communications*, vol. 50, pp. 1926-1934, Dec. 2002.
- [9] R. U. Nabar, H. Bölcskei, V. Erceg, D. Gesbert and A. J. Paulraj, "Performance of multi-antenna signaling techniques in the presence of polarization diversity," *IEEE Transactions on Signal Processing*, vol. 50, pp. 2553-2562, Oct. 2002.
- [10] F. Rashid-Farrokhi, A. Lozano, G. J. Foschini and R. A. Valenzuela, "Spectral efficiency of wireless systems with multiple transmit and receive antennas," *Proc. IEEE Int. Symp. PIMRC*, 2000, pp. 373-377.
- [11] D. S. Baum, D. Gore, R. Nabar, S. Panchanathan, K. V. S. Hari, V. Erceg and A. J. Paulraj, "Measurement and characterization of broadband MIMO fixed wireless channels at 2.5 GHz," *Proc. IEEE ICPWC*, 2000, pp. 203-206.

- [12] R. Stridh, B. Ottersten and P. Karlsson, "MIMO channel capacity of a measured indoor radio channel at 5.8 GHz," *Proc. Asilomar Conf. Signals, Systems and Computers*, 2000, pp. 733-737.
- [13] J. P. Kermoal, L. Schumacher, P. E. Mogensen and K. I. Pedersen, "Experimental investigation of correlation properties of MIMO radio channels for indoor picocell scenarios," *Proc. IEEE VTC*, 2000, pp. 14-21.
- [14] A. L. Swindlehurst, G. German, J. Wallace and M. Jensen, "Experimental measurements of capacity for MIMO indoor wireless channels," *Proc. IEEE Signal Processing Workshop Signal Processing Advances Wireless Communications*, 2001, pp. 30-33.
- [15] D. Chizhik, J. Ling, P. W. Wolniansky, R. A. Valenzuela, N. Costa and K. Huber, "Multiple-input-multiple-output measurements and modeling in Manhattan," *IEEE J. Select Areas Commun.*, vol. 23, pp. 321-331, Apr. 2003.
- [16] T. L. Marzetta and B. M. Hochwald, "Capacity of a mobile multiple-antenna communication link in Rayleigh flat fading," *IEEE Transactions on Information Theory*, vol. 45, pp. 139-157, Jan. 1999.
- [17] J. H. Winters, J. Salz and R. D. Gitlin, "The impact of antenna diversity on the capacity of wireless communications systems," *IEEE Transactions on Communications*, vol. 42, pp. 1740-1751, Feb. 1994.
- [18] N. Al-Dhahir, C. Fragouli, A. Stamoulis, Y. Younis and A. Calderbank, "Space-time processing for broadband wireless access," *IEEE Commun. Mag.*, pp. 136-142, Sep. 2002.
- [19] S. Ariyavisitakul, "Turbo space-time processing to improve wireless channel capacity," *IEEE Trans. Commun.*, vol. 48, pp. 1347-1359, Aug. 2000.
- [20] G. Bauch and N. Al-Dhahir, "Iterative equalization and decoding with channel shortening filters for space-time coded modulation," *Proc. IEEE VTC*, 2000, pp. 1575-1582.
- [21] G. Caire and S. Shamai, "On the achievable throughput of a multiantenna Gaussian broadcast channel," *IEEE Trans. Information Theory*, vol. 49, pp. 1601-1706, Jul. 2003.
- [22] D. Chizhik, G. Foschini, M. Gans and R. Valenzuela, "Keyholes, correlations, and capacities of multielement transmit and receive antennas," *IEEE Trans. Wireless Commun.*, vol. 1, pp. 361-368, Apr. 2002.

- [23] C. Chuah, D. Tse, J. Kahn and R. Valenzuela, "Capacity scaling in MIMO wireless systems under correlated fading," *IEEE Trans. Information Theory*, vol. 48, pp. 637-650, Mar. 2002.
- [24] M. O. Damen, K. Abed-Meraim and J. C. Belfiore, "Diagonal algebraic space-time block codes," *IEEE Trans. Information Theory*, vol. 48, pp. 628-636, Mar. 2002.
- [25] V. M. Dasilva and E. S. Sousa, "Fading resistant modulation using several transmitter antennas," *IEEE Trans. Commun.*, vol. 45, pp. 1236-1244, Oct. 1997.
- [26] S. Diggavi, N. Al-Dhahir, A. Stamoulis and A. R. Calderbank, "Differential space-time coding for frequency-selective channels," *IEEE Communications Letters*, vol. 6, pp. 253-255, Jun. 2002.
- [27] S. N. Diggavi, N. Al-Dhahir and A. R. Calderbank, "Algebraic properties of space-time block codes in inter-symbol interference multiple-access channels," *IEEE Trans. Inform. Theory*, vol. 49, pp. 2403-2414, Oct. 2003.
- [28] S. N. Diggavi, B. C. Ng and A. Paulraj, "An interference suppression scheme with joint channel-data estimation," *IEEE J. Select. Areas Commun.*, vol. 17, pp. 1924-1939, Nov. 1999.
- [29] H. El-Gamal and A. R. Hammons, "A new approach to layered space-time coding and signal processing," *IEEE Trans. Inform. Theory*, vol. 47, pp. 2321-2334, Sep. 2001.
- [30] C. Fragouli, N. Al-Dhahir and W. Turin, "Reduced-complexity training schemes for multiple-antenna broadband transmissions," *Proc. IEEE WCNC*, 2002, pp. 78-83.
- [31] L. Godara, "Applications of antenna arrays to mobile communications. Part I. Performance improvement, feasibility, and system considerations," *Proceedings of The IEEE*, vol. 85, pp. 1031-1060, Jul. 1997.
- [32] L. Godara, "Applications of antenna arrays to mobile communications. Part II. Beamforming and direction-of-arrival considerations," *Proceedings of The IEEE*, vol. 85, pp. 1195-1245, Aug. 1997.
- [33] J. C. Guey, M. P. Fitz, M. R. Bell and W. Y. Kuo, "Signal design for transmitter diversity wireless communication systems over Rayleigh fading channels," *IEEE Trans. Commun.*, vol. 47, pp. 527-537, Apr. 1999.

- [34] A. R. Hammons and H. El-Gamal, "On the theory of space-time codes for PSK modulation," *IEEE Trans. Inform. Theory*, vol. 46, pp. 524-542, Mar. 2000.
- [35] L. Zheng and D. Tse, "Diversity and multiplexing: a fundamental tradeoff in multiple antenna channels," *IEEE Transactions on Information Theory*, vol. 49, pp. 1073-1096, May 2003.
- [36] S. M. Alamouti, "A simple transmit diversity technique for wireless communications," *IEEE Journal on Selected Areas in Communications*, vol. 16, pp. 1451-1458, Oct. 1998.
- [37] V. Tarokh, H. Jafarkhani and A. R. Calderbank, "Space-time block codes from orthogonal designs," *IEEE Transactions on Information Theory*, vol. 45, pp. 1456-1467, Jul. 1999.
- [38] W. Su and X. Xia, "Two generalized complex orthogonal space-time block codes of rates 7/11 and 3/5 for 5 and 6 transmit antennas," *IEEE Transactions on Information Theory*, vol. 49, pp. 313-316, Jan. 2003.
- [39] X. Liang, "A high-rate orthogonal space-time block code," *IEEE Communications Letters*, vol. 7, pp. 222-223, May 2003.
- [40] V. Tarokh, N. Seshadri and A. R. Calderbank, "Space-time codes for high data rate wireless communication: performance criterion and code construction," *IEEE Transactions on Information Theory*, vol. 44, pp. 744-765, Mar. 1998.
- [41] P. W. Wolniansky, G. J. Foschini, G. D. Golden and R. A. Valenzuela, "V-BLAST: an architecture for realizing very high data rates over the rich-scattering wireless channel," *IEEE International Symposium on Signals, Systems, and Electronics (ISSSE)*, pp. 295-300, Oct. 1998.
- [42] G. D. Golden, G. J. Foschini, R. A. Valenzuela and P. W. Wolniansky, "Detection algorithm and initial laboratory results using V-BLAST space-time communication architecture," *IEE Electronics Letters*, vol. 35, pp. 14-16, Jan. 1999.
- [43] H. Wang and X. Xia, "Upper bounds of rates of complex orthogonal space-time block codes," *IEEE Transactions on Information Theory*, vol. 49, pp. 2788-2796, Oct. 2003.
- [44] X. Liang, "Orthogonal designs with maximal rates," *IEEE Transactions on Information Theory*, vol. 49, pp. 2468-2503, Oct. 2003.

- [45] X. Liang and X. Xia, "On the nonexistence of rate-one generalized complex orthogonal designs," *IEEE Transactions on Information Theory*, vol. 49, pp. 2984-2988, Nov. 2003.
- [46] H. Jarfarkhani, "A quasi-orthogonal space-time block code," *IEEE Transactions on Communications*, vol. 49, pp. 1-4, Jan. 2001.
- [47] O. Tirkkonen, A. Boariu and A. Hottinen, "Minimal non-orthogonality rate 1 space-time block code for 3+ tx antennas," *Proc. IEEE 6th Int. Symp. Spread-Spectrum Techniques and Applications (ISSSTA)*, pp.429-432, Sep. 2000.
- [48] N. Sharma and C. B. Papadias, "Improved quasi-orthogonal codes through constellation rotation," *IEEE Transactions on Communications*, vol. 51, pp. 332-335, Mar. 2003.
- [49] W. Su and X. Xia, "Signal constellations for quasi-orthogonal space-time block codes with full diversity," *IEEE Transactions on Information Theory*, vol. 50, pp. 2331-2347, Oct. 2004.
- [50] L. Xian and H. Liu, "Space-time block codes from cyclic design," *IEEE Communications Letters*, vol. 9, pp. 231-233, Mar. 2005.
- [51] L. Xian and H. Liu, "Optimal rotation angles for quasi-orthogonal space-time codes with PSK modulation," *IEEE Communications Letters*, vol. 9, pp. 676-678, Aug. 2005.
- [52] N. Sharma and C. B. Papadias, "Full-rate full-diversity linear quasi-orthogonal space-time codes for any number of transmit antennas," *EURASIP J. Applied Signal Proc.*, no. 9, pp. 1246-1256, Aug. 2004.
- [53] L. Xian and H. Liu, "Rate one space-time block codes with full diversity," *IEEE Transactions on Communications*, vol. 53, pp. 1986-1990, Dec. 2005.
- [54] H. Shin and J. H. Lee, "Upper bound on the error probability for space-time codes in fast fading channels," *Proc. IEEE Vehicular Technology Conference (VTC)*, Sep. 2002, pp. 243-246.
- [55] S. Sandhu and A. Paulraj, "Union bound on error probability of linear space-time block codes," *Proc. IEEE International Conference on Acoustics, Speech, and Signal Processing (ICASSP)*, May 2001, pp. 2473-2476.
- [56] G. Gritsch, H. Weinrichter and M. Rupp, "A tight lower bound for the bit error ratio of space-time block codes," *Proc. IEEE Vehicular Technology Conference (VTC)*, May 2004, pp. 728-732.

- [57] J. Liu and E. Gunawan, "An exact union bound on the BER for the combined system of ideal beamforming and Alamouti's STBC," *Proc. IEEE ICICS-PCM*, Dec 2003, pp. 1488-1491.
- [58] Y. Li and B. Vucetic, "Tight upper bound for bit error probability of combined space-time block codes and ideal beamforming," *IEE Electronics Letters*, vol. 40, pp. 1434-1435, Oct. 2004.
- [59] G. Gao and A. M. Haimovich, "BER analysis of MPSK space-time block codes with differential detection," *IEEE Communications Letters*, vol. 7, pp. 314-316, Jul. 2003.
- [60] L. Xian and H. Liu, "Exact error probability for space-time block coded MIMO systems over Rayleigh fading channels," *IEE Proceedings-Communications*, vol. 152, pp. 197-201, Apr. 2005.
- [61] L. Xian and H. Liu, "An adaptive power allocation scheme for space-time block coded MIMO systems," *Proc. IEEE Wireless Communications and Networking Conference (WCNC)*, pp. 504-508, Mar. 2005.
- [62] L. Xian, R. Punnoose and H. Liu, "Space-time block coded GMSK with low-complexity linear receiver," *Proc. IEEE International Conference on Communications (ICC)*, pp. , Jun. 2006.
- [63] L. He and H. Ge, "A new full-rate full-diversity orthogonal space-time block coding scheme," *IEEE Communications Letters*, vol. 7, pp. 590-592, Dec. 2003.
- [64] A. Sezgin, E. A. Jorswieck and H. Boche, "Performance criteria analysis and further performance results for quasi-orthogonal space-time block codes," *Proc. of IEEE ISSPIT*, pp. 102-105, 2003.
- [65] D. Wang and X. Xia, "Optimal diversity product rotations for quasi-orthogonal STBC with MPSK symbols," *IEEE Communications Letters*, vol. 9, pp. 420-422, May 2005.
- [66] H. Jafarkhani and N. Hassanpour, "Super-quasi-orthogonal space-time trellis codes for four transmit antennas," *IEEE Transactions on Wireless Communications*, vol. 4, pp. 215-227, Jan. 2005.
- [67] J. Hou, M. H. Lee and J. Y. Park, "Matrices analysis of quasi-orthogonal space-time block codes," *IEEE Communications Letters*, vol. 7, pp. 385-387, Aug. 2003.

- [68] B. A. Sethuraman, B. S. Rajan and V. Shashidhar, "Full-diversity, high-rate space-time block codes from division algebras," *IEEE Transactions on Information Theory*, vol. 49, pp. 2596-2616, Oct. 2003.
- [69] O. Damen, A. Chkeif and J. Belfiore, "Lattice code decoder for space-time codes," *IEEE Communications Letters*, vol. 4, pp. 161-163, May 2000.
- [70] X. Li, T. Luo, G. Yue and C. Yin, "A squaring method to simplify the decoding of orthogonal space-time block codes," *IEEE Transactions on Communications*, vol. 49, pp. 1700-1703, 2001.
- [71] V. Tarokh, H. Jafarkhani and A. R. Calderbank, "Space-time block coding for wireless communications: performance results," *IEEE Journal of Selected Areas on Communications*, vol. 17, pp. 451-460, 1999.
- [72] V. Tarokh and H. Jafarkhani, "A differential detection scheme for transmit diversity," *IEEE Journal of Selected Areas on Communications*, vol. 18, pp. 1169-1174, 2000.
- [73] H. Jafarkhani and V. Tarokh, "Multiple transmit antenna differential detection from generalized orthogonal designs," *IEEE Transactions on Information Theory*, vol. 47, pp. 2626-2631, 2001.
- [74] J. G. Proakis, "Digital communications," (McGraw-Hill, 2001, 4th edition).
- [75] J. G. Proakis, "Probabilities of error for adaptive reception of M-phase signals," *IEEE Transactions on Communication Technology*, vol. 16, pp. 71-81, 1968.
- [76] G. Gao and A. M. Haimovich, "BER analysis of MPSK space-time block codes with differential detection," *IEEE Communications Letters*, vol. 7, pp. 314-316, 2003.
- [77] J. H. Horng, L. Li and J. Zhang, "Adaptive space-time transmit diversity for MIMO systems," *Proc. of IEEE VTC'03*, Apr. 2003, pp. 1070-1073.
- [78] T. Lo, "Adaptive space-time transmission with side information," *Proc. of IEEE WCNC'03*, Mar. 2003, pp. 601-606.
- [79] M. Seo and S. W. Kim, "Power adaptation in space-time block code," *Proc. of IEEE Globecom'01*, Nov. 2001, pp. 3188-3193.
- [80] G. Ganesan, P. Stoica and E. G. Larsson, "Diagonally weighted orthogonal space-time block codes," *Proc. of Asilomar Conference on Signals, Systems and Computers*, Nov. 2002, pp. 1147-1151.

- [81] W. H. Wong and E. G. Larsson, "Orthogonal space-time block coding with antenna selection and power allocation," *IEE Electronics Letters*, vol. 39, pp. 379-381, Feb. 2003.
- [82] X. Zhang and M. P. Fitz, "Space-time code design with continuous phase modulation," *IEEE Journal of Selected Areas on Communications*, vol. 21, pp. 783-792, Jun. 2003.
- [83] W. Zhao and G. B. Giannakis, "Reduced complexity receivers for layered space-time CPM," *IEEE Transactions on Wireless Communications*, vol. 4, pp. 574-582, Mar. 2005.
- [84] J. K. Cavers, "Space-time coding using MSK," *IEEE Transactions on Wireless Communications*, vol. 4, pp. 185-191, Jan. 2005.
- [85] G. Wang and X. Xia, "An orthogonal space-time coded CPM system with fast decoding for two transmit antennas," *IEEE Transactions on Information Theory*, vol. 50, pp. 486-493, Mar. 2004.
- [86] D. Wang, G. Wang and X. Xia, "An orthogonal space-time coded partial response CPM system with fast decoding for two transmit antennas," *IEEE Transactions on Wireless Communications*, vol. 4, pp. 2410-2422, Sep. 2005.
- [87] P. A. Murphy and G. E. Ford, "Cochannel receivers for CPM signals based upon the Laurent representation," *Proc. of Virginia Tech. Symp. Wireless Personal Communications*, 1996.
- [88] G. K. Kaleh, "Simple coherent receivers for partial response continuous phase modulation," *IEEE Journal of Selected Areas on Communications*, vol. 7, pp. 1427-1436, Dec. 1989.
- [89] P. A. Laurent, "Exact and approximate construction of digital phase modulations by superposition of amplitude modulated pulses (AMP)," *IEEE Transactions on Communications*, vol. 34, pp. 150-160, Feb. 1986.
- [90] G. L. Lui, "Threshold detection performance of GMSK signal with $BT=0.5$," *Proc. IEEE MILCOM*, Oct. 1998, pp. 515-519.
- [91] D. G. Manolakis, V. K. Ingle and S. M. Kogan, "Statistical and adaptive signal processing," McGraw-Hill, 1999.
- [92] S. L. Marple, "Digital spectral analysis with applications," Prentice-Hall, 1987.

- [93] W. H. Gerstacker, R. R. Muller and J. B. Huber, "Iterative equalization with adaptive soft feedback," *IEEE Transactions on Communications*, vol. 48, pp. 1462-1466, Sep. 2000.
- [94] E. de Carvalho and D. T. M. Slock, "Burst mode noncausal decision-feedback equalizer based on soft decisions," *Proc. of IEEE VTC*, pp. 414-418, 1998.
- [95] H. Artés, D. Seethaler and F. Hlawatsch, "Efficient detection algorithms for MIMO channels: a geometrical approach to approximate ML detection," *IEEE Transactions on Signal Processing*, vol. 51, pp. 2808-2820, Nov. 2003.
- [96] A. Boariu and D. M. Ionescu, "A class of nonorthogonal rate-one space-time block codes with controlled interference," *IEEE Transactions on Wireless Communications*, vol. 2, pp. 270-276, Mar. 2003.
- [97] M. Z. A. Khan and B. S. Rajan, "Space-time block codes from coordinate interleaved orthogonal designs," *Proc. IEEE International Symposium of Information Theory*, Jul. 2002, p. 275.
- [98] M. Z. A. Khan, B. S. Rajan and M. H. Lee, "On single-symbol and double-symbol decodable STBCs," *Proc. IEEE International Symposium of Information Theory*, Jul. 2003, p. 127.
- [99] M. Z. A. Khan, B. S. Rajan and M. H. Lee, "Rectangular coordinate interleaved orthogonal designs," *Proc. IEEE Globecom*, Dec. 2003, p. 2004-2009.

